

VU Research Portal

Last Glacial climate variability in eastern and central Europe as recorded in loess deposits

Bokhorst, M.P.

2009

[Link to publication in VU Research Portal](#)

citation for published version (APA)

Bokhorst, M. P. (2009). *Last Glacial climate variability in eastern and central Europe as recorded in loess deposits*. [PhD-Thesis - Research and graduation internal, Vrije Universiteit Amsterdam]. Ipskamp Drukkers BV.

General rights

Copyright and moral rights for the publications made accessible in the public portal are retained by the authors and/or other copyright owners and it is a condition of accessing publications that users recognise and abide by the legal requirements associated with these rights.

- Users may download and print one copy of any publication from the public portal for the purpose of private study or research.
- You may not further distribute the material or use it for any profit-making activity or commercial gain
- You may freely distribute the URL identifying the publication in the public portal ?

Take down policy

If you believe that this document breaches copyright please contact us providing details, and we will remove access to the work immediately and investigate your claim.

E-mail address:

vuresearchportal.ub@vu.nl

Last Glacial climate variability in eastern and central Europe as recorded in loess deposits

VRIJE UNIVERSITEIT

LAST GLACIAL CLIMATE VARIABILITY
IN EASTERN AND CENTRAL EUROPE
A S R E C O R D E D I N
LOESS DEPOSITS

ACADEMISCH PROEFSCHRIFT

ter verkrijging van de graad Doctor aan
de Vrije Universiteit Amsterdam,
op gezag van de rector magnificus
prof.dr. L.M. Bouter,
in het openbaar te verdedigen
ten overstaan van de promotiecommissie
van de faculteit der Aard- en Levenswetenschappen
op maandag 18 mei 2009 om 15.45 uur
in de aula van de universiteit,
De Boelelaan 1105

door

Mark Peter Bokhorst

geboren te Haarlemmermeer

promotor:
copromotor:

prof.dr. J.F. Vandenberghe
dr. C.J. Beets

reading committee:

prof.dr. M. Frechen
prof.dr. H. Hooghiemstra
prof.dr. F. Lehmkuhl
prof.dr. S.B. Marković
dr. M.A. Prins

Voorwoord

Waarom noemen ze dit eigenlijk een proefschrift? Dat heb ik mijzelf gedurende mijn hele promotie afgevraagd. Een proeve van bekwaamheid, dat ligt voor de hand, maar bekwaam in wat? In wetenschappelijk onderzoek doen? Je kritisch opstellen tegenover het werk van jezelf en dat van anderen? Zelf een eigen onderzoek aan laten sluiten op de stand van zaken in de literatuur? Dat lijkt meer op een groot afstudeeronderzoek.

Nee, het betekent meer. Het is ook: de proef om de (on)juistheid te bewijzen van wat anderen gedaan hebben. Toen het idee, dat geresulteerd heeft in het eerste hoofdstuk van dit proefschrift ontstond, ging ik voor het eerst tegen de gevestigde orde in. En dat heb ik geweten. Natuurlijk kwam mijn paper bij de verkeerde reviewer, die mijn gehele idee met de grond gelijk maakte in een review op verwijtende toon.

Proefschrift betekent dus ook: 'scientific world'-proof geschrift. De kunst beheersen om je werk geaccepteerd te krijgen in de vastgeroeste gevestigde orde. Dat is mij menigmaal zwaar gevallen en heeft ervoor gezorgd dat ik diverse malen serieus heb gedacht dat ik dit niet zou kunnen. Dit geeft mij aanleiding om als eerste mijn hartelijke dank uit te spreken aan mijn promotor, Jef Vandenberghe. Niet alleen wil voor alle vruchtbare wetenschappelijke discussies die we hebben gehad, maar ook voor de onvoorwaardelijke steun en peptalks die hij mij steeds weer bood als ik het niet meer zag zitten, soms zelfs in hoge frequentie. Gesprekken met Jef hebben mij steeds weer moed gegeven om de draad weer op te pakken, en uiteindelijk met resultaat! Natuurlijk wil ik ook mijn copromotor Kay Beets bedanken, in het bijzonder voor zijn ideeën om nieuwe proxy's uit te testen op mijn monsters. Ondanks alle pijn en moeite heeft dit in ieder geval al één mooie publicatie over dit thema opgeleverd.

Dit proefschrift betekent dus ook: behoorlijke beproeving. De beproeving van vier jaar op een kamertje met één harde deadline: het einde van het geld na vier jaar. En tot die tijd je eigen deadlines stellen en nakomen. Vooral dat laatste heb ik als erg lastig ervaren, met alle gevolgen vandien voor mijn humeur. Hier noem ik graag mijn ouders, die veel steun hebben gegeven en geduld hebben opgebracht als het weer eens 'don't mention the p-word' was, en mijn steun en toeverlaat Karel van der Hee. Onze relatie is op de proef (!) gesteld, maar hij heeft mij door dik en dun gesteund, ook tijdens piekermomenten midden in de nacht.

Het sociale aspect van de dagelijkse koffiepauze om tien uur was vaak een reden om op tijd op de VU te verschijnen, om toch maar weer door te gaan. Hier ontstond het contact met mede-aio's, vooral na de fusie van de afdelingen Kwartairgeologie en PalPal. Geleidelijk werd ik met hen kind aan huis op de Donderdorst van GeoVU'sie, gingen we regelmatig met elkaar een hapje buiten de VU eten en weet ik wat meer. Hier wil ik graag mijn hartelijke dank uit laten gaan aan al mijn collega's voor de vele honderden discussies over van alles en nog wat, maar meestal over helemaal niets, die we onder het genot van (het proeven van) koffie op E3 hebben gehad. Graag laat ik even hun namen passeren: Bert Boekschoten (als eerste omdat hij vaak aanstichter is van de meest bizarre onderwerpen en omdat hij dit soort bedankjes verschrikkelijk vindt), Emma Versteegh, Aafke Brader, Els Ufkes, Ron Kaandorp, Alex Wright, Philip

Ward, Ane Wiersma, Geert-Jan Vis, José Joordens, Ronald van Balen, Kees Kasse, Sjoerd Bohncke, Jef Vandenbergh, Maarten Prins, Cedric van Meerbeeck, Hans Renssen, Jens Zinke, Margot Saher, Jochem Jongma, Didier Roche, Orson van de Plassche, Martin van Breukelen, Frank Peters, Ko van Huissteden, Anco Lankreijer, Suzan Verdegaal, Hubert Vonhof, Gerald Ganssen en natuurlijk in het bijzonder mijn kamergenoten Stefan Engels en Hanneke Bos. Daarnaast noem ik ook graag mijn eerdere kamergenoten Vincent Post, Boris van Breukelen, Gu Oude Essink, Igor Mendizabal en Margriet Groenendijk. Met al deze mensen is een band ontstaan en ik hoop dat deze nog lang voort kan blijven duren, al waaieren velen uit, soms ver weg van de VU. In het bijzonder wil ik graag de naam van Mirjam Vriend noemen. Zij was meer dan een collega. Met haar ben ik al tijdens mijn studie op veldwerk geweest en op de VU hadden we dezelfde missie. Dit heeft geleid tot vele wetenschappelijke discussies over de aanpak van ons onderzoek en natuurlijk tot een verdere versterking van onze band. Kort na haar promotie overleed Mirjam aan een klimongeluk.

Het schrijven van een proefschrift betekent dus ook het mogen proeven van de universitaire wereld, met alle bijbehorende mogelijkheden en vrijheden. Mogen proeven van onderzoek doen en natuurlijk: van veldwerk. Voordat ik begon aan mijn onderzoek was ik wat sceptisch tegenover oost Europa, maar daar ben ik volledig van teruggekomen! Leuke mensen, talen en de Oekraïense keuken was een ontdekking. Herewith I like to thank all my colleagues and friends I met in central and eastern Europe: Slobodan Marković and his family, Tivadar Gaudenyi, Nebojsa Milojković, Natasha Gerasimenko, Zhanna Matviishina, Maria Łanczont, Pál Sümegi and Manfred Frechen and his team. Natuurlijk ook de studenten die mee op veldwerk waren en met hun afstudeerscriptie mijn onderzoek ondersteund hebben: Erhard Pots, Hans Leuversing, Jasper Wassenburg en tweede chauffeur Sander Zwart. En monsters nemen betekent monsters analyseren. Mijn dank gaat uit naar Martin Konert, Roel van Elsas, Maurice Hooyen, Bas van der Wagt, Mark Dekkers, Paul Smit, Bart de Vries, Martine Hagen, Nel Slimmen en de veel te vroeg gestorven Hetty Schäfer voor hun hulp bij de duizenden analyses die mijn veldbezoeken tot gevolg hadden.

Als promovendus mag je ook proeven van het geven van universitair onderwijs. Vijf jaar heb ik het eerstejaarsveldwerk naar de Brabantse Wal met veel plezier medebegeleid. Graag noem ik mijn teamgenoten Kay Beets, Vincent Post, Stefan Engels en alle anderen die in deze jaren meegeweest zijn naar Brabant en de Ardennen.

Voor mij was dit proefschrift de proef op de som. Bij mijn afstuderen lag een onderzoekscarrière voor de hand. Ik wilde promoveren en kwam erachter dat deze specifieke manier van benaderen van mijn vakgebied het niet was voor mij. Bij het schrijven van een proefschrift kreeg ik echter ook het doceren even op proef. En dat is bevallen, het is mijn nieuwe baan geworden.

Contents

General introduction	11
State of the art of research on last-glacial climate evolution over Europe and the North-Atlantic	11
Loess deposits	13
Loess as an archive of climate information	15
Research objectives	16
Outline of the thesis	17
1 Validation of wiggle matching using a multi-proxy approach and its paleoclimatic significance	21
1.1 Introduction	23
1.2 Methods	23
1.3 Results	25
1.4 Discussion	37
1.5 Conclusions	39
2 Pedo-chemical climate proxies in Late Pleistocene Serbian-Ukrainian loess sequences	41
2.1 Introduction	43
2.2 Site description and lithostratigraphy	45
2.3 Sediment-geochemical approach and methods	46
2.4 Chronology of the four sections	49
2.5 Results	53
2.6 Discussion	55
2.7 Conclusions	60
3 Comparing the $\delta^{13}\text{C}$ of soil carbonates and soil organic matter as paleo-precipitation indicators in late Quaternary European loess deposits	63
3.1 Introduction	65
3.2 Methods	67
3.3 Results	69
3.4 Discussion	72
3.5 Possible secondary processes affecting $\delta^{13}\text{C}_{\text{som}}$	73
3.6 Conclusion	74

4 Atmospheric circulation patterns in eastern and central Europe during the Weichselian Pleniglacial inferred from loess grain-size records	77
4.1 Introduction	79
4.2 Methods	80
4.3 Descriptions of study regions and sites	84
4.4 Chronostratigraphic subdivision	88
4.5 Endmember composition and interpretation	89
4.6 Analysis of the geographical variation and temporal evolution of EM proportions and mass accumulation rates	92
4.7 Discussion of grain-size variability	96
4.8 Implications for atmospheric circulation during the Weichselian Pleniglacial in central and eastern Europe	98
4.9 Conclusions	100
Synthesis	103
Registration of millennial scale climate oscillations in loess	103
Are the found proxy variations related to Dansgaard-Oeschger cycles?	104
Can registered millennial scale climate oscillations in central and eastern Europe bridge Chinese and Atlantic climatic evolution?	106
What can be contributed to the reconstruction of the climate development in eastern and central Europe during the Weichselian Pleniglacial?	107
Future research	108
References	109
Summary	119
Samenvatting	123

General introduction

Changes in our planet's climate are a major topic of public interest. CO₂ concentration, sea level and air temperature are rising (IPCC, 2007) and it generally comes to be accepted that climate change is a fact. The first indications of changes in ecological systems are also measured and economies are slightly adjusting to the consequences of warming.

The consequences may express themselves in intensification of the water cycle (e.g. Ward et al., 2007). When this happens dryer summers and wetter winters may be expected at intermediate latitudes. In lowland areas flooding frequencies may intensify in winter, resulting in major water storage capacity problems. Water resources can become scarcer in desert areas, influencing agricultural potentials.

For economies that have to anticipate to climate change it is of major importance to predict the climate changes in the nearby future as exactly as possible. Extrapolations of the climate change of the last decennia still show a scatter of scenarios. To be able to make more reliable predictions, better knowledge on the functioning of short-term climate changes is essential. The studies presented in this thesis intend to contribute to a better understanding of short-term (millennial to centennial scale) climate changes in eastern and central Europe, under natural conditions in the recent geological past.

State of the art of research on last-glacial climate evolution over Europe and the North-Atlantic

Long-term climate changes, responsible for periodic cycles of glacial periods and interglacial periods, are orbitally forced. Milutin Milankovitch postulated that the position of earth in her path around the sun and the shape of that pathway changes on a scale of ten thousands to a hundred thousand years (Milankovitch, 1941; Hays et al., 1976). This results in changes in the distribution of solar radiation over the seasons and over the earth's surface. A chain of processes on earth responds to these changes, leading to alternations of glacial and interglacial periods.

Relatively small differences in irradiation between summer and winter, over the year or over the hemispheres, result in weakly pronounced seasons. Large differences in irradiation result in large snow accumulation at higher latitudes. Albedo reinforces reflection of the radiation and further growth of ice caps at the poles, eventually resulting in a glacial climate. The ice starts to melt again when growing irradiation at 65° N reaches a threshold value.

Short-scale climate oscillations, discovered more recently (Lehman, 1993) have a sub-Milankovitch duration of 7 ka or less and are characterized by more sudden climate changes. These Bond-cycles cannot directly be explained by orbital forcing due

to their short duration and abrupt character. Such cycles were registered primarily as high-frequency sand (Ice Rafted Debris, IRD) deposits in oceanic records at subtropical latitude and were explained by major ice rafting events, with a repetition period of about 11-7 ka (Heinrich, 1988; Hemming, 2004). Even shorter abrupt climate changes, with duration of 1.5 ka or a multiple thereof, were found in the $^{18}\text{O}/^{16}\text{O}$ ratios in ice cores from the Greenland ice sheet in the GRIP and GISP2-drilling projects (Dansgaard et al., 1990; GRIP, 1993; Grootes et al., 1993, Mayewski and Bender, 1995; NorthGRIP, 2004). Comparable oscillations were discovered in foraminifer's compositions in ocean floor sediment from the Atlantic Ocean, indicating changes in seawater temperature (Bond et al., 1993). These cycles are characterized by climate warming within decades (e.g. Cortijo et al., 1997; Voelker, 2002). In paleoclimatological studies from the late 1990's and early 2000's these cycles were found in deposits spread around the world, mainly in ocean records (for a review see e.g. Rahmstorf, 2002). In the late 1990's it was discovered that even centennial scale oscillations must have existed during the last glacial (for a review see e.g. Voelker, 2002 (on Marine Isotope Stage 3))

A proper understanding of the processes involved in, and more specific, the triggering factor of millennial scale climate oscillations is essential to be able to describe actual and predict future climate changes. However, both are still under discussion. A major step in a series of cause and effect processes responsible for millennial or centennial scale climate changes is the breakdown of the so-called conveyor belt of thermo-haline ocean circulation near Iceland, where ocean surface waters sink. Also other causes have been proposed. MacAyeal (1993) suggests Heinrich events are triggered by ice sheet instability itself. Ganopolski and Rahmstorf (2001) modeled oscillations comparable to Dansgaard-Oeschger from noise of several artificial signals. They suggest Dansgaard-Oeschger events appear when a threshold value is reached in the noise of various parameters. Alley et al. (2001) published comparable modeling of a stochastic resonance process as the trigger of these cycles. Some authors suggest the cycles might have been triggered from the tropical Pacific (e.g. Clement and Cane, 1999), while another group of scientists suggest solar forcing as the major trigger (Van Geel et al., 1999).

Considering millennial scale climate oscillations, detailed records from the landmasses, considering the whole Weichselian Pleniglacial, are limited. However, several proxy records show promising results. Continuous pollen records from several regions in France show high-resolution climate variability, probably related to Dansgaard-Oeschger cycles (e.g. Reille and De Beaulieu, 1990; Reille et al., 2000; Veres, 2007). Speleothem records in (among other locations) China (e.g. Cosford et al., 2008), France (e.g. Genty, 2003) and Austria (e.g. Spötl and Mangini, 2002; Spötl et al., 2006) show detailed $\delta^{18}\text{O}$ records resembling to smaller parts of the last glacial. Local lacustrine and peat deposits in Europe have provided small parts or some interstadials of the Weichselian Pleniglacial (e.g. Van Huissteden, 1990; Behre and Van der Plicht, 1992; Mol, 1997; Bos et al., 2001; Kasse et al., 2003; Hiller et al., 2004). Recent development

in research to chironomid-records as paleoclimatic proxies is promising (e.g. Engels, 2008).

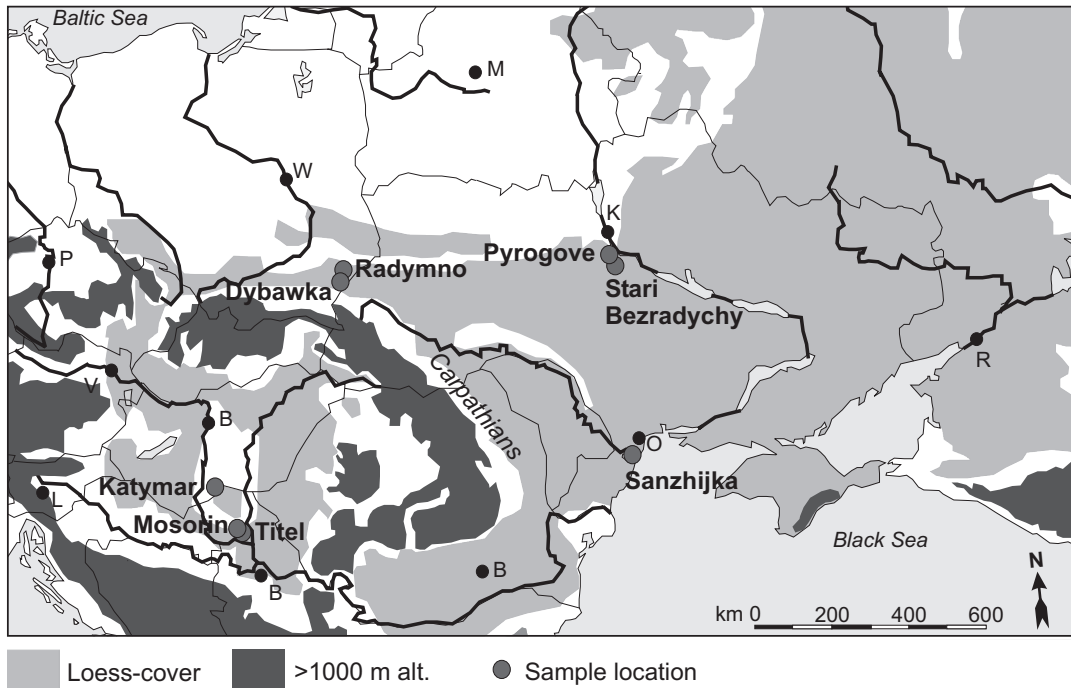
To improve our understanding of the functioning of millennial scale climate change it is important to identify frequency and amplitude, driving mechanism and areas where the signal started and was most intense. Therefore, we need an accurate comparison between the expression of the cycles in different climate proxy records and at different locations around the world. Composition of the Greenland ice, lake fills, loess grain-size distributions and so on, may all be originating from different forcing and different regions, and thus reflect different (paleo-)climatic conditions.

A major problem in correlating past climate behavior at different places is accurate dating of the records. To find out whether a proxy registration of a climate oscillation leads or lags the registration of the same climate oscillation at another location by another proxy, the oscillation registrations at both locations need to be matched first. This has proven to be possible by key signals that occur over the whole globe or over large distances, such as methane concentrations in air bubbles enclosed in ice, or volcanic ashes (e.g. Blunier et al., 1998; Mudelsee, 2001; Landais et al., 2006, Lowe et al., 2007). But records of terrestrial sediments are influenced by varying deposition rates, periods of non-deposition and erosion. Apart from that, the most appropriate approach is by absolute dating. However, present-day dating techniques are not sufficiently precise. The ^{14}C -method ranges only up to 40 ka. Luminescence dating techniques cover ages of the whole last glacial, but are not accurate enough to date millennial scale climate variations. These dating limitations are a major problem for the interpretation of terrestrial sediments as paleoclimatic information carriers.

Loess deposits

Loess as a terrestrial product is pre-eminently suitable for the registration of climate changes (Ding et al., 2002). The unstratified loess-paleosol sediments were first scientifically described by Luigi Ferdinando Marsigli in 1726 in the Danube River valley and later in more detail by Karl von Leonhard in 1820 near Heidelberg (Germany). In 1882, Ferdinand von Richthofen first described these sediments as eolian (Von Richthofen, 1882). He described a high similarity between eastern European loess and Chinese loess, suggesting a comparable origin. It can be defined as an unstratified, relatively homogenous, yellowish, generally silt-sized (5.5 - 63 μm in diameter), eolian deposit (e.g. Rousseau et al., 2007). Loess consists for the major part of quartz, combined with other minerals like (K-)feldspars, clay minerals and carbonates. The geochemical composition is dependent on the source regions of the loess.

In general, loess is rich in calcium carbonate. The calcium carbonate content in normal loess ranges from 10 to about 25%. High concentrations are found in illuviation zones just below interglacial or interstadial soils, often in nodules, while these soils themselves are eluviated from calcium carbonate. Calcium carbonate is also present



0.1

as coatings on loess grains and in root hollows, and in land snails having built their carbonate shell via plants or directly from the soil in stressful conditions (Goodfriend et al., 1999).

At intermediate latitudes loess was the dominant eolian deposit and was mainly deposited in glacial times. Its distribution on the Eurasian continent is from Normandy (France), via central Europe, Ukraine and Russia (fig. 0.1), Tadjikistan and Kazakhstan to central China. It is generally found as blanket deposits over existing landscapes, in basins, in wind shadows of river terraces and at foot slopes of mountain ranges. Loess may be present at upwind slopes and less on downwind slopes of mountain ranges and at high altitudes (e.g. Goossens and Gross, 2002).

Loess deposits are not only found in Quaternary, but also in Tertiary deposits in China (e.g. Ding et al., 1998; Guo et al, 2001; Vandenberghe et al., 2004) and is very useful for paleoclimatic reconstructions (e.g. Kaakinen et al., 2006). But a considerable increase in loess deposition on the Eurasian continent is related to the onset of the Pleistocene, about 2.4 million years BP (Ding et al., 1993) and is indicative for relatively cold periods. Chinese loess deposits have probably major source areas in the large Chinese and Mongolian deserts, such as Taklimakan, Tengger and Gobi (Sun, 2002).

0.1 Loess distribution and locations of the eight sampled loess sections in eastern and central Europe. The dark shaded area indicates mountain ranges over 1000 m altitude. P = Prague, W = Warszawa, M = Minsk, K = Kiev, R = Rostov, V = Vienna, L = Ljubljana, B = Budapest / Belgrade / Bucharest, O = Odessa.

European loess is suggested to have sources in river plains and in proglacial areas of northern Europe during and directly after glacial periods (Frechen et al., 2003), last glacial ice margins near mountain ranges like the Alps and Carpathians (Újvári et al., 2008) and areas with intensive periglacial weathering during the Pleniglacial (Wright, 2007). However, loess deposits mostly consist of a mixture of deposits from various sources ranging from very nearby to very distant, up to intercontinental. Apart from that, the thickest European loess deposits, having the highest sedimentation rates, are found at relatively large distances from these proglacial zones, like in the Pannonian Basin. This suggests that, apart from loess availability in the source region, conditions favoring deposition play a major role in loess distributions.

Loess as an archive of climate information

The grain-size distribution of loess deposits is highly dependent on wind strength, transport distance and material availability in potential source regions (see also Chapter 4). Gradients in geographical distribution of loess and identification of source areas can be used to reconstruct wind directions (Prins and Vriend, 2007). However, the grain-size composition can change after deposition due to physical and chemical weathering processes, possibly affecting mainly the clay-fraction (see also Chapter 4). When wet periods are also combined with high temperatures, leached soil profiles such as a luvisol, rendzina or even a chernozem will develop. Percolating rainwater dissolves leachable elements like Ca, Sr and Mg, and transports them over a short or a large vertical distance. Soils are depleted in concentrations of these elements, while the zones below these soils are enriched (see also chapter 2). Therefore, concentrations of relatively badly solvable elements, combined with low concentrations of easily solvable elements, can be used as indicators for wet periods.

In order to exclude secondary clay formation in deriving wind energy from grain-size distribution data, Vandenberghe et al. (1985) introduced the U-ratio, defined as the ratio of relative grain-size components transported mainly in suspension clouds (16-44 μm) and the components transported mainly in dust plumes, but excluding the clay fraction (5.5-16 μm). Herewith also sand and coarse silt deposits (>44 μm), mainly transported by saltation (Mabbutt, 1977), and therefore often dependent on very local conditions, are excluded.

As stated before, loess can be considered as a mixture of different deposits with different sources. The components of this mixture can be recognized from detailed grain size analyses using laser techniques, and quantified by endmember analysis (Weltje and Prins, 2007). Changes of endmember fluxes in a set of samples indicate changes of loess distributions by, for example, changes in dominant wind directions (Prins and Vriend, 2007).

Apart from pedogenesis, other secondary processes may also affect the deposits. For instance, wet periods or periods with low or no loess deposition can result in concentration of organic matter, originating from intensified vegetation development or long periods of (scarce) vegetation coverage respectively.

The presence of CaCO_3 in the soil is in the first place controlled by the concentration in the primary loess, just after deposition. After deposition soil moisture saturated with CO_2 , dissolves the CaCO_3 . The $^{13}\text{C}/^{12}\text{C}$ -ratio of soil CO_2 is controlled by the type of vegetation (C3 or C4 or a mixture) and its degradation. Exchange of mainly HCO_3^- determines the $^{13}\text{C}/^{12}\text{C}$ -ratio of the present C. Reprecipitated soil carbonate, often as coatings on root hollows (rhizoliths) or grains, is therefore indicative of the vegetation type that was present during this redeposition process. The vegetation type, in its turn, is indicative for the humidity conditions.

During soil formation percolating rainwater favors the formation of nano-magnetic minerals ($<0.4\ \mu\text{m}$) (e.g. Maher et al., 1994; 2002; Maher and Thompson, 1995; Nawrocki et al., 1999). Magnetic properties of loess are considered useful for paleoclimatic reconstructions (for a review see Tang et al., 2003). The presence of these minerals is reflected in the magnetic susceptibility (MS) signal of the loess. In most cases high values indicate high precipitation intensities, while also the opposite relation has been found (Hatté et al., 2001; Rousseau et al., 2002).

Research objectives

As stated before, relatively little is known on the impact of millennial scale climate oscillations on the landmasses during the last glacial period (75-12 ka BP, Martinson et al., 1987). The thick loess deposits in China have high enough resolution to detect millennial scale climate oscillations (e.g. Porter and An, 1995; Vandenberghe and Nugteren, 2001; Vriend, 2007). The western and eastern European last glacial and interglacial loess hardly exceeds 10 m. The European loess belt is extensive, and the last glacial and interglacial loess in central Europe is locally up to 20 m thick, suggesting that the resolution here can also be high enough to find millennial-scale cycles.

Key questions:

1. To what extent are millennial scale climate oscillations registered in the last-glacial loess deposits of central Europe? What is the reliability of these cycles? Can they contribute to bridge millennial scale climate information as derived from loess records on the Chinese Loess Plateau and from North Atlantic marine records?
2. To what extent can conclusions be drawn on the climatic conditions, mainly wind circulation patterns, over central Europe during the last glacial?

For these purposes eight loess sections covering the last glacial period throughout the eastern and central European plain were sampled at 5-cm resolution (fig. 0.1). In total 23 IRSL-dates and four ^{14}C -dates provided the anchor points for the time frame reconstruction of seven sections. The data collection was focused on both primary and

secondary climate proxies to have indications of wind intensities, wind directions and also relative changes in temperature and precipitation.

Outline of this thesis

When two loess records at different locations have to be matched by comparing their respective patterns of oscillations to each other (“wobble matching”), dating precision is the major problem. The standard deviations of the IRSL-technique are in most cases about 10%. As the research is focused on cycles with a duration of about 1.5 ky between 75 and 12 ka BP, the IRSL-technique does not provide enough precision to perform reliable wobble matching.

The precision problem might be (partly) anticipated using many luminescence dates, or by focusing on other properties of each wobble than its age. In Chapter 1 we discuss three more or less independent loess proxies (grain-size <5.5 μm , MS and the leachate Ba/Sr-ratio (see also Chapter 2)) that are used to label each oscillation found in two loess records, which are within a distance of only 5 km. This multi-proxy approach results in clearly more precise wobble matching than can be reached with a single proxy approach.

Reliability of wobble matching or climate reconstruction may be improved by using many independent proxies. New relatively easily measurable proxies contribute to this approach. In Chapter 2 we discuss a pilot study of new proxies that potentially can indicate paleo-precipitation intensities. These proxies are based on elements that are active in soil chemical processes. The elements differ in their ability to dissolve in percolating water. All proxies are element ratios to eliminate control by initial composition of the sediment. All ratios consist of the concentration of a relatively immobile element, divided by the concentration of an element that is easily dissolved and washed out. The proxies are tested and compared on loess from sections in three different present-day climate conditions.

$^{13}\text{C}/^{12}\text{C}$ -values of organic matter and soil carbonates as potential paleo-precipitation proxies are discussed in Chapter 3. The $\delta^{13}\text{C}$ -value of organic matter ($\delta^{13}\text{C}_{\text{som}}$) is more and more accepted as such a proxy (e.g. Rousseau et al., 2002). The $\delta^{13}\text{C}$ -value of soil carbonates ($\delta^{13}\text{C}_{\text{sc}}$) is directly related to $\delta^{13}\text{C}_{\text{som}}$. However, only few studies have been done to $\delta^{13}\text{C}_{\text{sc}}$ as a proxy for paleo-precipitation and they are once compared for this purpose (Wang and Folmer, 1998). The reliability of $\delta^{13}\text{C}_{\text{som}}$ and $\delta^{13}\text{C}_{\text{sc}}$ as paleo-precipitation proxies is discussed by comparing both records, measured on loess from the Titel section (Serbia).

A connection between all sampled sections for this thesis is presented in Chapter 4. As stated before, the sections can only be connected via proxies that are comparable in all sections. For example the U-ratio (Vandenberghe, 1985) is a reliable proxy for a connection on a European scale, as loess is (slightly) affected by post-depositional processes and consists of a mixture of different deposits, originating from different sources or being transported by different mechanisms (e.g. Vriend, 2007). Endmember

analysis unmixes the loess in parts that represent deposits from comparable source regions or coherent transport mechanisms. When the model is run over the loess grain-size dataset from eight sections as a whole, the resulting endmember distributions in each single section can be compared. Based on the results of the endmember analysis results and assuming that the relations between paleo-wind directions and endmember distributions on the Chinese Loess Plateau are also valid in the European loess belt, a reconstruction of the dominant wind directions in central Europe during the Early, Middle and Late Pleniglacial is suggested and discussed.



VALIDATION OF WIGGLE MATCHING USING A MULTI-PROXY APPROACH AND ITS PALEOCLIMATIC SIGNIFICANCE

With Jef Vandenberghe. Published in Journal of Quaternary Science, doi: 10.1002/jqs.1271

ABSTRACT

The research to global, millennial-scale climate oscillations during the last glacial requires wiggle matching. One method for adequate wiggle matching is based on the dating of the climate proxy records. Luminescence dating methods are needed for estimates of last glacial ages in terrestrial records. However, such dating methods are not accurate enough for millennial scale wiggle matching. It is shown that a multi-proxy comparison of two sections that are situated close to each other may improve considerably the accuracy of wiggle matching. The method is tested by an application on two loess sections of last glacial age in Vojvodina, Serbia. The climate proxies include magnetic susceptibility, leachate Ba/Sr and grain-size. Firstly, single proxy-wiggle matches between both sections are analysed, successively with the same and with different proxies. Secondly, a multi-proxy wiggle match based on all three proxies of the two sections is presented and compared to the single-proxy tests. In such a procedure, it becomes clear which wiggles are mainly determined by local conditions and which have a more extended significance. It is concluded that a multi-proxy approach results in the best and the most unique wiggle matches.

1 Validation of wiggle matching using a multi-proxy approach and its paleoclimatic significance

1.1 Introduction

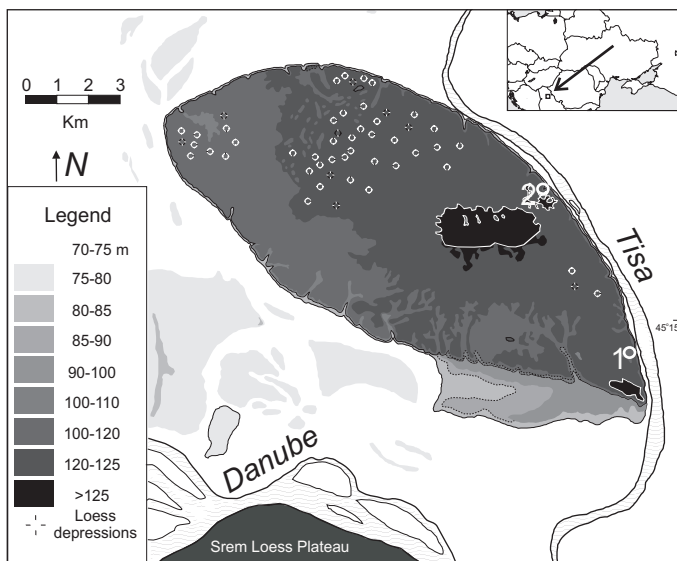
There is a continuous search for records containing millennial-scale climate oscillations, allowing better understanding of them. Those short-scale records have been found all around the globe (e.g. Leuschner and Sirocko, 2000) and are often related to climate variations recorded in the Greenland ice sheet as described by Bond et al. (1993). To examine whether millennial-scale climate oscillations from a specific study area are related to those in the GRIP or GISP2 ice cores, wiggle matching is often applied. In many cases tele-connections are based on one or a few proxies from one location and a varying number of absolute age estimates (e.g. Bowen et al., 2002; Chen et al., 1997; Hatté et al., 1999; Little et al., 1997; Rousseau et al., 2002; Watts et al., 1996). Others base their correlation on two or more locations situated close to each other, while one proxy is used (e.g. Leuschner and Sirocko, 2000; Nawrocki et al., 1999).

Terrestrial evidence for millennial-scale variability is often found in loess records. The presence of little organic matter in loess and the maximum age determination of approximately 45 ka hamper the applicability of ^{14}C -dating. To cover the complete range of the last glacial, in which most millennial scale oscillations are found, luminescence dating techniques are applied in these types of records. However, luminescence techniques have in most cases a standard deviation of $\pm 10\%$. When considering a millennial scale cycle of about 1.5 ky duration (Bond et al., 1997), up to ten cycles might fit in one standard deviation with ages equivalent to the early part of marine isotope stage (MIS) 4. Moreover, no separation can be made between wiggles that are due to large-scale climate oscillations and wiggles that are due to coincidental local situations or processes.

The hypothesis in this chapter is that the millennial (to centennial) scaled oscillations can be matched with more certainty and reliability using a multi-proxy approach than with a single-proxy approach. In this way one can easier separate local oscillations from regional to global scale climate oscillations.

1.2 Methods

The suggested wiggle matching method was applied on two loess sections situated close to each other. The sections have comparable environmental conditions. The Titel loess plateau is located near the confluence of the rivers Tisa (Tisza/Theiss) and Danube in the region of Vojvodina, Serbia (fig 1.1). A former brickyard and river cut exposure near the village of Titel shows 20 meters of loess deposition since the beginning of the Last Interglacial. A gully exposure near the village of Mošorin is located only 6 km from the Titel section and has 15 metres of loess deposition in the same period. Both sections



1.1

were sampled at 5-cm resolution. In each section 5 samples were taken for luminescence dating. All samples were analysed for magnetic susceptibility, the ratio of leachable barium (Ba) and strontium (Sr) and grain-size distribution.

It is supposed that the magnetic susceptibility is a signal mainly created by very small ($<0.4 \mu\text{m}$) magnetic grains, formed and deposited by water percolating through the soil (e.g. Maher et al., 1994; 2002; Maher and Thompson, 1995; Nawrocki et al., 1999). It is considered by those authors as a reliable proxy for paleo-precipitation intensities. The measurements were carried out with 2 g dry sample on a KLY-2 susceptibility bridge (AGICO, Brno, Czech Republic) (Dekkers, 1997). All values are averages of triplicate measurements.

The Ba/Sr-ratio consists of a conservatively leachable element (Ba) and an easily leachable element (Sr). These two elements are liberated from clay minerals by the same weathering process. But Sr is transported before Ba. This differential rate of leaching is especially clear at relatively low precipitation intensities. Therefore the Ba/Sr-ratio is considered as a paleo-precipitation proxy in dry to moderately humid climates (Bokhorst et al., 2008; Chapter 2). Both elements were measured after the leaching of 100 mg sample in 1 N HNO_3 , using a Liberty II Varian ICP-AES.

The grain-size, just like the sedimentation rate, appears to be a good indicator for wind energy (e.g. Liu, 1985; Vandenberghe et al., 1997; Nugteren and Vandenberghe, 2004). The grain-size distribution was measured between 0 and $2000 \mu\text{m}$ in 57 intervals and performed on a FRITSCH A22 laser grain-size analyser. The pre-treatment was done according to the procedure by Konert and Vandenberghe (1997). The fraction 5.5-

1.1 Location of the sections near Titel (1) and Mošorin (2) on the Titel loess plateau in Serbia (after S.B. Marković). The grey tone represents the altitude above sea level.

16 μm is used, which is mainly transported as suspension load over large distances and therefore relatively continuously deposited (Prins et al., 2007). It is not, or only hardly, affected by secondary processes like soil formation (Vandenberghe et al., 2004).

The luminescence samples were pretreated under weak red light. The 4 to 11 μm fraction was stimulated by infrared light (IRSL). The dose rate samples were calculated from the amounts of potassium (K), uranium (U) and thorium (Th). The average water content in the samples was estimated at 20%. For further information on the used dating method see Frechen et al. (1996).

Initially, statistically reliable oscillations in each individual proxy record were separated from noise based on three standard deviations of the used measurement technique of each proxy signal. Since it is our objective to demonstrate the differences between single-proxy and multi-proxy correlations, we first establish a temporal frame in which only information from one individual proxy and the dating results are used. Several single-proxy wiggle matching possibilities are carried out between the sections. This is done to simulate single-proxy wiggle matches where no more information is available. Next, the three proxies of the single sections are compared and climatic oscillations are identified on the base of these comparisons. Finally, multi-proxy wiggle matching is carried out using all six proxy records and dating results.

1.3 Results

Site description

In the Vojvodina region, northern Serbia, typical loess is found on six discontinuous plateau uplands between the alluvial plains of the Danube, Tisa, Sava and Tamiš rivers (Marković et al., 2008). The Titel loess plateau (45°14'N, 20°19'E) is situated in the central part of the Vojvodina region, near the confluence of the rivers Danube and Tisa. It is a loess island with remarkable cliffs created by fluvial erosion. For this study, two sites were chosen at the eastern edge of the Titel loess plateau (fig. 1.1). The stratigraphic units are based on current chronostratigraphic interpretations in the Vojvodina region (Serbia) (Marković et al., 2004; 2005; 2006; 2007; 2008). The prefix 'V' refers to the standard Pleistocene loess-paleosol stratigraphy in Vojvodina.

The Titel section (fig. 1.2a, left) is located in an old brickyard quarry about 1 km north of the village of Titel. In this section the Holocene soil consists of a chernozem of about 80 cm (V-S0), followed by a thin transition horizon (V-S0a) containing small CaCO_3 -nodules. The soil complex contains crotovinas. The Upper Pleniglacial loess contains an incipient soil of 2 m at the top (V-L1-1S1) and a smaller one between 3.70 m and 4.10 m (V-L1-1S2). The top of the Middle Pleniglacial loess is marked by a soil complex containing two incipient soils (V-L1-2S1 and V-L1-2S3) and a more developed mollic horizon, possibly representing a chernozem (V-L1-2S2). The central part of the Middle Pleniglacial deposits contain three incipient soils (V-L1-2S4 – V-L1-2S7), separated by loess containing Mn-spots (V-L1-2L1 – V-L1-2L4), while the lower part becomes sandier. The base of the Middle Pleniglacial loess is marked by an incipient soil

Field code	Section	Depth (m)	Equivalent dose (Gy)	Equivalent dose, 1 σ	Dose rate (Gy/ka)	Dose rate, 1 σ	Age (ka)	Age, 1 σ
Sb2.30	Titel	2.30	271.3	46.9	3.16	0.24	15.0	2.8
Sb5.00	Titel	5.00	734.4	26.8	3.89	0.29	25.1	2.2
Sb8.00	Titel	8.00	984.0	11.6	4.00	0.29	32.7	2.6
Sb11.35	Titel	11.35	1066.0	30.3	3.54	0.26	52.7	4.0
Sb15.40	Titel	15.40	1545.2	23.8	3.90	0.29	69.3	5.2
Sv2.5	Mošorin	2.50	220.5	17.4	3.82	0.28	10.2	1.1
Sv5.0	Mošorin	5.00	575.8	36.1	3.98	0.30	25.3	2.5
Sv7.55	Mošorin	7.55	762.4	36.3	3.83	0.29	34.9	3.1
Sv9.75	Mošorin	9.75	1439.7	88.0	3.78	0.29	66.7	6.5
Sv12.55	Mošorin	12.55	1339.8	62.4	3.92	0.30	59.9	5.4

T 1.1

(V-L1-2S7). The Lower Pleniglacial loess (V-L1-3) becomes clearly coarser and contains many sandy layers. The lower part is finer and contains Mn-spots. The last interglacial deposit contains a soil complex, consisting of a 40 cm-thick weakly developed soil (V-S1a), followed by a 2 m-thick chernozem (V-S1). Both soils contain crotovinas. The lower part of S1 contains large nodules of CaCO_3 .

The Mošorin section is located 6 km NNW of the Titel section, in a small valley cut (fig. 1.2a, right). The Holocene soil (V-S0) is clearly visible and consists of a 65-cm thick dark chernozem, followed by a thin transition horizon (V-S0a) containing small CaCO_3 -nodules. The soil complex contains crotovinas. The Upper Pleniglacial loess contains an incipient soil of 1 m at the top (V-L1-1S1) and a smaller one between 3.40 m and 4.30 m (V-L1-1S2). The top of the Middle Pleniglacial loess is marked by a more developed mollic horizon of 30 cm (V-L1-2S1). The Middle Pleniglacial deposits are marked by two incipient soils with a thickness of 1,6 and 1 m respectively (V-L1-2S2 and V-L1-2S3). The Lower Pleniglacial loess (V-L1-3) is slightly coarser and contains Mn-spots. The last interglacial deposit contains a soil complex, consisting of a 50 cm-thick weakly developed soil (V-S1a), followed by a 1,8 m-thick chernozem (V-S1). Both soils contain crotovinas. The lower part of S1 contains large nodules of CaCO_3 .

The individual proxy records in the Titel section

The magnetic susceptibility curve (fig. 1.3a, left) shows a base value of about $5 \times 10^{-6} \text{ m}^3/\text{kg}$, which is probably the initial value after deposition. In the top part two oscillations with low amplitude ($<5.5 \times 10^{-6} \text{ m}^3/\text{kg}$) are found. The central part of the curve shows one double oscillation of about 1.5 m thickness and one single oscillation of 0.4 m thickness. Both show values up to about $7 \times 10^{-6} \text{ m}^3/\text{kg}$. The maximum values, representing interglacial conditions, range up to $2 \times 10^{-5} \text{ m}^3/\text{kg}$ and are found between 17.5 to 19.5 m depth.

The Ba/Sr-record (figs. 1.2b, left and 1.3b, left) varies more than the magnetic susceptibility curve. The base value is about 0.35. In the top part of the curve one weak oscillation (value 0.4) is found at 3.5 m depth. The central part of the curve shows one double oscillation with a thickness of about 1 m and 4 thinner oscillations (about 0.5 m) with maximum values ranging between 0.65 and 0.85. In the lower part three weak oscillations (thickness <0.4 m, maximum value <0.5) are found, while the basal part of sections shows values up to 1.5, representing interglacial conditions. The general shape of the curve is comparable to that of the magnetic susceptibility curve, while nine oscillations are found in the Ba/Sr curve and four in the magnetic susceptibility curve (interglacial part not counted). Both patterns of oscillations are completely different in size and position.

The grain-size curve (figs. 1.2a, left and 1.3c, left), representing only the 5,5-16 μm fraction, show values between 12% and 30%. The record shows a thick top part (thickness >3 m) with very high values (23 to 28%), suggesting interglacial conditions. The central part of the curve shows two oscillations, one with a thickness of about 2 m and both with a value of about 22%. The lower part of the section shows two oscillations with maximum values of 17% and a weaker one of 14%. The basal part of the section shows values up to 28%, indicating interglacial conditions.

The individual proxy records in the Mošorin section

The magnetic susceptibility curve (figs. 1.2a, right and 1.3a, right) shows a base value of about $5 \times 10^{-6} \text{ m}^3/\text{kg}$, comparable to the Titel section. In the top part two thin oscillations (<0.3 m) with a value of about $6.5 \times 10^{-6} \text{ m}^3/\text{kg}$ and one weak oscillation with a value of $5.5 \times 10^{-6} \text{ m}^3/\text{kg}$ are found. The central part of the curve shows one double oscillation of about 1.5 m thickness and one single oscillation of 0.4 m thickness. Both show values up to about $7 \times 10^{-6} \text{ m}^3/\text{kg}$. The maximum values, representing interglacial conditions, range up to $1.8 \times 10^{-5} \text{ m}^3/\text{kg}$ and are found between 12.5 to 14.5 m depth.

The base value of the Ba/Sr-record (fig. 1.3b, right) is about 0.3. The top part shows no clear oscillations, while the central part shows four oscillations, ranging between 0.6 and 0.75. The lower part shows two weak oscillations (value about 0.4) and one clearer oscillation (value 0.6). The basal part of the section shows a maximum of 0.85, indicating interglacial values.

The grain-size curve (fig. 1.3c, right) shows high values (26-30%) in the top 3.7 m. The central part shows three relatively thick oscillations (>0.5 m) with values of about 24%, while the lower part shows two oscillations with values of 21% and 19%. The basal part of the section is again characterised by high values (maximum 29%), indicating interglacial values.

Chronology

The ages resulting from luminescence analyses are shown in table 1.1 and plotted next to the proxy curves in figs. 1.2-1.5. The samples are all in chronological order, except the lowest one in the Mošorin section which shows a very small overlap within one

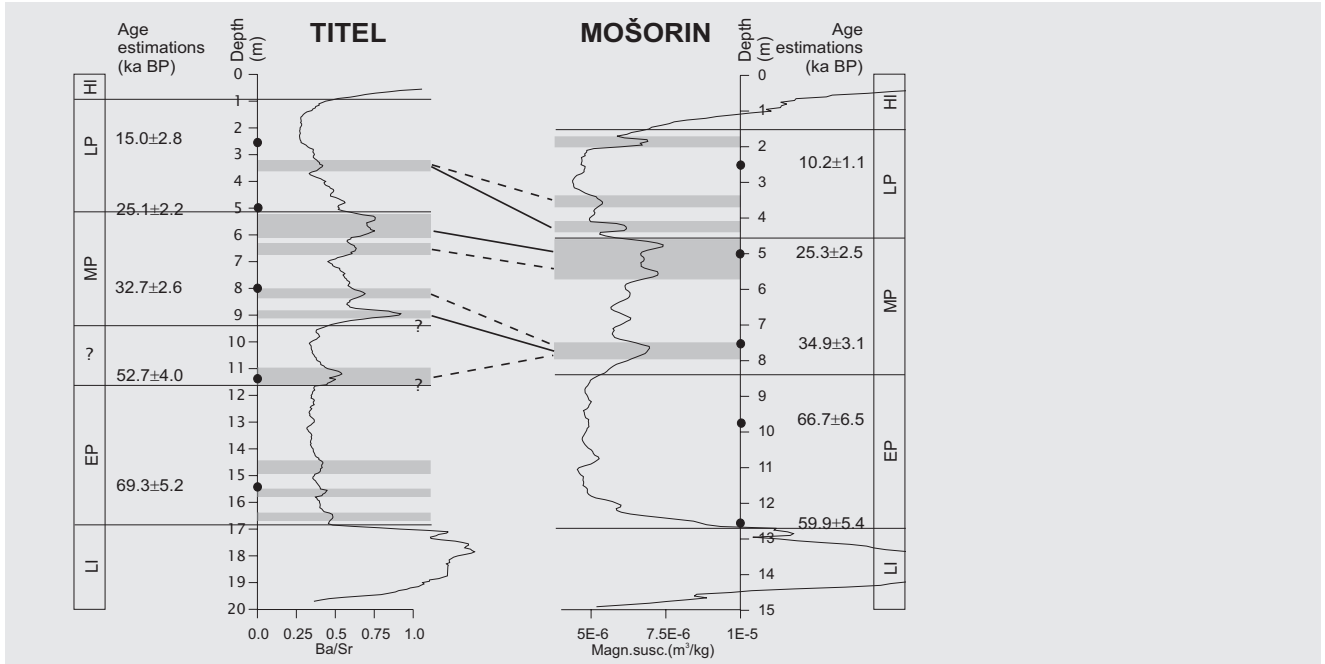
standard deviation with the one at a depth of 9.75 m. The chronology is based on the luminescence dating results and the most obvious boundaries between the Late, Middle and Early Pleniglacial deposits. It has been pointed out that terrestrial and marine stages correlate well (e.g. Woillard and Mook, 1982; Vandenberghe, 1985; Vandenberghe et al., 1997). Therefore the chronology used here is based on the marine isotope stage (MIS) boundaries by Martinson et al. (1987) at 12 ka BP (MIS 2-1), 24 ka BP (MIS 3-2), 59 ka BP (MIS 4-3), 75 ka BP (MIS 5-4). The interpreted chronostratigraphical boundaries in the Vojvodina loess sections are based on expected high values of magnetic susceptibility, fine grain-size fraction and Ba/Sr-ratio in Holocene (MIS 1) and Last Interglacial (MIS 5) deposits, low values in Late (MIS 2) and Early Pleniglacial (MIS 4) deposits and intermediate values in Middle Pleniglacial (MIS 3) deposits (Porter et al., 1992). The individually interpreted boundaries are shown as horizontal lines, when the dating results and the curve shape suggest a unique, most probable position for the considered boundary. Uncertain boundaries or zones are marked with a question mark in the figures.

Chronology of the Titel section, single proxy approach

The magnetic susceptibility record, combined with the IRSL-datings and field descriptions, enable the subdivision in chronostratigraphical units corresponding with the marine isotope stages (fig. 1.3a, left). The most obvious division based on the curves fits all available age information. The high values in the top and bottom of the section (values over $1 \times 10^{-5} \text{ m}^3/\text{kg}$) indicate Holocene and Last Interglacial deposits respectively. They more or less correspond to the soil and paleosol that were found in the field. The low values between 1.3 and 5 m depth and between 10 and 17 m depth indicate Late and Early Pleniglacial deposits respectively. The part between, with values between 6×10^{-6} and $7.5 \times 10^{-6} \text{ m}^3/\text{kg}$, indicates Middle Pleniglacial deposits. This corresponds more or less to the zone containing relatively high density of incipient soils (fig. 1.2a, left). The Middle-Early Pleniglacial boundary is at 10 or at 11.4 m; although the luminescence date at 11.4 m fits in that chronostratigraphical frame only within two standard deviations.

The Ba/Sr record contains five recognizable parts, enabling a straightforward chronostratigraphic framework (fig. 1.2b, left). The transitions between the Holocene-Late Pleniglacial deposits, Late-Middle Pleniglacial deposits and Late Pleniglacial-Last Interglacial deposits can be drawn at 1, 5.2 and 17 m respectively. However, the oscillation between 11 and 12 m may be part of Middle or Early Pleniglacial deposits, as it corresponds to an incipient soil in the field like the others in the Middle Pleniglacial deposits, while the part of the record between 9.5 and 11 m shows a base value comparable to the Early Pleniglacial deposits (fig. 1.2b, left). The IRSL dating at 11.4 m suggests this oscillation is more likely part of the Middle Pleniglacial deposits.

The chronostratigraphic framework of the grain-size record is less straightforward, because there are no low values (that are indicative for Late Pleniglacial deposits) at depths where the dating results and the field stratigraphy indicate Late Pleniglacial deposits (fig. 1.2a, left). As a result, the exact location of the boundary between Holocene



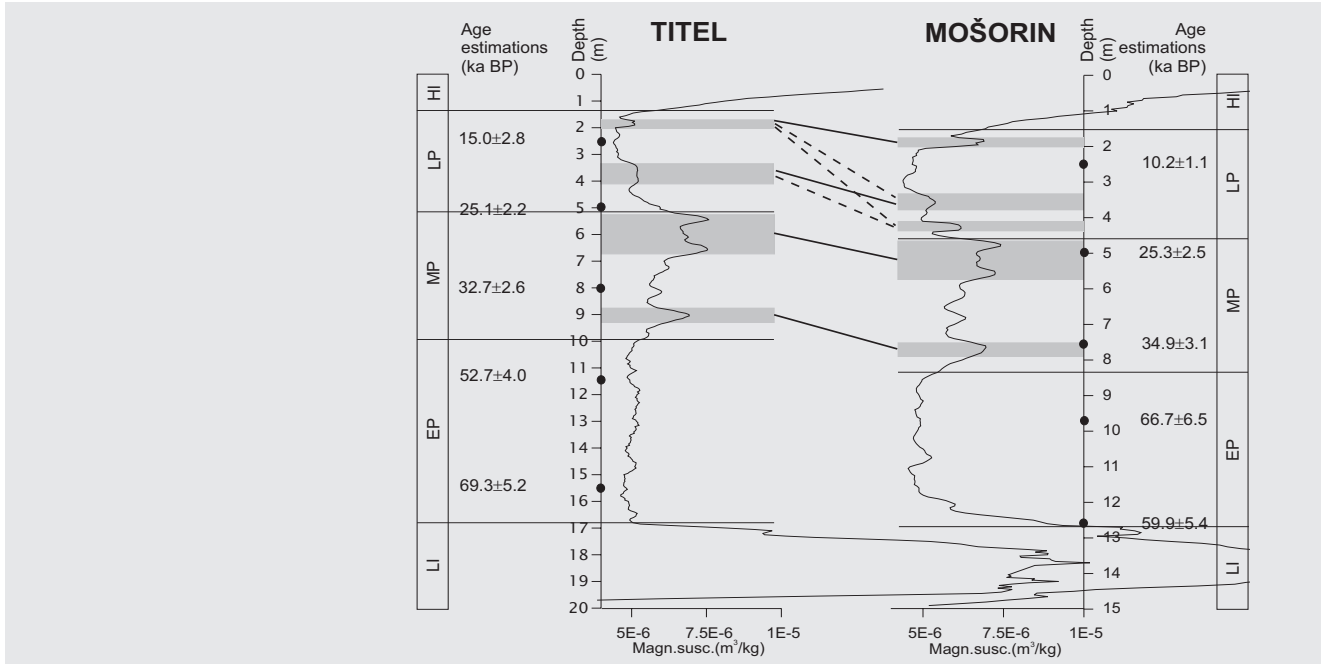
1.2b

and Late Pleniglacial deposits is uncertain. The transition is drawn at 3.4 m depth, based on the thick incipient soil in the top of the section and the dating at 2.5 m, which can be interpreted as Holocene age within two standard deviations. As a result, also the Late-Middle Pleniglacial transition is hard to draw. It was drawn at 5 m depth, based on the thick incipient soil starting at 5 m, the dating at 5 m and the slight increase in value at this depth. The Middle-Early Pleniglacial transition is also hard to define, considering the lowest values at 10.6 m that are lower than those in the Late Pleniglacial deposits, but not yet as low as in the Early Pleniglacial deposits. The Late Pleniglacial-Last Interglacial transition, however, was interpreted more easily at 17 m and corresponds to field observations (fig. 1.2a, left).

Chronology of the Mošorin section, single proxy approach

The magnetic susceptibility record enables the subdivision in chronostratigraphical units corresponding with the marine isotope stages in a more or less obvious way. The boundaries between the Holocene-Late Pleniglacial, Late-Middle and Middle-Early Pleniglacial deposits were drawn at 1.6, 4.7 and 8.3 respectively (fig. 1.2a, right). However, the exact location of the Early Pleniglacial-Last Interglacial boundary is less

1.2b Single-proxy wiggle match between the Ba/Sr-ratio in the Titel section (left) and the magnetic susceptibility record in the Mošorin section (right). HI=Holocene, LP=Late Pleniglacial, MP=Middle Pleniglacial, EP=Early Pleniglacial, LI=Last interglacial.



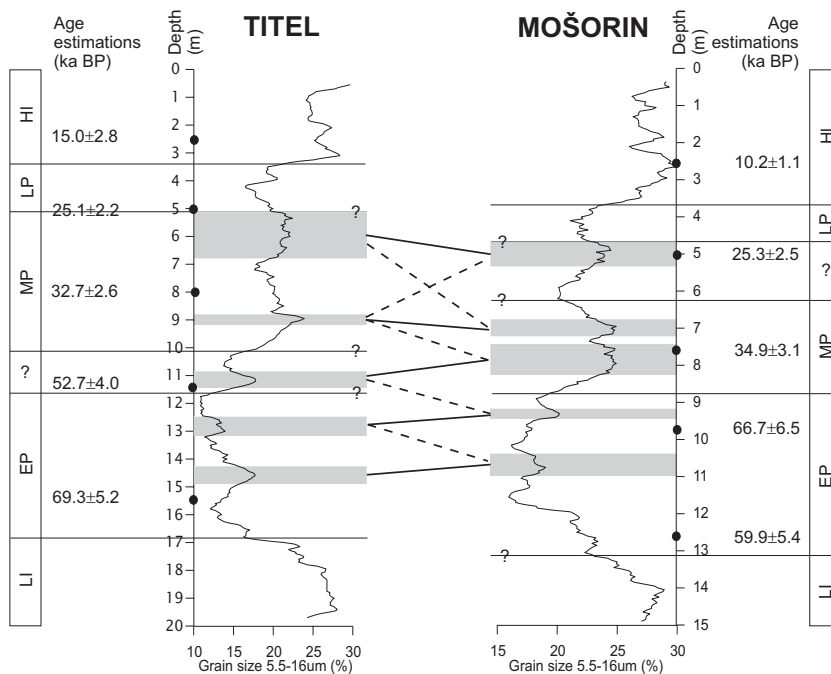
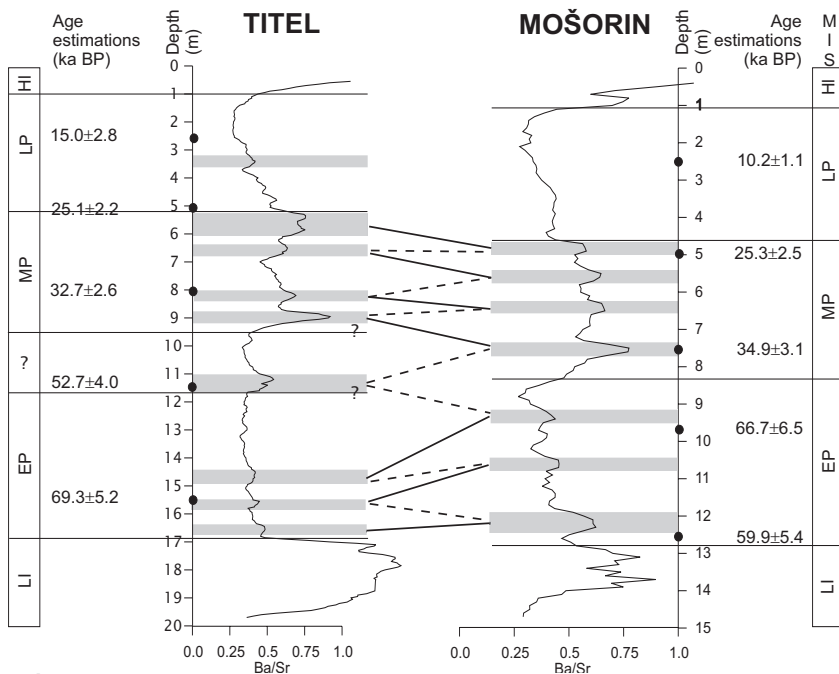
1.3a

certain, as the value at 12.6 m depth suggests a Last Interglacial age, while the dating at this depth cannot fit in this period within two standard deviations. Therefore the transition line was drawn just below the dating, at 12.8 m. It has to be noted that also the dating result at 2.5 m depth can only be interpreted as Late Pleniglacial age using two standard deviations.

The chronology of the Ba/Sr record enables an obvious interpretation (fig. 1.3b, right). The transitions of the Holocene-Late Pleniglacial, Late-Middle and Middle-Early Pleniglacial deposits were drawn at 1, 4.7 and 8.3 m respectively. The choice for the Early Pleniglacial-Last Interglacial transition, however, was controlled by the dating result at 12.6 m, indicating an Early Pleniglacial age.

The grain-size record (fig. 1.3c, right) shows no clear Late Pleniglacial part. The Holocene deposits are about 3.8 m thick, confirmed by a dating at 2.5 m depth. The Late-Middle Pleniglacial transition is therefore unclear and can be drawn at 4.8 m, below some low values at about 4 - 4.5 m, or at 6.2 m, below some low values at about 6 m. The Middle-Early Pleniglacial transition is clearer and could be drawn where values drop below 20% at 8.8 m. The transition Early Pleniglacial-Last Interglacial was controlled by the dating at 12.6 m.

1.3a Single-proxy wiggle match between the magnetic susceptibility records at Titel and Mošorin. HI=Holocene, LP=Late Pleniglacial, MP=Middle Pleniglacial, EP=Early Pleniglacial, LI=Last interglacial.



1.3b Single-proxy wiggle match between the Ba/Sr-ratios at Titel and Mošorin. HI=Holocene, LP=Late Pleniglacial, MP=Middle Pleniglacial, EP=Early Pleniglacial, LI=Last interglacial.

1.3c Single-proxy wiggle match between the 5.5-16 µm grain-size records at Titel and Mošorin. HI=Holocene, LP=Late Pleniglacial, MP=Middle Pleniglacial, EP=Early Pleniglacial, LI=Last interglacial.

Independent wiggle matching between different single proxies of the sections

The matching of the wiggles is marked by lines between grey bars in figs. 1.2-1.5. When more matches are possible within the age frame using two standard deviations, these are also given. When the amount of possibilities is too numerous the most obvious ones are shown only. The best match between two oscillations is shown with a thick line, other possibilities by dashed lines. All single-proxy wiggle matches are based only on the proxy curves and age information.

In the first graph the grain-size record from the Titel section is matched with the magnetic susceptibility record from the Mošorin section (fig. 1.2a, right). The Late Pleniglacial deposits in the Mošorin section contain three oscillations, while the equivalent in the Titel section contains none. In the Middle Pleniglacial deposits the Titel record contains two or three significant wiggles, while Mošorin contains two. The thickest wiggle in the Mošorin section, at about 5 m depth is dated at 25.3 ± 2.5 ka BP. With this information it is most obvious that it matches the thick oscillation at about 6 m depth at Titel. In the lower part of the Middle Pleniglacial deposits it remains arbitrary which oscillation in the Titel section matches the one at 7.8 m in Mošorin, as the one at 9 m in Titel may seem to fit better considering the ages, while the Middle-Early Pleniglacial transition and the datings using two standard deviations, suggest a match with the one at 11.2 m. The magnetic susceptibility record shows no significant oscillations in the Early Pleniglacial deposits, while the Titel record shows two, so that no matches are possible in these parts of the sections.

In fig. 1.2b the grain-size record in the Titel section is replaced by the Ba/Sr record. The Late Pleniglacial deposits in the Titel section show one oscillation, while the Mošorin section shows three in the equivalent part. Considering the available age information, a match of the Titel oscillation with the one at 1.9 m at Mošorin is not likely, while a match with the one at 4.2 m is the most obvious interpretation. The thick oscillation at about 5 m depth in Mošorin can be matched with two oscillations close to each other at 5.7 m or to the whole zone between 5.2 and 6.7 m depth in Titel. The lowermost oscillation in the Middle Pleniglacial deposits in the magnetic susceptibility record can be matched with three oscillations in the Ba/Sr record. Three oscillations in Late Pleniglacial deposits in Titel cannot be matched, as there are no significant oscillations in this age zone in the magnetic susceptibility record in Mošorin.

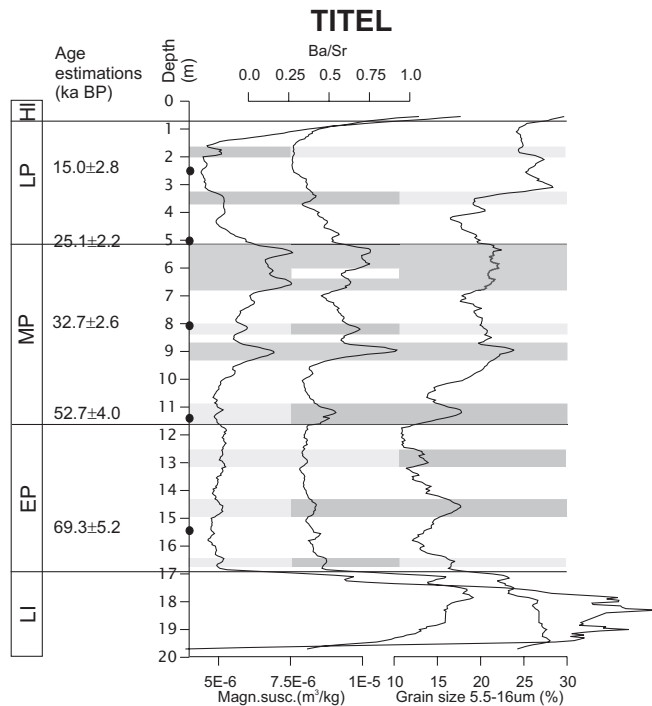
Independent wiggle matching between similar single proxies of the two sections

When matching both magnetic susceptibility records (fig. 1.3a) the Late Pleniglacial in Titel shows two oscillations, while Mošorin shows three. Considering the ages, the upper one at Titel (1.8 m) can be matched to all Late Pleniglacial oscillations in Mošorin, while the shape of the curves suggest that the upper one is the most obvious. The other oscillations in the Late Pleniglacial parts in both sections have a twofold matching possibility. The major parts of the Middle Pleniglacial deposits show one thick and one

thinner oscillation that can be matched uniquely within the available age uncertainty ranges. The Early Pleniglacial shows no oscillations in either records.

The Ba/Sr records (fig. 1.3b) show no matching possibilities in the Late Pleniglacial, but many oscillations in Middle and Early Pleniglacial deposits, making many matches possible. The most obvious matches considering the shapes of the curves and the age information are indicated in fig. 1.3b. However, the oscillation at 11.3 m depth in the Titel section is difficult to match. Within two standard deviations it could be matched to the one at 7.6 m or to the one at 9.3 m depth.

When both grain-size records are compared (fig. 1.3c) no unique match can be made. In total five oscillations have many possibilities of which the most probable are shown. In choosing the most obvious unique oscillation it is problematic to match the oscillations at 11.2 m and 12.8 m in the Titel section: both might be related to the oscillation at 9.2 m in the Mošorin section, but the two lowermost luminescence datings at Mošorin hinder the correlation to the Titel correlation at 11.2 m. The most obvious possibility is to match all five oscillations synchronically.

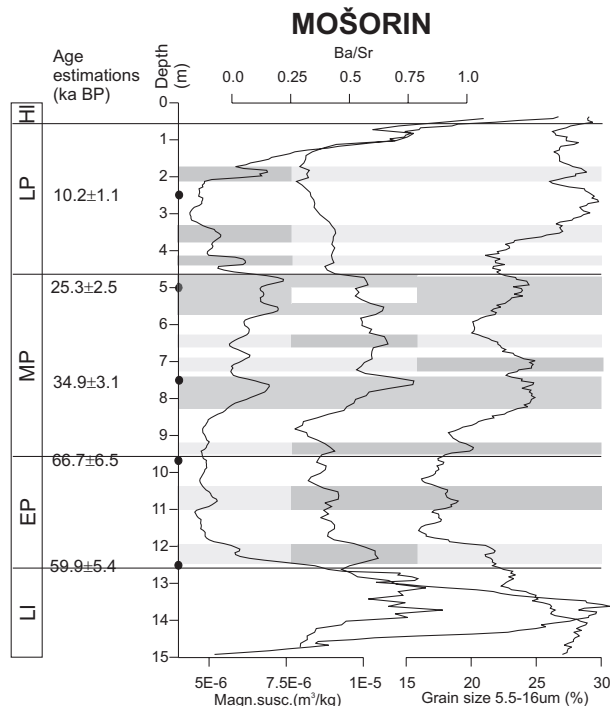


1.4a Multi-proxy wiggle match of all three proxies (grain-size, magnetic susceptibility and Ba/Sr), within the Titel section. HI=Holocene, LP=Late Pleniglacial, MP=Middle Pleniglacial, EP=Early Pleniglacial, LI=Last interglacial. The related oscillations per section are marked with a continuous dark grey bar. Light grey bars are shown where an oscillation is missing in the indicated record, while it is registered in another record at the same depth.

Multi-proxy wiggle matching per section

In contrast with previous inter-profile attempts for correlation between two single proxies we now apply an intra-matching of three proxy records within each of the sections (fig. 1.4a-b). The chronological interpretation is more obvious than using the single proxy approach, as there is more information combined now.

The Titel section (fig. 1.4a) shows three matches of oscillations that are observed in each of the three proxy records (at 5-7 m (double peak) and 9 m) and three peaks that appear in two of the three records (at 3.5, 11.5 and 14.5 m). In the Mošorin section (fig. 2.4b) three matches between three proxy records may be made (at 4.5-5.5 m (double peak), and 7.5 m) and two peaks link two of the three records (9.5 m and 10.5 m). Apparently, the correlations at both individual sites show an obvious improvement in comparison with the previous attempts as the uncertainties of inter-profile correlations are absent. Indeed, this analysis is only an identification of wiggles at a single spot, not a correlation. But, when comparing both sections separately we observe an unequal number of peaks, while some previous correlations between both sections now disappear



1.4b Multi-proxy wiggle match of all three proxies (grain-size, magnetic susceptibility and Ba/Sr) within the Mošorin section. HI=Holocene, LP=Late Pleniglacial, MP=Middle Pleniglacial, EP=Early Pleniglacial, LI=Last interglacial. The related oscillations per section are marked with a continuous dark grey bar. Light grey bars are shown where an oscillation is missing in the indicated record, while it is registered in another record at the same depth.

in one or both of the sections. For instance, in the Titel section (fig. 1.4a) the 0.8 m thick oscillation in the magnetic susceptibility record at 3.3 m (fig. 1.3a) only partly correlates with low values in the Ba/Sr record. In the same section the small oscillation in the Ba/Sr-record at 15.8 m correlates with a negative peak in the grain-size record and thus was eliminated, while in fig. 1.3b it was attempted to correlate it with the record at Mošorin.

Multi-proxy wiggle matching using the proxy-data of both sections

Fig. 1.5 shows all available information combined in one graph, including the relation between the oscillations in the different proxy records of the two sections. The Titel section shows now ten oscillations, while the Mošorin section contains eleven (double peaks are counted for two). Eight oscillations can be matched reliably fitting most of the luminescence datings and are based on the properties of three proxy records in the two sections. The weak oscillation at 3.5 m depth in Titel is probably equivalent to the one at 3.5 m depth in Mošorin, considering the positions in the magnetic susceptibility curves and the rising grain-size curves, while no signal is obvious from the Ba/Sr curve. In addition, the Ba/Sr records suggest that the c. 1.5 m thick oscillations in the magnetic susceptibility and grain-size records, at about 6 m and 5 m depth respectively, consist of two oscillations that are statistically not separated.

1.4 Discussion

The combination of information in the multi-proxy wiggle matching results finally in eight unique matches. Two oscillations in Titel and three in Mošorin cannot be correlated at all: they are probably the result of different sedimentation patterns that maybe are due to, for instance, local topography, vegetation or wind turbulence.

The differing matching results of proxy oscillations prove that not all types of data are reliable indicators for the reconstruction of paleoclimatic changes. Different proxies register varying numbers of significant oscillations. This makes clear that there is a high chance that, when two different proxies are compared, many oscillations are not present in the opposite section. This may be due to different registration ability or to different sensitivity for climatic influences.

The combination of oscillations, as registered in three individual proxies, contains more information on potential oscillations than it is the case in the three proxies separately, while also more oscillations are identified than in any individual record. Three proxies register obviously more variation for improved identification of significant wiggles and for more reliable and safe matching than one or two proxies. Of course, more proxies will probably improve the reliability even more. The total improvement of the multi-proxy wiggle matching over the single-proxy matching examples is shown in table 1.2.

The double peak in magnetic susceptibility at the top of the Middle Pleniglacial deposits is a good marker for correlation. No confusion is possible, because this double-peak contrasts well with surrounding (lower) values of magnetic susceptibility. Similar

Titel proxy:		GS	Ba/Sr	MS	Ba/Sr	GS	All	-	MULTI-
Mošorin proxy:		MS	MS	MS	Ba/Sr	GS	-	All	PROXY
LP	Wiggles:								
	<i>Titel</i>	0	1	2	1	0	2	-	2
	<i>Mošorin</i>	3	3	3	0	0	-	3	3
	Matches	0	1	2	0	0	1	0	1
	Unique matches	0	0	0	0	0	1	0	1
MP	Wiggles:								
	<i>Titel</i>	2-3	4-5	2-3	4-5	2-3	5	-	5
	<i>Mošorin</i>	2	2	2-4	4	3	-	6	6
	Matches	2	2	2-3	4-5	2-3	4	4	5
	Unique matches	1	0	2	0	0	4	4	5
EP	Wiggles:								
	<i>Titel</i>	2-3	3	0	3	3	3	-	3
	<i>Mošorin</i>	0	0	0	3	2	-	2	2
	Matches	0	0	0	3	3	1	1	2
	Unique matches	0	0	0	0	0	1	1	2
TOTAL	Wiggles:								
	<i>Titel</i>	5	9	4	9	5	10	-	10
	<i>Mošorin</i>	5	5	5	7	5	-	11	11
	Matches	2	3	4	7-8	5	6	5	8
	Unique matches	1	0	2	0	0	6	5	8

T 1.2

peaks are present in the Ba/Sr-ratio but are surrounded by other peaks that may lead to correlation problems. Such problems are, however, avoided by correlations of multiple proxy records instead of single proxy records as appears from the present study.

It is also clear that in cases where unequivocal wiggle matching is problematic, as in the present study, specific correlations may be confirmed by absolute datings. However, this is not possible in all circumstances, and for those cases the described method of multi-proxy matching is even more necessary. When no datings were used at all, the amount of matching possibilities will increase again. For instance, when matching without datings it might have been likely to correlate the oscillation at 11.3 m at Titel with the oscillation at 7.8 m in Mošorin. With the available datings we have, such a correlation is unlikely. A certain number of datings are therefore necessary to confirm the chronological framework. On the other hand, increasing the amount of datings would (probably) not result in more or different matching possibilities in this short-distance exercise. However, when correlations are extended over larger distances, the proxy curves probably show less similarity. In that case, a higher dating resolution and/or more proxies would be necessary to achieve the same result.

T 1.2 The amounts of wiggles per section, matches and unique matches per marine isotope stage in the Late (LP), Middle (MP) and Early Pleniglacial (EP). Results are shown for the five examples of single-proxy wiggle matching presented in figs. 1.2a-b and 1.3a-c and for the multi-proxy matching in figs. 1.4a-b and 1.5. MS = magnetic susceptibility, GS = grain-size 5.5-16 μm .

1.5 Conclusions

When evaluating the reliability of wiggle matching it is concluded that most single-proxy wiggle matches of terrestrial records should be considered carefully. Comparing proxies that express different environmental conditions or processes may cause doubtful matching. Matching between the same proxies or related proxies might have a better result. The presented results show that a multi-proxy approach, applied on two nearby sections, can strongly improve the reliability of wiggle matching because it separates local from regional or global signals. It may thus be useful to do a short-distance multi-proxy matching before a tele-connection is done.



PEDO-CHEMICAL CLIMATE PROXIES IN LATE PLEISTOCENE SERBIAN- UKRAINIAN LOESS SEQUENCES

With Kay Beets, Slobodan Marković, Natalia Petrovna Gerasimenko, Zhanna Nikolajevna Matviishina and Manfred Frechen. Published in Quaternary International, doi: 10.1016/j.quaint.2008.09.003

ABSTRACT

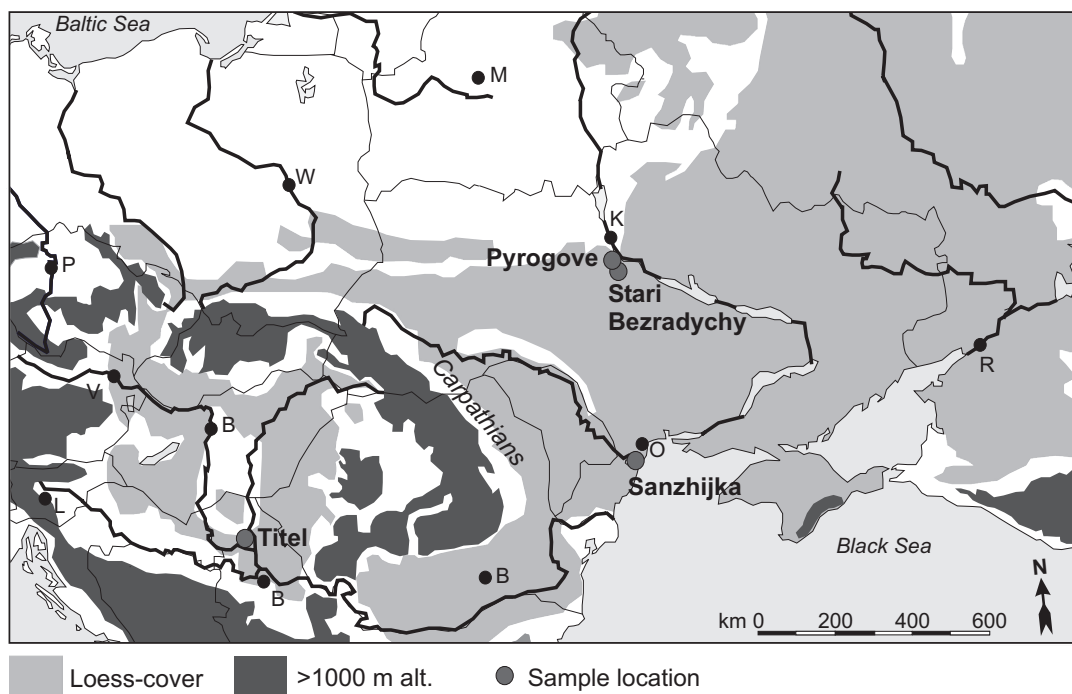
The last glacial-interglacial loess-paleosol sequences of Serbia and Ukraine provide a good climate reconstruction potential for this part of Europe. We studied four loess sections distributed over an area with present-day moist to semi-arid climates. In this chapter we show that in addition to traditional paleoclimate proxies, such as grain-size distribution as proxy for wind-strength and source aridity, and magnetic susceptibility as proxy for precipitation (and temperature), pedo-chemical elemental ratios, obtained by selective sediment leaching procedures, function as sensitive recorders of variations in weathering intensity due to changes in precipitation and temperature. Especially, the earth alkaline element ratios of Ba/Sr and Sr/Ca are subject to strong variations as a result of carbonate dissolution/precipitation and variable cation exchange capacity on clay minerals along the elemental sequence of Ca-Sr-Ba. As shown by the close similarity to the magnetic susceptibility records in the different loess sections, these ratios reflect the effects of weathering intensity as a result of precipitation changes. The fact that Ba/Sr unequivocally shows higher values in both soils and paleosols in the four studied sections over the present-day climate gradient, singles this elemental ratio out as an interesting paleoclimate proxy.

2 Pedo-chemical climate proxies in Late Pleistocene Serbian-Ukrainian loess sequences

2.1 Introduction

Detailed climate information from terrestrial records of last glacial age can be a major key in investigating the geographical extent and significance of millennial scale climate oscillations. Loess deposits are locally relatively thick in Central and Eastern Europe, containing ten to twenty meters of last glacial deposits (e.g. Marković et al., 2008; Novothny et al., in press; Rousseau et al., 2001). This implies that the sedimentation rates were high enough for the registration of millennial scale paleoclimatic variations. We investigated four sections in eastern and central Europe (fig. 2.1). Studies on the paleoclimatic records of the Titel section in Serbia and on the Pyrogove section in northern Ukraine are published in this paper for the first time, while sections in the region have been studied for their paleoclimatic significance (e.g. Marković et al., 2004; 2005; 2006; 2007; 2008; Rousseau et al., 2001; Gerasimenko, 2006). The section Stari Bezdychy in northern Ukraine was studied for its pollen content before by Gerasimenko (2001; 2006). Compiled pollen records of many sites in the area resulted in a detailed temporal and vegetational succession interpretation of the complex loess-paleosol record at this location. The stratigraphy of the fourth section, Sanzhijka in southern Ukraine, was described by Matviishina et al. (1990). In this paper we present the ratios of chemically leached (or 'free') elements that were tested on their potential application as proxies for interstadial climate conditions.

The grain-size distribution in loess research can be a good climate proxy for changes in wind intensity (Vandenberghe and Nugteren, 2001; Sun et al., 2002; Vandenberghe et al., 1985; 1997; 1998). The grain-size distribution serves as an allogenuous proxy, as its compositional change is a direct result of climate change. Temperature and precipitation affect post-depositional processes that change some of the compositional properties of the sediment, and therefore proxies that indicate these in-situ processes are considered as authigenous. However, proxies for temperature and precipitation intensity are few and still insufficiently known. Magnetic susceptibility (MS) is often found enhanced in paleosols relative to loess and interpreted as a proxy for paleoclimatic variations, and especially as a proxy for precipitation amounts (Heller and Evans, 1995; Heller and Liu, 1982; 1984; 1986; Kukla, et al., 1988; Kukla and An, 1989; Maher et al., 1994; 2002; Maher and Thompson, 1995; Nawrocki et al., 1999; Porter et al., 2001). In addition, carbon isotopes ($\delta^{13}\text{C}$) in organic matter and soil carbonates have been used as qualitative proxies for paleo-precipitation and/or paleo-vegetation coverage (Hatté et al., 1999; Gu et al., 1991; Rousseau et al., 2002). However, the $\delta^{13}\text{C}$ proxy on organic matter is not always applicable, due to post-depositional processes affecting the proxy signal, as discussed in Chapter 3.



2.1

Ratios of the bulk chemical element composition have been used successfully for the determination of the origin of loess particles (Gallet et al., 1996; 1998; Jahn et al., 2001; Buggle et al., 2008; Újvári et al., 2008). Gallet et al. (1996) showed that a ratio of Ba and Sr, measured by bulk chemistry (XRF) analyses on loess from the Luochuan section on the Chinese Loess Plateau, shows high similarity to a MS record. The Ba/Sr ratio results were therefore explained as controlled by pedo-chemical processes, related to climate variability. The Sr content is systematically depleted in carbonates, a process that can be interpreted as a result of pedogenesis. Ba, however, does not seem to enrich or deplete and shows stable values in paleosols relative to loess parts. The ratio of Ba and Sr can therefore be considered as chemical indicator for pedogenesis as a result of paleoclimatic changes. The Ba/Sr-ratio is also related to leaching intensity (Retallack, 1994) and applied to find origins of stream water (Land et al., 2000).

In this chapter we extrapolate and apply this principle. We assume that a ratio of an element that does not show depletion during weathering relative to a preferentially depleted element, may be used as an indicator for paleoclimatic changes. These changes are mainly controlled by weathering susceptibility of Ca-Mg-Sr-Ba, and weathering intensity controlled by precipitation. Four ratios, Ba/Sr, Mg/Ca, Mg/Sr and Sr/Ca, following this principle and constructed from these elements, were tested as potential paleoclimatic proxies.

2.1 Locations of the sections. P = Prague, W = Warszawa, M = Minsk, K = Kiev, R = Rostov, V = Vienna, L = Ljubljana, B = Budapest / Belgrade / Bucharest, O = Odessa.

The elemental ratios were measured in loess/paleosol samples from four locations in Serbia (Vojvodina) and Ukraine. These four locations are distributed over an area with three different present-day climates. The sampled sediments were deposited during the Late Pleistocene. Visible soils and other pedological indications in the field, together with luminescence and ^{14}C AMS dating are used to construct the chronostratigraphy of the loess records, and to subdivide the deposits into last Interglacial, the Lower, Middle and Upper Pleniglacial and the Holocene. The elemental ratio records are compared with the visible soils and the clay fraction, as these indicate interstadial or interglacial conditions. The MS record is also used for comparison, where MS is assumed to represent also in-situ formation of magnetisable minerals as a function of precipitation (e.g. Maher et al., 2002).

2.2 Site description and lithostratigraphy

The studied transect runs from the south-eastern part of the Carpathian (Pannonian) Basin to the north-eastern Black Sea coast and ends in central Ukraine (fig. 2.1). These locations represent different present-day climatic conditions and cover a range of different, mostly steppic environments, following temperature and precipitation gradients. Stratigraphic interpretations illustrate the diversity of Late-Pleistocene climates and environments in northern Serbia and Ukraine (Matviishina et al., 1990; Gerasimenko, 2001; Markovic et al, 2008; figs. 2.3a-d).

The Last Interglacial (MIS 5) and the Holocene soils are encoded as S1 and S0 respectively, while Lower, Middle and Upper Pleniglacial deposits are indicated as L1-3, L1-2 and L1-1 respectively (fig. 2.3a-d). Subdivisions in other (incipient) soils and loess parts are encoded after their local stratigraphy (Matviishina et al., 1990; Gerasimenko, 2001; Markovic et al., 2008; figs 2.3a-d).

Serbia (Vojvodina)

In the Vojvodina region, Northern Serbia, typical loess is found on six discontinuous plateau uplands between the alluvial plains of the Danube, Tisa, Sava and Tamiš rivers (Marković et al., 2008). The Titel loess plateau is situated in the central part of the Vojvodina region, near the confluence of the rivers Danube and Tisa. It is a loess island with remarkable cliffs created by fluvial erosion. The present-day mean annual temperature in the investigated area is 11°C with a maximal average monthly temperature in July of 21°C and a minimal average monthly temperature in January of -1°C . The mean annual precipitation of 550 mm is evenly distributed over the seasons with a peak of ~ 95 mm in June.

For this study, a site was chosen at the south-eastern edge of the Titel loess plateau, where the sedimentation rate is higher than in other parts of this loess plateau. The Titel section is located ($45^{\circ}14'\text{N}$, $20^{\circ}19'\text{E}$) in an old brickyard quarry about 1 km north of the village of Titel. The total thickness of the investigated profile is about 20 m (for a description of the section see fig. 2.3a).

Ukraine

About 70% of the territory of Ukraine consists (morphologically) of flat land, almost completely covered with loess deposits. The sections Stari Bezradychy and Pyrogove are located in central Ukraine near Kiev. The Sanzhijka site is situated in south-western Ukraine, near Odessa. The present annual precipitation ranges from about 500 mm in the central to about 300 mm in the south-western Ukrainian regions. The average present-day July and January air temperatures vary from 19°C to 22°C and from –6°C to –2°C in central and south-eastern Ukraine, respectively.

The Stari Bezradychy section is located 20 km south of Kiev (50°11'N, 30°33'E). The stratigraphic interpretation of the section at Stari Bezradychy is partly based on the description by Gerasimenko (2001). The total thickness of the investigated loess-paleosol sequence exposed in a gully is about 8.5 m (for description see fig. 2.3b). The section at Pyrogove is located in a local brickyard quarry and has a thickness of 12.80 m (49°13'N, 28°28'E) (for description see fig. 2.3c). The Sanzhijka section is located 30 km south of Odessa (46°14'N, 30°37'E). The interpretation of the exposure at Sanzhijka is partly based on the description by Matviishina et al. (1990) (for description see fig. 2.3d).

2.3 Sediment-geochemical approach and methods

Sampling

To obtain a high-resolution record, samples of about 40 grams were taken at 5-cm intervals at the Titel, Pyrogove and Sanzhijka sections, and at the lower part of the Stari Bezradychy site. The uppermost 6.5 m of the Stari Bezradychy section was sampled at 3.3 cm resolution. The MS and grain-size determination methods are described in §2.3 and §2.4. Samples for geochemical analyses were obtained each 5 cm at the Titel site and 10 to 20 cm at the Ukrainian sections.

Geochemical elements analyses

We propose that variations in geochemical composition in loess-paleosol sequences caused by pedological processes can be easily illustrated by specific, targeted, leaching chemistry, instead of using the bulk geochemical composition. All samples were studied for their Ba, Sr, Mg and Ca content, using a mild leaching-procedure targeting more specifically the carbonate phase. To verify our assumption that the leachate fraction proportionally represents the in-situ formed geochemical component, we made a comparison between the 1N HNO₃-leachate fraction and the bulk composition of a selection of 30 samples from loess and paleosol units at Titel. The samples were selected as representing a range with a large variability in MS and grain-size measurements. The elements Ca, Mg and Sr were measured for bulk and leaching chemistry analyses. Ba could only be measured by the leaching method, for technical reasons in the XRF procedure. A high similarity between the records of the bulk and leachate analyses would indicate that the variations of the element values are mainly due to pedological

processes. In that case, these elements measured by leaching may be used as potential indicators for paleoclimatic variations.

Bulk sediment analysis (XRF)

Samples are dried overnight at 120°C in an oven to remove absorbed water. The LOI (Loss on ignition) is determined by heating the sample to 900°C. LOI replicates indicate a precision of better than 2%. Fused beads are made by mixing 4 grams of LiCO₃ flux with 1 g of sample. The fused beads are created with a Panalytical Perl'X 3, using a custom heating program with a maximum temperature of 900°C. The 28mm-beads are measured on a Panalytical MagicX'Pro, using a Rh-tube at 40 kV and 90 mA for all major elements. Matrix correction is done by fundamental parameter model in the software. Calibration lines are generated from 30 USGD, NIST, BMR and JGS standards.

Trace elements are measured on pressed pellets, which are composed of 4.5 grams of dried (120°C) sample powder and 0.45 g of wax, pressed at 20 tons/cm². All trace-elements are run with a Rh tube (60 kV, 60 mA) on a Panalytical MagicX'Pro. The matrix corrections are done by both fundamental parameter analyses and Rh Compton. Calibration lines are generated for all major elements and trace elements from 30 international rock standards from the USGS, NIST, BMR and JGS.

Leaching procedure

Leaching in 1N HNO₃ will cause CaCO₃ to dissolve, releasing Ca, CO₂ and the Mg, Sr and Ba (and more) which belong in the CaCO₃ lattice. Any salts present, such as CaSO₄ and NaCl will also dissolve. Moreover, exchangeable, adsorbed cations will be released from sites on clay minerals or from goethite, brucite, gibbsite (FeOOH (Fe(OH)₃), Mg(OH)₃, Al(OH)₃), which are part of normal weathering sequences during soil formation.

100 mg of dry sample was taken up in 5 ml 1N HNO₃ and left for ~20 hours. After centrifuging 1 ml of the resulting solution the sample was pipetted off and the solution was diluted to a total of 10 ml. The elemental composition (Ca, Mg, Sr and Ba) of the leachable sediment fraction was determined using a Liberty II Varian ICP-AES. The in-run precision for all the measured elements is better than 1.5%. The reproducibility of duplicate measurements (n = 9) is 6.7%.

Element Ratio composition

The selection of tested element ratios was based on several principles. 1. Precipitation stimulates weathering and pedological processes. Temperature also stimulates weathering, but in a dry and warm environment weathering plays a much smaller role (e.g. Van der Hoven and Quade, 2002). 2. Present allogenous carbonates dissolve in percolating rainwater and reprecipitate under influence of acids excreted by vegetation (Merian, 1991). 3. Weathering results in a changing mineral composition and thus in a changing cation exchange capacity (CEC) (McBride, 1994). 4. Weathering also results in the production of 'free' elements, dependent on availability and weathering susceptibility of these elements. 5. Free elements are transported through the soil with percolating

rainwater, dependant on their solubility ($Ba < Sr < Mg < Ca$) and ability to retain to clay (Perel'man, 1977). The elements reprecipitate in carbonates or remain dissolved and wash out. 6. Elements may remain in the soil due to their role in ecology, expressed by their biogenic coefficient. All measured elements are taken up by plants, while Ca is much more important with a biogenic coefficient of 0.17, versus 0.02, 0.06 and 0.04 for Mg, Sr and Ba respectively (Perel'man, 1977).

Ba/Sr

The element Ba becomes available for pedologic processes by weathering of mainly K-feldspars (e.g. Perel'man, 1977) and is stronger retained to clay than Sr (Nesbitt et al, 1980). Sr is also produced from K-feldspar and from Ca-feldspar (Negrèl, 2006), but it has a larger susceptibility to weathering than Ba (Land et al., 2000). In contrast to Ba, after release Sr may form complex carbonate salts together with mainly Ca during reprecipitation (Brantley et al., 1998). However, both Ba and Sr form no important minerals on their own (Stueber, 1978; Puchelt, 1972) and have a comparably little importance for vegetation (biogenic coefficients 0.04 and 0.06 (Perel'man, 1977)). The Ba/Sr ratio is therefore controlled by the weathering intensity and leaching intensity.

Mg/Ca

Mg and Ca are mainly present in carbonate salts, primary present in loess deposits. Mg is also produced by the weathering of pyroxenes, amphiboles and biotite. Ca is mainly produced by weathering of Ca-feldspars. Mg retains much stronger to clay than Ca, due to the large difference in atomic diameter (Perel'man, 1977). Therefore, more Ca will reprecipitate as carbonate salts. A ratio of Mg/Ca would increase in paleosols, due to increased production of Mg compared to Ca and a stronger leaching of Ca relative to Mg.

Mg/Sr

Sr and Mg are both present in primary carbonates, while the Mg-content can be enriched from pyroxene, amphibole, biotite weathering and Sr mainly from K-feldspar and Ca-feldspar weathering. Both elements can form complex carbonate precipitates with Ca. However, Mg retains stronger to clay minerals than Sr. Therefore, increasing leaching intensity would increase the Mg/Sr ratio.

Sr/Ca

As stated before, Ca and Sr are mainly present in primary carbonates. Due to its size, Ca attaches less strongly to clay than Sr. More Ca will reprecipitate in secondary carbonates relative to Sr, enhanced by vegetation. A ratio of Sr/Ca will therefore increase with increased weathering and leaching.

Magnetic susceptibility

The MS signal originates from sub-micron (0.4-0.001 μm) magnetic grains, of which the major part is formed after deposition by percolating rainwater (Maher, 1998). The most dominant minerals causing the susceptibility signal are magnetite (Fe_3O_4) and maghemite (Fe_2O_3). They have respectively a 1000 and 500 times higher susceptibility than other iron-oxide minerals like goethite, hematite or lepidocrocite (Schwertmann and Taylor, 1977).

The low-field or initial susceptibility (χ , expressed per unit mass or m^3/kg) of dry samples was measured with a KLY-2 type susceptibility bridge (AGICO, Brno, Czech Republic). The measuring frequency was 920 Hz and the r.m.s. field amplitude 300 A/m (0.375 mT). The sensitivity of the instrument is 4×10^{-8} SI (for a 10 cm^3 sample), while typical values for samples in the present study are at least one to two orders of magnitude higher (see also Dekkers, 1997). All values are averages of triple measurements.

Grain-size analyses

Samples were pre-treated following Konert and Vandenberghe (1997). First, the loess was boiled with 10 ml 30% H_2O_2 , resulting in the oxidation of organic matter. Carbonates were dissolved by boiling with 10% HCl, and 0.05 N dispersant ($(\text{NaPO}_3)_6$) was added to the solution. The grain-size was measured using a FRITSCH A22 laser grain-size analyser. In this paper the $<5.5 \mu\text{m}$ grain-size interval is used. This fraction is partly produced after deposition of the loess and thus may be considered as being influenced by secondary processes. This proxy indicates the primary clay and clay fraction content, combined with additional clay illuvation, production of clay by chemical weathering and production of clay fraction by physical weathering.

2.4 Chronology of the four sections

Infrared stimulated luminescence (IRSL) measurements were carried out on six samples at Titel, three at Stary Bezradychy, and two at Pyrogove sites. Polymineral fine-grained material ($4\text{-}11\mu\text{m}$) was prepared for the determination of the equivalent dose, as described by Frechen et al. (1996). The samples were beta irradiated by a 90Sr beta source in at least seven dose steps with five discs each and a maximum radiation dose of 750 Gray (Gy). All discs were stored at room temperature for at least four to six weeks after irradiation. The irradiated samples were preheated for 1 minute at 230°C before infrared stimulation. Equivalent dose values were determined using IRSL. A Schott BG39/Corning 7-59 filter combination was placed between a photomultiplier and the aliquots for IRSL measurements. A 10s IR exposure was applied to obtain their IRSL signals. The equivalent dose was obtained by integrating the 1-10s region of the IRSL decay curves using an exponential fit. Alpha efficiency was estimated to a mean value of 0.08 ± 0.02 for all samples (cp. Lang et al., 2003). Dose rates for all samples were

Field code	Section	Depth (m)	Equivalent dose (Gy)	Equivalent dose, 1 σ	Dose rate (Gy/ka)	Dose rate, 1 σ	Age (ka)	Age, 1 σ
Sb2.30	Titel	2.30	271.3	46.9	3.16	0.24	15.0	2.8
Sb5.00	Titel	5.00	734.4	26.8	3.89	0.29	25.1	2.2
Sb8.00	Titel	8.00	984.0	11.6	4.00	0.29	32.7	2.6
Sb11.35	Titel	11.35	1066.0	30.3	3.54	0.26	52.7	4.0
Sb15.40	Titel	15.40	1545.2	23.8	3.90	0.29	69.3	5.2
Ub-2	Stari Bezr.	5.17	677.2	33.1	3.21	0.25	36.9	3.4
Ub-3	Stari Bezr.	6.07	988.7	52.7	3.64	0.27	47.5	4.4
Ub-1	Stari Bezr.	6.50	811.4	65.6	3.00	0.24	47.3	5.3
Ug-1	Pyrogove	0.55	159.0	40.4	3.06	0.22	9.1	2.4
Ug-2	Pyrogove	6.10	413.4	25.0	3.14	0.22	17.5	1.6

T 2.1

Depth (m)	¹⁴ C-lab code	¹⁴ C uncal. (y)	¹⁴ C cal.+corr. (y BP)
2.30	GrA-21628	20,790 \pm 170	24,950 \pm 600
5.00	GrA-21616	26,970 \pm 330	31,520 \pm 680
8.00	GrA-21612	33,850 \pm 730	40,750 \pm 2250
11.35	-	-	-
15.40	-	-	-

T 2.2

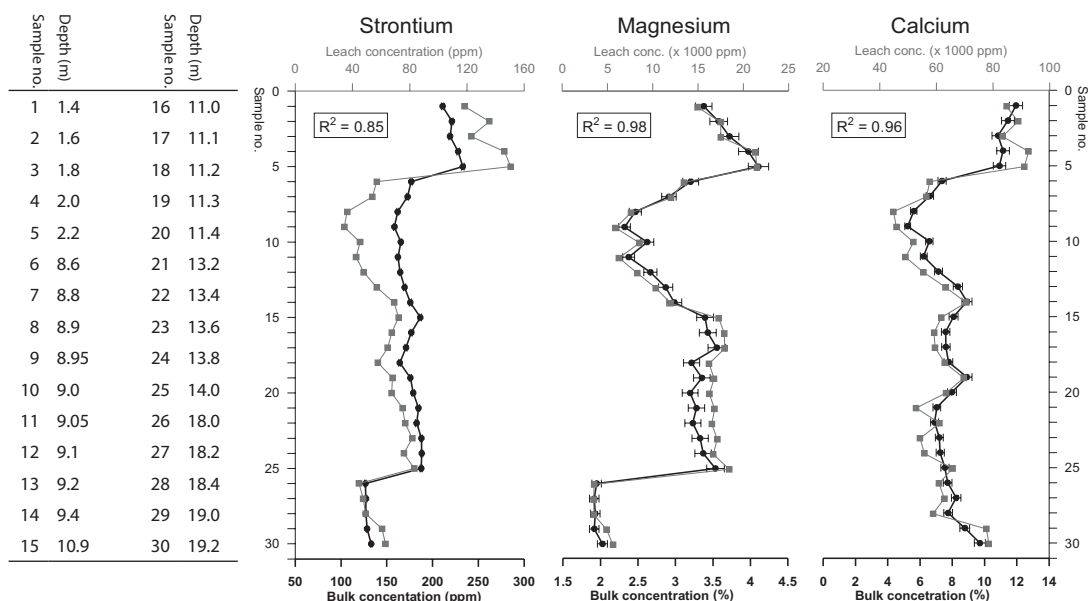
calculated from potassium (K), uranium (U) and thorium (Th) contents, as measured by gamma spectrometry in the laboratory, assuming radioactive equilibrium for the decay chains. The amount of U is probably slightly underestimated, because a small part of the zircon in the loess samples was not destructed during the chemical preparation, causing an underestimation of the dose-rate and so resulting in a slight overestimation of the deposition age. Cosmic dose rate was corrected for the altitude and sediment thickness, as described by Aitken (1985) and Prescott and Hutton (1995).

The natural moisture content of the sediment was estimated to 20 \pm 5% for all samples (weight water content). This estimation is based on the actual moisture content, much dryer than 20%, and an assumed moisture content during the last glacial, that was probably 40-80% (Frechen et al., 2001a). A moisture content increase of 25% to 35% in a sand sample in Belgium resulted in -10% dose rate alteration (Frechen et al., 2001b). This suggests that an eventual underestimation of the moisture sample will result in slight age underestimation (Frechen, 2001a).

AMS-¹⁴C dating was done on carbonate shells of mixed assemblages of land snail from 2.30, 5.00 and 8.00 m depth below surface at Titel. The data are calibrated

T 2.1 Results of IRSL dating (on 4-11 μ m) from samples from the sections Titel, Stari Bezradychy and Pyrogove.

T 2.2 Uncalibrated and calibrated and corrected AMS ¹⁴C age estimations from the Titel section. For the ¹⁴C calibration data from Lake Suigetsu in Japan (Kitagawa and Van der Plicht, 2000) were used.



2.2

according to Kitagawa and Van der Plicht (2000). When radiocarbon dating land snails, it has to be taken into account that the uptake of carbonate by the snails may be an open system introducing the uptake of dead carbon (e.g. Goodfriend et al., 1999). A land snail switches to direct carbonate take-up from the soil when there is only few vegetation available. The AMS dates are therefore probably too old, as it is unknown which percentage of the measured carbonate has a source of direct uptake. The species found in the Titel area are *Clausilia*, *Chondrula*, *Granaria*, *Helicopsis*, *Ena*, *Pupilla*, *Succinea*, *Trichia* and *Vallonia*. (Markovic et al., 2008). For example, Pigati et al. (2004) calculated the dead carbon reservoir effect for *Pupilla* and *Vallonia* for a site in Arizona, USA. Their results show that *Vallonia* species show a higher deviation than the *Pupilla*, with a maximum of ~6% for samples of 25,000 ^{14}C years. Although most species occurring in Serbia were not measured by Pigati et al. (2004) this study shows there can be a variable dead carbon contribution depending on the species of land snail.

The results of the IRSL and ^{14}C AMS analyses are displayed in tables 2.1 and 2.2 respectively. The IRSL age estimates in the Titel section, ranging from 69.3 ± 5.2 ka to 15.0 ± 2.8 ka, increase with depth and confirm a deposition during the Last Glacial. The

2.2 Correlations between results of leachate chemistry and bulk-chemistry of the elements Sr (a), Mg (b) and Ca (c) on 30 samples from the Titel section. The table on the left shows the depths of the samples used for bulk chemistry analysis.. The elements Sr, Mg and Ca show an acceptable correlation, which indicates that the variation in the leach-chemistry results of these elements is not caused by variations in lithology. The bulk concentration of Ba was not measured.

Figure 1 displays the lithological column and geochemical profiles of the V-S0 core. The lithological column on the left shows depth from 0 to 20 cm, with various sediment types labeled (V-S0a, V-L1-1S1, V-L1-1L1, V-L1-1S2, V-L1-1L2, V-L1-2S1, V-L1-2S2, V-L1-2S3, V-L1-2S4, V-L1-2S5, V-L1-2S6, V-L1-2L4, V-L1-2S7, V-L1-3, V-S1a, V-S1). The profiles on the right show magnetic susceptibility ($10^{-5} \text{ m}^3/\text{kg}$) from 4 to 9, Ba/Sr from 0.25 to 1.0, and Mg/Sr from 100 to 300. Shaded regions indicate specific depth intervals. A legend at the bottom identifies the lithological patterns.

2.3a

upper three IRSL age estimates are younger than the AMS-¹⁴C dates from the same depths. This discrepancy may be explained from the possible dead carbon reservoir effect of the AMS-¹⁴C dates and/or an underestimation of the moisture content in the IRSL samples. Nevertheless, all dating results from the Titel section confirm the age of the assigned stratigraphic units.

The IRSL age estimates in Stari Bezradychy increase with depth. They range from 47.5 ± 4.4 ka to 36.9 ± 3.4 ka giving evidence for a deposition age during the Middle Pleniglacial. However, the lowermost sample does not confirm that the loess at 6.50 m is deposited during the Lower Pleniglacial as suggested by the stratigraphic field description. Soil moisture underestimation might have underestimated the age. The IRSL age estimate at 6.10 m confirms that the major part of the Pyrogo section is deposited during the Upper Pleniglacial. The chronology of the Sanzhijka section is based on unpublished TL dates by Zhanna Nikolajevna Matviishina.

2.5 Results

Correlation of bulk and leachate chemistry analyses

The results of the bulk XRF-analyses and the leachate ICP-procedure show similar behaviour for all measured elements ($R^2 > 0.85$) (fig. 2.2). This indicates that variations in the bulk chemistry results for these elements- are controlled by carbonate minerals and other 1N HNO₃ leachable fractions (fig. 2.2). The leachate chemistry results are plotted together with the grain-size and MS results in figs. 2.3a-d.

Grain-size, MS, and leaching geochemistry results per loess section

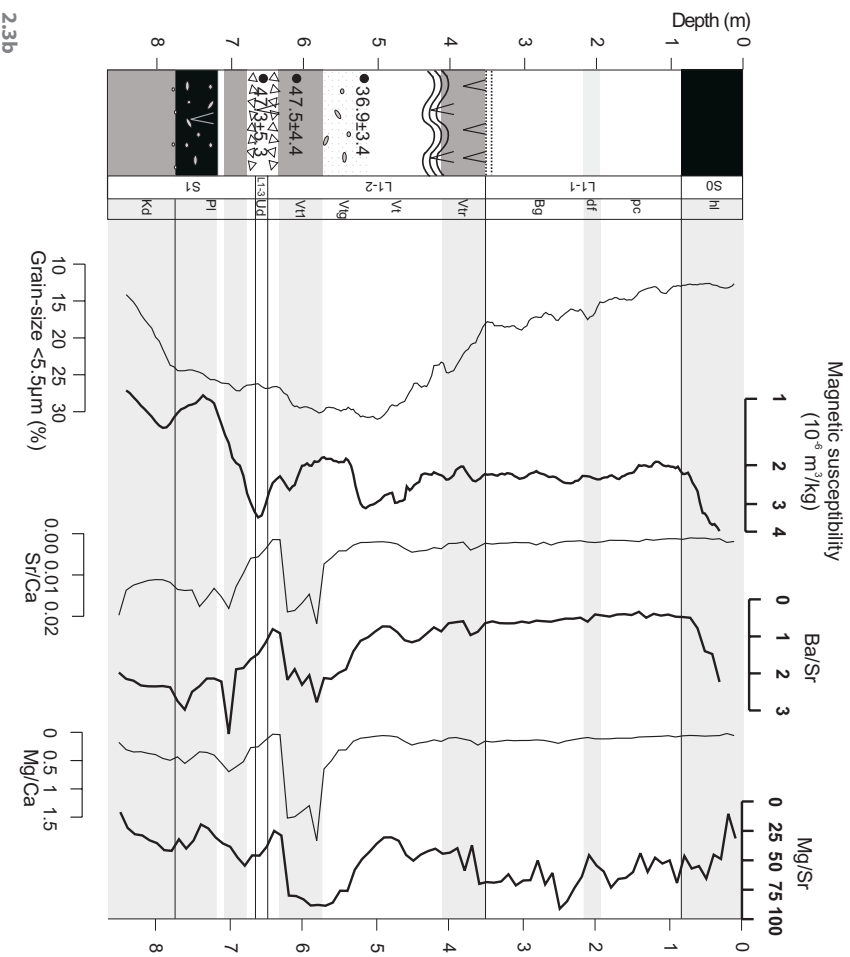
The Titel section, Serbia

The clay fraction (%) in the Titel section shows a clear relation with the paleosols and incipient soils (fig. 2.3a). The MS record increases at the top of V-S0 and in units V-S1 and V-L1-2, but shows no significant response to the incipient soils in units V-L1-1 and V-L1-3. However, the clay fraction record shows a clear relation to the weak soil formation of V-L1S1 (between 0.8 and 3 m, fig. 2.3a), indicating that the conditions during this period were not favouring magnetic mineral formation.

The Ba/Sr-ratio behaves similar as clay percentage and MS ($R^2 = 0.60$ and 0.85 respectively, table 2.3). There is a clear resemblance in V-L1-2 between Ba/Sr, MS and clay percentage between 5 m and 10 m. Strikingly, in the V-L1-1 and the V-L1-3 loess the Ba/Sr ratio shows a better resemblance to MS than to the clay percentage record, while the oscillation at 11.2 m in the Ba/Sr record is registered in the clay percentage record but not in the MS record. The Mg/Sr record show comparable response as Ba/Sr at several depths, like the oscillations at 5.5 m and at 11.2 m, but also show an opposite response, comparable to Sr/Ca and Mg/Ca, at 8.5 m and in V-S1.

The correlation between MS and Sr/Ca and Mg/Ca is strongly negative (table 2.3). High values in the MS or clay percentage records correspond to low values in the Sr/Ca and Mg/Ca records at e.g. 6.5 m, 9 m or in V-S1 and V-S0. However, zones with low

Stari Bezradychy (Ukraine)



2.3b Results of leach-chemical analyses and grain size distributions of the Stari Bezradychy section (Ukraine). The encoding of the stratigraphic units refer to Gerasimenko (2001). For the legend see fig. 2.3a. The dating results in the left column are IRSL datings. The Holocene soil is exposed as 80 cm thick remnant of a chernozem (hl). The uppermost 3.50 m of the section correlates with the Upper Pleniglacial Prychernomorsk (pc) and Bug (Bg) loess units interrupted by the Dofniovka incipient paleosol (df) at a depth of about 2.00 m from the top of the profile. Some coarse material layers indicate erosion events posited at a depth of 3.50 m. The sediments between 3.50 and 6.70 m were deposited most likely during the Middle Pleniglacial and correlate with the Vytachiv complex (Vt). A brown rendzina soil is intercalated between 3.50 and 4.10 m (Vtr), containing frost cracks both at the top and the bottom of the soil. About 4.10 m below surface, some cryoturbation structures were found. Some root hollows, black manganese nodules and strong gley spots are exposed between 5.40 and 5.90 m below surface (Vg). Between 5.90 and 6.40 a gleysol is exposed (Vtr). The Lower Pleniglacial Uday loess (Ud) is exposed only between 6.50 and 6.60 m from the top of the profile. A frost crack was found below 6.40 m, and two layers containing calcium-carbonate prisms are intercalated at 6.50 m and at 6.80 m below surface. The last interglacial Pryluky pedocomplex (Pl) appears below the prismatic carbonate layer and consists of a truncated thin dark brown soil, 10 cm loess and a chernozem soil below with many crotovinas and is intercalated by a frost crack exposed at 7.30 m below topographic surface. The Kaydaky soil complex (Kd) is posited at a depth interval from 7.75 to 8.50 m and is a truncated brown forest – pseudogley soil superimposed to the top of the Mid-Pleistocene glaciofluvial deposits related to the Dnieper stage.

values of these ratios are mostly followed by high values, e.g. at 2.5 (below V-S0), at 7 m (below the incipient soil at 6.5 m (V-L1-2S3)) and at 11.2 m (below the peaks at 10.2 m), suggesting reprecipitation of soil carbonates at those depths.

The Stari Bezradychy section, Ukraine

All elemental ratios register the Vt1 unit in the Middle Pleniglacial deposits, while the clay percentage and MS do not (fig. 2.3b). The mismatch between clay percentage and MS records, and the visible soils in the field, explain the low correlation between clay percentage or MS with any of the elemental ratio records (table 2.3). Only Sr/Ca and Ba/Sr seem to register the Holocene soil (hl) and the last interglacial soils (Pl and Kd). No proxies clearly register the Vitachiv soil in the upper part of the Middle Pleniglacial (Vtr) and the Dofinivka incipient soil (df).

The Pyrogove section, Ukraine

Mainly in the lower part of the Pyrogove section, the clay percentage record shows clear oscillations, suggesting/indicating paleoclimatic variations. Although the MS signal shows less variation, it has some resemblance to the clay percentage variation (fig. 2.3c). Both Sr/Ca and Ba/Sr show increasing values in the actual (hl) and last interglacial soil (Kd), while the ratio records seem less sensitive for the incipient soils throughout the section. A good match was found between MS and Ba/Sr ($R^2=0.66$, table 2.3).

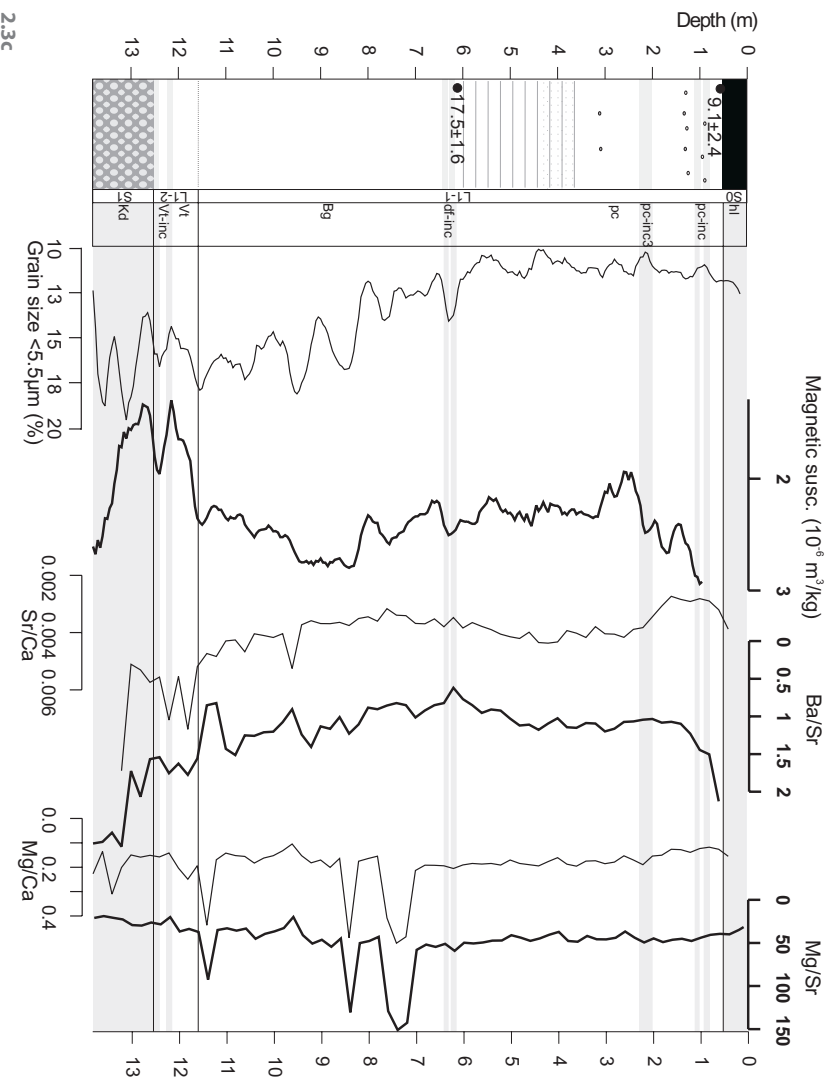
The Sanzhijka section, Ukraine

The clay percentage and MS records show generally high values in the soil complexes and lower values in the thicker loess parts. In Sanzhijka clay percentage, MS, Sr/Ca, Ba/Sr and Mg/Ca match to paleosols in the Middle Pleniglacial (codes starting with Vt) and Holocene (hl) deposits, indicating interstadial climate conditions during these periods (fig. 2.3d). Clay percentage and MS seem to be sensitive recorders of the Prychernomorsk (pc) and Dofinivka (df) paleosols, while none of the elemental ratios are. A good match was found between MS and Ba/Sr ($R^2=0.72$, table 2.3), while also MS and Sr/Ca relate to each other to some amount ($R^2=0.55$), indicating both Ba/Sr and Sr/Ca are sensitive for related (climate) conditions.

2.6 Discussion

The clay fraction and MS results in the different sections show clear resemblance to each other in Titel ($R^2=0.71$) and Sanzhijka ($R^2=0.64$). Mainly in Titel the records show a good parallel to many incipient soils, described in the field. This match indicates that both proxies recorded related conditions that are controlled by climate variability. In Stari Bezradychy and Pyrogove these records do not match ($R^2=-0.03$ and -0.16 , respectively). The main reason is probably that these proxies register a different (climate) process. An increasing amount of fine fraction may indicate clay production due to increased chemical or physical weathering related to climate variability, but may also indicate

Pyrogove (Ukraine)



2.3c Results of leach-chemical analyses and grain size distributions of the Pyrogove section (Ukraine). For the legend see fig. 2.3a. The dating results in the left column are IRSL datings. The Holocene soil consists of 50-cm thick dark brown mollic material (h). The Upper Pleniglacial Prychennomorsk loess unit (pc, 0.50 m to 6.20 m depth) has a horizontal bedding in its lower part and is intercalated by weak soils at 0.8 m, 1.00 m and 2.00 m below the surface (pc-inc1 – pc-inc3 respectively), including some light brown organic matter accumulations. Carbonate spots are found at 0.85 m and 1.30 m, as well as brown root spots found at 1.30 m and 3.10 m. Small manganese nodules are visible at a depth interval between 3.70 m and 4.30 m below the surface. Two incipient soils are intercalated between 6.20–6.45 m, correlated to the Dofnivka unit (df-inc1 and df-inc2). The lower part of the Upper Pleniglacial loess (6.45–11.60 m) is interpreted as Bug loess (Bg). The Middle Pleniglacial Vtarchiv loess starts possibly at 11.60 m and ends sharply at 12.50 m (Vt). Two incipient soils are intercalated at 12.10 and 12.50 m (Vt-inc1 and Vt-inc2). The material becomes coarser and contains gravel, more clay and a more humus-rich soil below 12.50 m. This lower part of the sequence is designated to represent the middle Pleistocene Dnieper till deposits (Kd).

a decrease in wind intensity, a turning wind resulting in a change of source area, or other changes in material availability upwind. An increase of the MS signal indicates an improvement of conditions favouring the production of magnetic minerals, possibly due to an increase in precipitation.

A climate warming or an increase in precipitation may result in a change of both clay percentage and MS records, like in Titel and Sanzhijka, but not necessarily, like in Stari Bezradychy and Pyrogove. This will also have an impact on the results of the elemental ratio records and could explain the different behaviour of the ratios at different locations. We suggest that bioturbation in paleosols, frost wedge formation, cryoturbation and the formation of prismatic layers have disturbed mainly the MS signal in the Stari Bezradychy section. This can explain the registration failure of the MS signal, compared to the present paleosols.

The Ba/Sr record

Ba/Sr shows high positive correlations to MS in the sections Titel, Pyrogove and Sanzhijka ($R^2=0.85$, 0.66 and 0.72 respectively, table 2.3). In all sections Ba/Sr shows higher values in interglacial and Middle Pleniglacial deposits relative to the Upper and Lower Pleniglacial deposits. Apart from that, Ba/Sr matches to several paleosols and incipient soils that were described in the field. In Titel these paleosols and incipient soils show an outstanding match to the Ba/Sr record. The paleosol encoded V-L1-2S7, at 11.2 m (fig. 2.3a), is not registered in the MS signal, while it is by the Ba/Sr ratio. This indicates that the Ba/Sr ratio is a more sensitive proxy for climate variability than MS at this location.

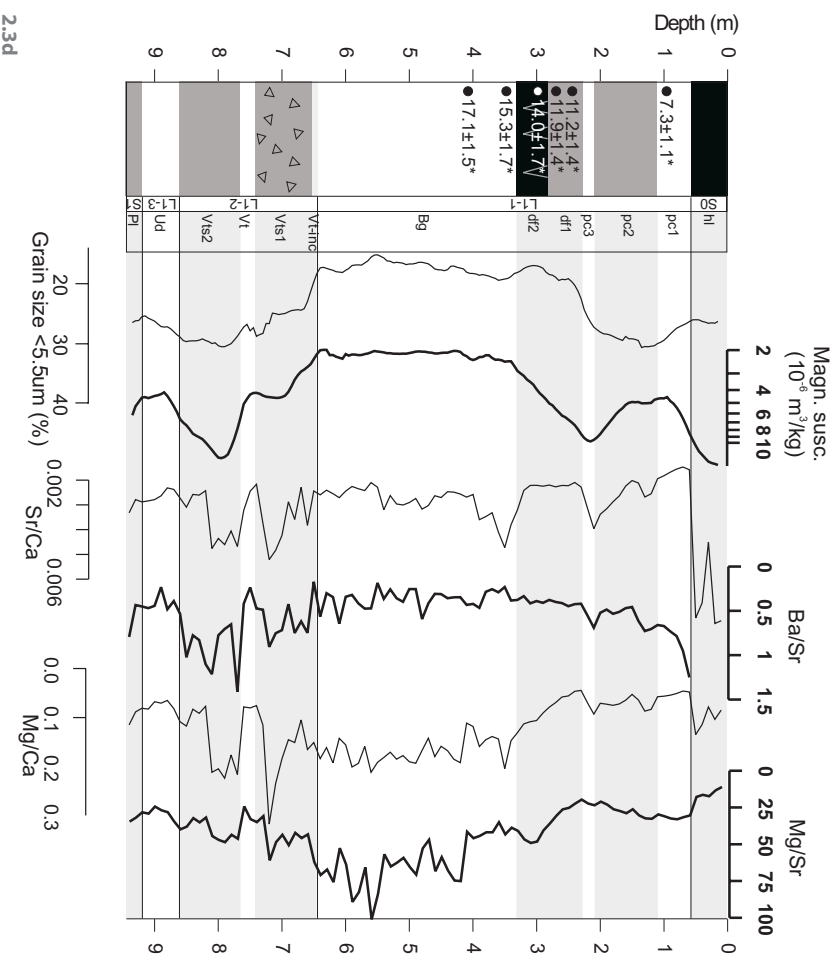
In general, the Ba/Sr records show no clear parallel to other ratio records containing Sr, indicating the element Ba controls the ratio variation. Apparently the 'free' Ba content is strongly controlled by changing weathering intensities, which is also strongly related to the development of many soils.

At Stari Bezradychy the correlation between MS and Ba/Sr is low ($R^2=-0.11$, table 2.3). This may again be explained by a possible breakdown of the magnetic minerals, and thus of the MS signal. Despite this low correlation, Ba/Sr registered climate variability also at this location, as indicated by the match between Ba/Sr and the Middle Pleniglacial and last interglacial paleosols.

The Sr/Ca record

In general, Sr/Ca shows higher values in interglacial paleosols and in some interstadial paleosols in all Ukrainian sections. This indicates that at these locations Sr/Ca is at least in some cases sensitive to paleoclimatic variability. Where Sr/Ca does not show higher values parallel to paleosols, the clay percentage or MS records did not either. This indicates that the climatic ameliorations resulting in these paleosols were weak, and not favouring the production of clays, magnetic minerals or wash-out of 'free' elements in the soil.

Sanzhijka (Ukraine)



2.3d Results of leach-chemical analyses and grain size distributions of the Sanzhijka section (Ukraine). The encoding of the stratigraphic units refer to Matviishina et al. (1990). For the legend see fig. 2.3a. The datings in the left column (in ky BP), marked with a *, are unpublished TL-data by Zhanna Nikolajevna Matviishina. The top of the section contains a Holocene chernozem soil (tl). Beneath the Holocene soil a second soil complex is intercalated, consisting of three greyish to brown soils, one in Prychernomorsk deposits (pc) and two in Dofnivka deposits (df), all of late Upper Pleniglacial age. The lowermost soil is designated to represent a chernozem. A 20-cm thick loess layer (pc3) marks the first transition between the soils, a series of ice-wedge casts marks the transition to the third soil. Between 3.30 and 6.50 m Upper Pleniglacial Bug loess is found (Bg). This loess is loamy at the base. The transition to the Middle Pleniglacial Vitrachiv deposits (Vt) is marked by an incipient soil (Vt-inc). Two reddish brown soils are intercalated in the loess between 6.50 and 8.70 m below surface (Vts1 and Vts2). The uppermost of these soils contains abundant slats, mainly gypsum. According to Matviishina et al (1990) this soil is heavily cryoturbated. However, during the sampling this was not observed. The lower soil is loamy and a little browner than the first one. The Lower Pleniglacial Uday loess (Ud) has a thickness of only 50 cm, covering a loamy and brownish prismatic soil, which probably represents a Pryluky soil complex (Pl).

The strong parallel to the Mg/Ca records in mainly Titel and Stari Bezradychy indicates that the shapes of the curves are mainly controlled by the behaviour of the element Ca. Apparently the dissolution and transport of Ca, caused by percolating water, is the major process that controls the registration of interglacial and interstadial climate conditions.

However, the correlation of Sr/Ca to MS is often strongly negative in Titel, indicating a higher mobility of Sr relative to Ca. This is mainly the case in Titel. Loess parts are indicated by higher values than paleosols. Ca controls the record, considering the match to Mg/Ca. We assume that the high CaCO_3 -content in this section plays a major role (16% average compared to 3-11% average in the Ukrainian sections), while the Sr content is comparable to the Ukrainian sections. Vegetation might also have played a role in preventing an amount of Ca from wash-out, as the biogenic coefficient of Ca is much higher (0.17) than of Sr (0.06) (Perel'man, 1977). As a result, Sr washed out to a larger degree than Ca. This resulted in a registration of paleosols by lower values than in loess parts.

It needs to be noted that the correlation to MS is strongly different between Stari Bezradychy and Pyrogove ($R^2 = -0.57$ and $+0.35$ respectively, table 2.3), while the sections are separated only 20 km and are formed under comparable climate conditions. The probable cause is a breakdown of the MS signal in Stari Bezradychy in the lower part of the Middle Pleniglacial loess.

Reprecipitation indications in Sanzhijka are found mainly below the Upper Pleniglacial soil complex, while oscillations in the soil complex in the lower Middle Pleniglacial are found in the soil. This indicates that the upper soil complex was probably formed under wetter conditions than the lower soil complex.

R^2	Sr/Ca	Ba/Sr	Mg/Ca	Mg/Sr
Titel				
Grain-size <5.5 μm	-0.34	0.60	-0.78	-0.80
MS	-0.63	0.85	-0.76	-0.64
Stari Bezradychy				
Grain-size <5.5 μm	0.31	0.21	0.44	0.05
MS	-0.57	-0.11	-0.27	0.12
Pyrogove				
Grain-size <5.5 μm	0.20	0.14	0.04	-0.11
MS	0.35	0.66	0.38	0.06
Sanzhijka				
Grain-size <5.5 μm	0.20	0.36	-0.42	-0.66
MS	0.55	0.72	-0.28	-0.61

T 2.3 Correlations (R^2) between the leach-chemical ratios tested as potential paleoclimatic proxies and the clay fraction (grain-size <5.5 μm) and the MS-record.

The Mg/Ca and Mg/Sr records

Mg/Ca and Mg/Sr show a high correspondence to each other, mainly in Titel, Pyrogove and Sanzhijka, indicating Mg controls the shape of the curve. In the Ukrainian sections the curves do not seem to respond to processes responsible for soil formation, as they show no parallel to most paleosols. Mainly in Titel and Sanzhijka the values of the curves are lower in paleosols than in loess parts, resulting in a strongly negative correlation to the clay fraction and MS (table 2.3). This indicates that Mg washes out more strongly than Ca or Sr. This can be explained by the high CaCO_3 content in Titel (16% average) and Sanzhijka (11% average) compared to Stari Bezdychy (6%) and Pyrogove (3%). Also uptake by vegetation may partly prevent Ca from wash-out processes (the biogenic coefficient of Mg is 0.02 (Perel'man, 1977)), while the higher solubility of Mg compared to Sr may have caused preferential wash-out of Mg.

Paleoclimatic implications

The overall variability of all elemental ratio records and MS is more expressive in Titel than in Stari Bezdychy and Pyrogove. This implies that the climate situation favoured leaching processes better at the location Titel than in northern Ukraine. Probably the interglacials and interstadials during the last 130 ka were wetter in northern Serbia than in northern Ukraine, similar as to the present-day situation.

The climate registration by the elemental ratio records in Sanzhijka shows an intermediate between those in the Stari Bezdychy and Titel sections. Here the Holocene soil is registered by the Sr/Ca and Mg/Ca records, while indications for reprecipitation are found below the Upper Pleniglacial soils (at 2.5 and 2.1 m, fig. 2.3d). This suggests that the climate in southern Ukraine was possibly slightly wetter than in Northern Ukraine, but still dryer than in northern Serbia during the last glacial and interglacial.

All sections show soil complexes in the (lower part of the) Middle Pleniglacial deposits and in the Upper Pleniglacial deposits. In Titel, Stari Bezdychy and Pyrogove the registration of the Middle Pleniglacial soils is better than the Upper Pleniglacial soils. This indicates that during the interstadials of the Middle Pleniglacial the climatic conditions favoured leaching by weathering, and the release of earth alkaline elements from primary minerals. These interstadials were probably wetter than the interstadials in the Upper Pleniglacial. However, in Sanzhijka the MS signal and the Ca-containing records show both soil complexes. This might be explained by its southerly position, with warm conditions favouring chemical weathering, resulting in higher production of magnetic minerals and conditions that stimulate the mobility of Ca.

2.7 Conclusions

A study of four last-glacial loess-paleosol sections in Serbia and Ukraine indicates that ratios of earth alkaline elements can be used as proxies for weathering controlled, leaching favouring conditions. In three of four sections the Ba/Sr ratio shows a high correlation to MS, in the fourth, the breakdown or absence of magnetic minerals bias

the correlation. In relatively wet climatic conditions the Ba/Sr ratio more clearly registers interstadials than the MS signal. Therefore we conclude that the leachable Ba/Sr ratio in loess-paleosol sequences has a good potential as a weathering intensity proxy. More specifically, it can be interpreted as an indicator for rainfall and precipitation amount that favour leaching of these elements from primary minerals. Sr/Ca also shows promising results in the Ukrainian sections, and may also be interpreted as a proxy for interglacial and interstadial climate conditions, mainly precipitation, in loess. The spatial range of Last Glacial and Interglacial climate conditions where these proxies are applicable may be pointed out by further research.



COMPARING THE $\delta^{13}\text{C}$ OF SOIL CARBONATES AND SOIL ORGANIC MATTER AS PALEO- PRECIPITATION INDICATORS IN LATE QUATERNARY EUROPEAN LOESS DEPOSITS

With Kay Beets, Slobodan Marković and Harro Meijer. Submitted to Global Biogeochemical Cycles

ABSTRACT

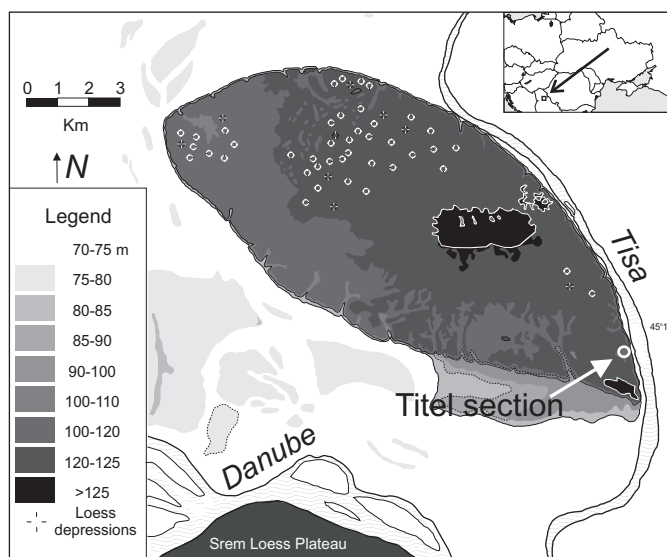
We present new evidence from a continuous, well-dated last glacial-interglacial loess section at Titel in Serbia, that shows that the $\delta^{13}\text{C}$ -value of soil organic matter ($\delta^{13}\text{C}_{\text{som}}$) and soil carbonate ($\delta^{13}\text{C}_{\text{sc}}$) strongly react to changes in (paleo-)precipitation and (paleo-) temperature. Two well reproduced paleo-precipitation records from this section, namely magnetic susceptibility and the Ba/Sr ratio, gave us the opportunity to check the preservation of the precipitation-signal in the $\delta^{13}\text{C}_{\text{som}}$ and the $\delta^{13}\text{C}_{\text{sc}}$. In this case $\delta^{13}\text{C}_{\text{som}}$ -record does not resemble the established paleo-precipitation records, while the $\delta^{13}\text{C}_{\text{sc}}$ -record does. We conclude that, at this location, the $\delta^{13}\text{C}_{\text{sc}}$ is probably a more evident paleo-precipitation proxy than $\delta^{13}\text{C}_{\text{som}}$. Possible mechanisms that lead to disturbance or even destruction of the original signal in the $\delta^{13}\text{C}_{\text{som}}$ and $\delta^{13}\text{C}_{\text{sc}}$ records are discussed.

3 Comparing the $\delta^{13}\text{C}$ of soil carbonates and soil organic matter as paleo-precipitation indicators in Late Quaternary European loess deposits

3.1 Introduction

The reconstruction of summer climatic conditions from loess records during the Last Glacial has proven to be difficult. Pollen grains are hardly preserved in the oxygenated loess deposits, with some exceptions (Rousseau et al., 2001). Malacological studies have also been hampered by the limited preservation of the aragonitic mollusks in paleosols (Wu et al., 2006). Several studies suggest that the $\delta^{13}\text{C}$ -value of soil organic matter ($\delta^{13}\text{C}_{\text{som}}$) in loess reflects the composition of the vegetation, and hence the sensitivity of plants to climatic stress (Lin et al., 1991; Wang et al., 1997; Hatté et al., 1999; Wang and Folmer, 1998; Liu et al., 2005). $\delta^{13}\text{C}_{\text{som}}$ is often accepted as a qualitative paleo-precipitation indicator (e.g. Cerling et al., 1989). Magnetic susceptibility in loess deposits is also considered as indicative for paleo-precipitation (e.g. Maher et al., 2002). However, in cases where the $\delta^{13}\text{C}_{\text{som}}$ records do not resemble the magnetic susceptibility records the interpretation is more complicated (Hatté et al., 2001; Rousseau et al., 2002).

Soil carbonates also preserve a record of carbon isotope composition ($\delta^{13}\text{C}_{\text{sc}}$) (Cerling, 1984; Cerling et al., 1989; Wang and Folmer, 1998). The carbonate record is dominantly influenced by the isotopic composition in the soil CO_2 , which is controlled by the $\delta^{13}\text{C}$ of living plants, therefore, $\delta^{13}\text{C}_{\text{sc}}$ can be considered as a proxy for precipitation (Salomons and Mook, 1986).



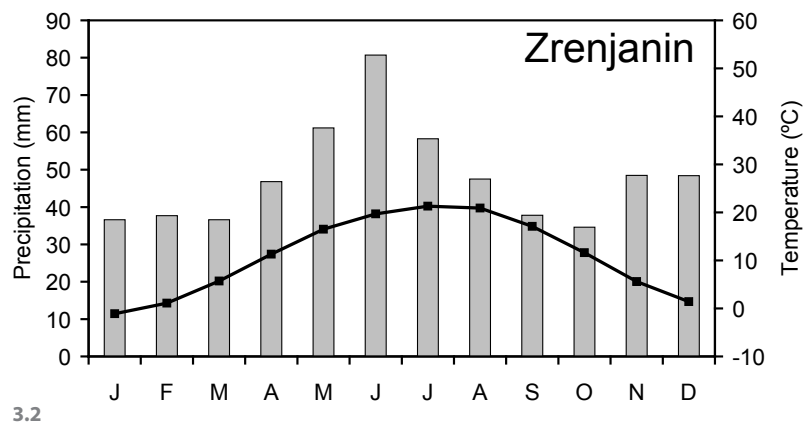
3.1 The location of the Titel section on the Titel Loess Plateau in Vojvodina, Serbia.

The Titel loess plateau in Vojvodina, Serbia, provides high resolution loess deposits of last glacial age (fig. 3.1). Two independent precipitation-controlled climate-records, magnetic susceptibility (MS) and the Ba/Sr-ratio, are well correlated ($R^2=0.82$). MS reflects in-situ formation of iron compounds due to weathering under influence of abundant rainfall (Maher et al., 2002). The Ba/Sr-ratio represents the progressive weathering of the alkaline earths, where Ba is better retained than Sr during ongoing weathering (Chapter 2). The clay fraction (grain-size $<5.5 \mu\text{m}$) record is probably affected by paleo-precipitation and also correlates well to MS ($R^2=0.73$) and to Ba/Sr ($R^2=0.62$). All records were well reproduced in a loess section 5 km away from Titel (Chapter 1). In this chapter we present the $\delta^{13}\text{C}_{\text{som}}$ and $\delta^{13}\text{C}_{\text{sc}}$ records in the Titel loess/paleosol-section and compare them with the available precipitation-proxy records, the total amount of organic carbon (TOC%) in the deposits, the C/N-ratio and the oxygen isotope composition of the soil carbonates ($\delta^{18}\text{O}_{\text{sc}}$). A detailed description of the Titel section can be found in Chapter 1.

Recording the $\delta^{13}\text{C}_{\text{som}}$ -signal and the $\delta^{13}\text{C}_{\text{sc}}$ -signal

In stressful dry conditions C4-plants prevail. They utilize a complex carbon cycle (C4), separating the uptake of carbondioxide and water necessary for their photosynthesis, and discriminate relatively little between the ^{13}C - and the ^{12}C -isotope (for a review see Salomons and Mook, 1986). This results in an average $\delta^{13}\text{C}_{\text{som}}$ of -12 ‰. Under environmental conditions without water-stress, plants that use the C3-cycle dominate. They have a $\delta^{13}\text{C}_{\text{som}}$ -value around -27 ‰. The amount of precipitation controls for a large part the C3/C4-composition of the vegetation (Salomons and Mook, 1986). When the $\delta^{13}\text{C}_{\text{som}}$ -value is below -20 ‰, the paleo-vegetation is considered as dominated by C3-plants. The $\delta^{13}\text{C}_{\text{som}}$ is often considered as an indication for C3/C4 composition of the vegetation, indicating moisture availability and hence paleo-precipitation.

Plant roots mostly dominate the isotopic composition of CO_2 in the soil ($\text{CO}_{2\text{soil}}$)



3.2 Actual precipitation and temperature data (1951-1990) of Zrenjanin, Serbia (45°24' N; 19°15' E; 85 m a.s.l.), about 18 km northeast of the section location.

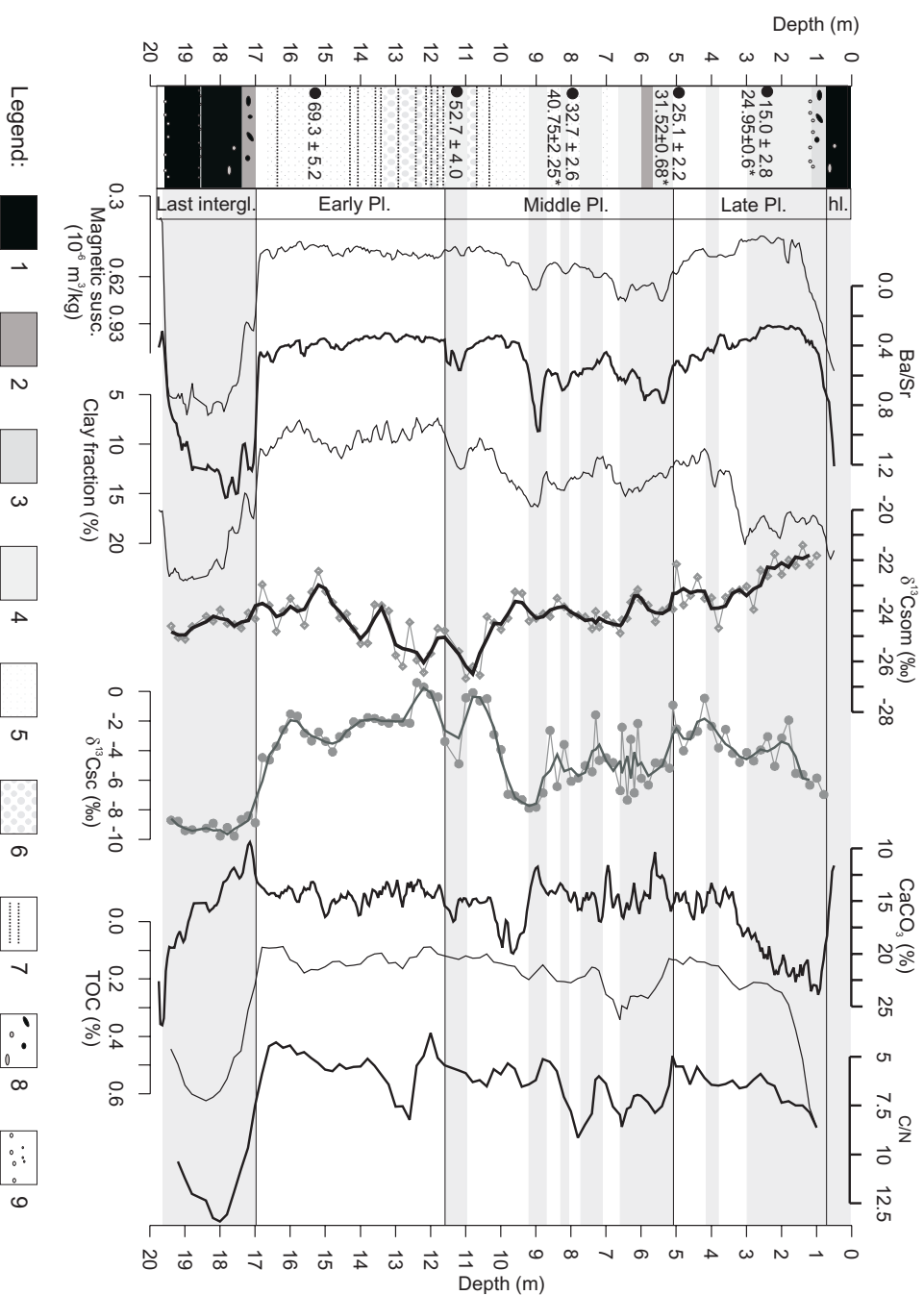
(Salomons and Mook, 1986). The root-exchange of CO_2 of C3-plants discriminates against ^{13}C and therefore the $\delta^{13}\text{C}$ of the CO_2 soil is higher than $\delta^{13}\text{C}_{\text{som}}$. C3-dominated vegetation types have an average $\delta^{13}\text{C}$ -value in CO_2 of -23‰ , while C4-dominated vegetation types have an average around -16‰ . The CO_2 equilibrates with the soil solution. The acidic soil solution dissolves any present limestone (CaCO_3). This initial limestone, depending on its origin, will mostly have higher $\delta^{13}\text{C}$ -values (between -2 and $+2\text{‰}$) when the carbonate has formed as a marine limestone (Salomons & Mook, 1986). The resulting $\delta^{13}\text{C}$ -values of the secondary CaCO_3 are between -13 and $+3\text{‰}$, where C3-dominated vegetation result in relatively low, negative values, while C4-dominated systems result in higher $\delta^{13}\text{C}_{\text{sc}}$ -values (Salomons and Mook, 1986).

$\delta^{18}\text{O}$ in soil carbonates

In an equilibrium situation the oxygen isotope composition of soil carbonates ($\delta^{18}\text{O}_{\text{sc}}$) registers the $\delta^{18}\text{O}$ value of precipitation. This value is slightly dependent on temperature and varies between approximately -5 and -9‰ in the temperate regions. Both signals respond in the same way to temperature changes, and thus should follow a parallel behaviour (Cerling and Quade, 1993). A temperature rise results in enrichment of $\delta^{18}\text{O}$ of precipitation, about $+0.6\text{‰}/^\circ\text{C}$ between 30° and 60° on the NH. During the period with the highest evaporation, mostly in the growing season, most soil carbonate is formed with another temperature dependent discrimination of about $-0.25\text{‰}/^\circ\text{C}$ (O'Neill et al, 1969). Apart from that, the $\delta^{18}\text{O}_{\text{sc}}$ value is a result of the type of carbonate present in the soil, that may be a mixture of detritic and authigenous carbonate. This mixture is controlled by the amount of precipitation that controls the formation of authigenous carbonate. The location Titel is characterized by a relatively dry climate with large precipitation fluctuations over the year, while the growing season is during the summer (fig. 3.2). Therefore, combined information of $\delta^{13}\text{C}_{\text{sc}}$ and $\delta^{18}\text{O}_{\text{sc}}$ from Titel may give insight in the origin of CaCO_3 in the soil, and thus in the reliability of $\delta^{13}\text{C}_{\text{sc}}$ and $\delta^{13}\text{C}_{\text{som}}$ as potential proxies for paleo-climatic conditions.

3.2 Methods

We analyzed samples taken at 20-cm intervals over a 20 meter section. The C/N-ratio was measured to check the soil organic matter composition and possible diagenetic alteration. The percentage of total organic carbon (TOC%) in the loess sediment was used to check the relative plant activity/vegetation density. The CaCO_3 -content ($\text{CaCO}_3\%$) was measured to determine the potential redistribution of CaCO_3 in the soil due to leaching, diffusion and reprecipitation. This would indicate an increase of rainfall influence on a part of the section, caused by higher precipitation intensities, non-deposition for a relatively long period, or a combination. The redistribution can be recognized by a thin layer containing low concentrations of CaCO_3 , underlain by a small zone of high concentrations.



3.3 Results of the $\delta^{13}\text{C}_{\text{sc}}$, $\delta^{13}\text{C}_{\text{som}}$, CaCO_3 , TOC% and C/N analyses compared to the magnetic susceptibility, Ba/Sr and clay fraction. The division in marine isotope stage equivalents is based on the IRL dating results and the general shapes of the strongly resembling curves. In all curves the interglacial values are plotted towards the right. Legend for section drawings: 1. chernozem soil, 2. other soils, 3. transition zone between soil and loess, 4. incipient soil, 5. loess containing spots, 6. loess containing coarse fractions, 7. sand layers, 8. crotoninas /root hollows, 9. carbonate concretions.

C/N-ratio and TOC%

About 10 mg of finely ground bulk loess sample was put into a silver cup. CaCO_3 was removed by leaving the sample in a HCl-gas environment for one night. Small drops of 10% HCl were added until no reaction could be observed anymore followed by a drying step at 60 °C. The silver cups were closed, tightly folded and put in a tin cup which was also closed and tightly folded. C and N% were measured using a Flash EA 1112 automatic elemental analyzer. Burning takes place in a He-environment at 1700°C. All samples were measured in duplicate. The results were also determined separately during the measurement of $\delta^{13}\text{C}_{\text{som}}$ and compared and averaged afterwards. The precision of C% and N% using the Flash analyzer was 0.05 and 0.011% respectively.

$\delta^{13}\text{C}_{\text{som}}$

For the $\delta^{13}\text{C}_{\text{som}}$ analyses the loess was sieved over a 1000 μm sieve. The loess was boiled with 1N HCl and washed with water 3 times after to remove the calciumcarbonate. The loess was then dried. Tin cups were filled with an amount of loess equivalent to 300-500 μg C. The tin cups were combusted in an elemental analyzer (Carlo Erba NA 2500), and the combustion CO_2 was isotopically ($\delta^{13}\text{C}$) and quantitatively analysed in an on-line connected continuous flow Isotope Ratio Mass Spectrometer (Micromass - now GV Instruments – Optima). The standard deviation of the measurements is approximately 0.15 ‰ (‰ PDB). One in five samples was measured in duplicate. The reproducibility is 0.275‰.

$\delta^{13}\text{C}_{\text{sc}}$ and $\delta^{18}\text{O}_{\text{sc}}$

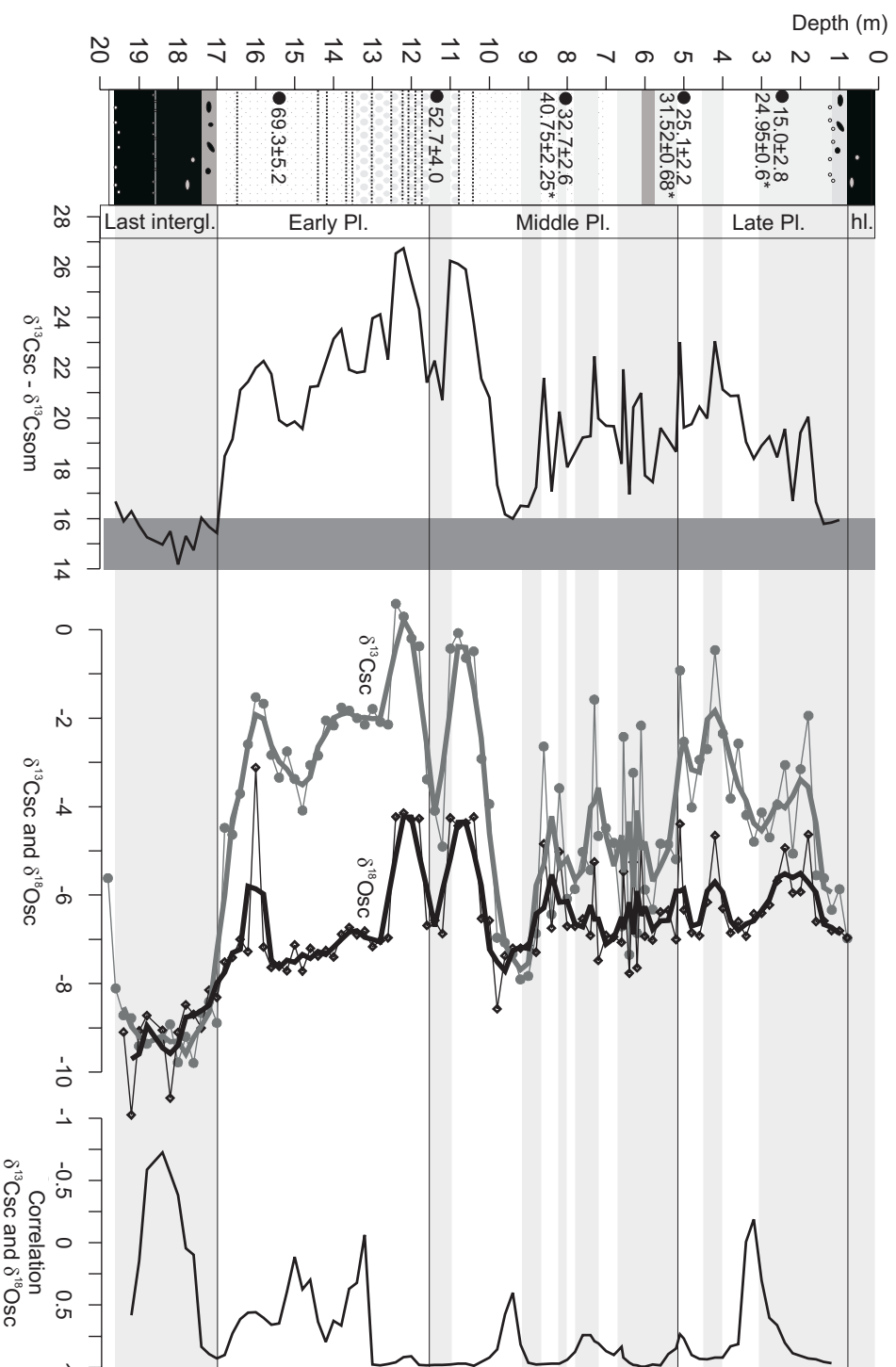
The samples for $\delta^{13}\text{C}_{\text{sc}}$ and $\delta^{18}\text{O}_{\text{sc}}$ analyses were dried and ground. A sub-sample (about ~100 μg) was measured using a GasBench equipped mass spectrometer. The liberated CO_2 is analyzed by Isotopic Ratio Mass Spectrometry using a Finnigan Delta plus. The standard deviations of the measurements for the $\delta^{13}\text{C}$ and $\delta^{18}\text{O}_{\text{sc}}$, are both approximately 0.12 ‰ (‰ PDB).

$\text{CaCO}_3\%$

About 100 mg of dry sample was left for one night in 5 ml 1N HNO_3 . After centrifuging 1 ml of the resulting sample solution was pipetted off and diluted to 10 ml. The amount of leachable Ca of the sediment was determined using a Liberty II Varian ICP-AES. The in-run precision for all the measured elements was better than 1.5 %. The reproducibility of duplicate measurements ($n = 9$) is 6.7 % for calcium and strontium. The $\text{CaCO}_3\%$ was finally calculated from the Ca content.

3.3 Results

In fig. 3.3 the results of the $\delta^{13}\text{C}_{\text{som}}$, $\delta^{13}\text{C}_{\text{sc}}$, TOC% and C/N analyses are plotted against depth with the MS-record, the Ba/Sr-record, the clay fraction content (see also Chapter 2) and the content of CaCO_3 from the Titel section. The $\delta^{13}\text{C}_{\text{som}}$ values have standard deviations ranging from 0.01 to 0.25 ‰, the standard deviations of the $\delta^{13}\text{C}_{\text{sc}}$



3.4 Results of the $\delta^{13}\text{C}_{\text{sc}} - \delta^{13}\text{C}_{\text{som}}$ record, reflecting the disequilibrium between these records. The $\delta^{13}\text{C}_{\text{sc}}$ versus $\delta^{18}\text{O}_{\text{sc}}$ records and their correlation show the indicate the reliability of the $\delta^{13}\text{C}_{\text{sc}}$ signal as a paleoclimatic proxy. The vertical shaded zone marking the 14-16 ‰-interval in the left graph indicates the isotopic equilibrium zone, as indicated by Cerling et al (1989). A legend for the section drawing on the left can be found in fig. 3.3.

values range from 0.06 to 0.24 ‰. The TOC% measurements were determined by two independent methods (see also methods section). The results show a correlation of 0.92. The double total organic N measurements have an R^2 of 0.76.

The proxy records have been subdivided in Last Interglacial deposits, Lower, Middle and Late Pleniglacial deposits and Holocene deposits. We assume a correlation of these deposits with Marine Isotope Stages (MIS) 5-1 respectively, based on Martinson et al. (1987) and Woillard and Mook (1982). We place the MIS 5-4 transition at 75 ka BP, 4-3 at 59 ka BP, 3-2 at 24 ka BP and 2-1 at 12 ka BP. Five IRSL dates and three AMS ^{14}C -dates corroborate the utilized subdivision (fig. 3.3). More detailed information on the chronology of this section can be found in Chapter 1.

Comparison of the $\delta^{13}\text{C}_{\text{som}}$, $\delta^{13}\text{C}_{\text{sc}}$, TOC% and C/N results with the MS and Ba/Sr records shows that the characteristic pattern of marine isotope stages is not always as clearly recognisable as in the Ba/Sr and MS records. The $\delta^{13}\text{C}_{\text{som}}$ curve shows higher values in the Early Pleniglacial than in the Last Interglacial deposits, while the values in the Middle and Late Pleniglacial deposits are about the same. The Late Pleniglacial to Holocene deposits transition is marked by increasing values. The total range of the $\delta^{13}\text{C}_{\text{som}}$ -variation is relatively low (~ 3 ‰). The $\delta^{13}\text{C}_{\text{sc}}$ -record shows a different pattern. All marine isotope stages are clearly recognisable and the curve shows a higher total range (~ 8 ‰) than the $\delta^{13}\text{C}_{\text{som}}$ -record. The Early and Late Pleniglacial deposits even show more variations in the $\delta^{13}\text{C}_{\text{sc}}$ -record than in the MS and Ba/Sr ones, while the Middle Pleniglacial deposits show comparable oscillations. These variations are resembled by the clay fraction record at equivalent depths. The C/N-ratio curve shows characteristic variation in all five marine isotope stages, while the Middle Pleniglacial deposits are relatively stable in contrast to $\delta^{13}\text{C}_{\text{sc}}$. A major oscillation at the base of the Middle Pleniglacial deposits, as registered in the magnetic susceptibility, clay fraction, Ba/Sr and $\delta^{13}\text{C}_{\text{sc}}$ records, was not registered in the C/N-ratio and TOC% records. However, the central part of the Early Pleniglacial deposits in the C/N-record shows a relatively high oscillation that has only an equivalent in the clay record. The CaCO_3 %-content shows increases followed by decreases between 19.5 to 17 m, between 10.2 and 8.8 m and in the top 3.2 to 0.4 m.

The $\delta^{18}\text{O}_{\text{sc}}$ signal shows relatively constant behaviour of -7 ± 1.5 ‰ above 9.5 m depth (fig. 3.4). On the contrary, the value difference between two low value zones near the Early to Middle Pleniglacial transition and very high values in S1, show an extraordinary large range of 6 ‰ between these two deposits. The $\delta^{18}\text{O}_{\text{sc}}$ record also shows a parallel behaviour to the $\delta^{13}\text{C}_{\text{sc}}$ record in the Middle and Late Pleniglacial deposits, except for two thin zones at approximately 9.5 and 3.2 m depth. However, the correlation is also worse in the Last Interglacial and the central part of the Early Pleniglacial deposits.

3.4 Discussion

When vegetation is present at the soil surface, plant roots and continuous decomposition of organic matter control the $\delta^{13}\text{C}$ -value of the soil CO_2 and hence that of the soil solution (and its equilibrium with the soil carbonates). The presence of organic carbon (~0.1 to 0.8 %, fig. 3.3) indicates that there was at least some vegetation continuously present at this location during the last glacial. The values of $\delta^{13}\text{C}_{\text{som}}$ are everywhere below -20 ‰, indicating that the vegetation was dominated by C3-plants. Cerling et al. (1989) show that under such vegetation type $\delta^{13}\text{C}_{\text{sc}}$ is 14 to 16 ‰ enriched with respect to the $\delta^{13}\text{C}_{\text{som}}$ at isotopic equilibrium. In that case the $\delta^{13}\text{C}_{\text{som}}$ and $\delta^{13}\text{C}_{\text{sc}}$ records should follow a more or less parallel pattern with a 14 to 16 ‰ difference. If this is not the case, a) the carbon isotopic signature is not simply transferred from the organic matter to the soil solution and the precipitated carbonate, or b) the soil carbonate is post-depositional overprinted, or c), what is likely to happen during dry periods, initial detrital calcite is not dissolved because of lack of acidic soil solution and soil carbonates will not be formed or only partly.

Our carbon isotope records do not show a parallel behaviour at all, and, following Cerling et al. (1989), the $\delta^{13}\text{C}_{\text{som}}$ -value does not reflect vegetation changes. However, the difference between the $\delta^{13}\text{C}_{\text{sc}}$ and $\delta^{13}\text{C}_{\text{som}}$ records is continuously higher than 14 to 16 ‰, except for the interglacials, and extremely varying (fig. 3.4). This suggests that secondary influence has biased the registration of the signal or has changed one of the signals after registration. Nevertheless, it is remarkable that the $\delta^{13}\text{C}_{\text{sc}}$ -record shows clear resemblance to the magnetic susceptibility ($R^2=-0.77$), Ba/Sr ($R^2=-0.80$) and clay fraction ($R^2=-0.82$) records, while the $\delta^{13}\text{C}_{\text{som}}$ does not at all ($R^2=-0.13$, -0.13 and $+0.34$ respectively) (fig. 3.3). Apart from that, the C/N-ratio and the TOC%-record broadly show parallel behaviour to the $\delta^{13}\text{C}_{\text{sc}}$ -signal in the Early, Middle and Late Pleniglacial deposits (fig. 3.3). This suggests that the soil carbonates preserved the original signal from the overprint shortly after deposition, while the $\delta^{13}\text{C}_{\text{som}}$ did not.

Other phenomena underline this statement. The depths at which the CaCO_3 -record shows deviations from its average value of 15% are indicative of enrichment or depletion of the carbonate by percolating water. All wash-out phenomena (low CaCO_3 -values) mark the wettest periods, based on MS and Ba/Sr, during the deposition of the loess and soil formation, respectively in the Last Interglacial, the early part of the Middle Pleniglacial and the Holocene deposits. The resulting accumulation of CaCO_3 is found in the deposits just below them. These maxima in CaCO_3 % coincide exactly with the highest values in the $\delta^{13}\text{C}_{\text{sc}}$ -record at the top of the Late Pleniglacial deposits (fig. 3.3). In the case of the Last Interglacial and Middle Pleniglacial deposits, the high $\delta^{13}\text{C}_{\text{sc}}$ values correlate with and underlie the highest values in the Ba/Sr-record. These high values in the $\delta^{13}\text{C}_{\text{sc}}$ record also coincide with observed soils in the field, related to interglacial and interstadial conditions. Marković et al. (2008) show that the Last Interglacial soil and the Middle Pleniglacial soil complex can be followed throughout the Vojvodina

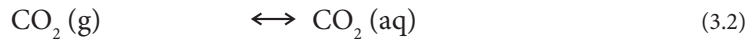
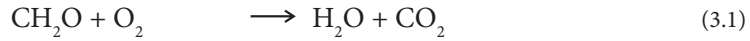
region. Malacological results from these soils in the area indicate relatively warm and moist conditions compared to the loess parts. These results also correlate well to our $\delta^{13}\text{C}_{\text{sc}}$ results.

The $\delta^{18}\text{O}_{\text{sc}}$ signal underlines the reliability of the $\delta^{13}\text{C}_{\text{sc}}$ record in two ways. First, the parallel behaviour of both signals during the Middle and Late Pleniglacial (fig. 3.4), except for two thin zones at about 9.5 and 3.2 m, suggest a reliable registration and preservation of the $\delta^{13}\text{C}$ -signal in the soil carbonates. However, in S1 and the central part of the Early Pleniglacial deposits, the signal was disturbed. Second, the relatively stable $\delta^{18}\text{O}_{\text{sc}}$ value in the central and top parts of the Middle Pleniglacial and the whole Late Pleniglacial deposits suggest a normal registration of the $\delta^{18}\text{O}$ value of the paleo-precipitation. Exceptions are a $\delta^{18}\text{O}_{\text{sc}}$ value of -10‰ in S1 and a value of -4‰ at 12.1 and 10.7 m. When this value range of 6‰ was completely caused by temperature changes, an unrealistic difference of 24 °C must have occurred between the Last Interglacial and Early Pleniglacial. We suggest that the low values in the Early Pleniglacial deposits are caused by incomplete registration of the paleo-precipitation signal in the soil carbonates due to drought. The preserved signal is possibly biased by detrital carbonates from nearby marine carbonate formations, possibly from the Dinaric Alps, having a $\delta^{18}\text{O}$ value of about $0 \pm 2\text{‰}$. Assuming a precipitation value of $-7 \pm 2\text{‰}$, a rough estimation can be made that about 43% of the present soil carbonate has registered the paleo-precipitation signal. The high values in S1 on the contrary, might be caused by a different climate system, like the monsoon system in China, where comparable interglacial values were found (e.g. Wang and Folmer, 1998; Liu et al., 2005).

The $\delta^{13}\text{C}_{\text{som}}$ record in this study differs significantly from the dataset presented by Hatté et al (2001), studying $\delta^{13}\text{C}_{\text{som}}$ in a loess section in the Rhine Valley in Germany. Their data show a registration of higher values during the glacial periods than during the interglacial periods, indicating more C4-vegetation during the glacial periods compared to the interglacial periods, reflecting increased drought-stress during glacials. In our data this is the other way round. This essential difference between these two European loess sections underlines that $\delta^{13}\text{C}_{\text{som}}$ is not reliable as a proxy for paleoclimatic conditions in every situation.

3.5 Possible secondary processes affecting $\delta^{13}\text{C}_{\text{som}}$

To understand the differences in behaviour of the $\delta^{13}\text{C}_{\text{som}}$ -records throughout the Eurasian continent we have to consider the decomposition process of dead organic matter. The larger part of dead plant tissue is decomposed after deposition. Indications of decomposition can be found in the TOC%-record in fig. 3.3. The values in the Middle Pleniglacial deposits are comparable to those in the Early and Late Pleniglacial deposits, while higher values can be expected, and no early Middle Pleniglacial oscillation like in the records of the independent proxies Ba/Sr, magnetic susceptibility and clay fraction content is recorded. The decomposition process can schematically be given by:



The influence of decomposition on the $\delta^{13}\text{C}_{\text{som}}$ -value is varying. Powers and Schlesinger (2002) found enrichment in the $\delta^{13}\text{C}$ of the remaining soil organic matter at 35 locations with varying tropical conditions in Costa Rica. However, Benner et al. (1987) found from experiments that the $\delta^{13}\text{C}$ -values of polysaccharide and lignin components of different plants deplete during decomposition. Ehlinger et al. (2000) and Wedin et al. (1995) showed that the activity of the processes that change the $\delta^{13}\text{C}_{\text{som}}$ -value of the remaining soil organic matter is dependent on the type of plant coverage during the decomposition. Koarashi et al. (2005) found that mainly the base-insoluble fraction of the soil organic matter remains after decomposition. Ehlinger et al. (2000) explain this strongly varying behaviour of $\delta^{13}\text{C}_{\text{som}}$ by a mixture of the remaining organic matter with microbial and fungal carbon residues accounting for the enrichment of the total $\delta^{13}\text{C}_{\text{som}}$ during decomposition. Ehlinger et al. (1997; 2000) and Sage and Monson (1999) show that the $\delta^{13}\text{C}_{\text{som}}$ -value is linearly related to (growing season) temperature. A research to the source of soil organic matter on the Chinese Loess Plateau confirms that also in Last Glacial loess deposits micro-organisms are responsible for degradation as well as enrichment of the $\delta^{13}\text{C}_{\text{som}}$ signal (Xie et al., 2004). However, they also point out that these degradation and enrichment processes are mainly active in interglacial and interstadial periods, and thus mainly affecting the $\delta^{13}\text{C}_{\text{som}}$ signal in paleosols.

Assuming that the $\delta^{13}\text{C}_{\text{som}}$ and $\delta^{13}\text{C}_{\text{sc}}$ records have had a parallel behavior shortly after deposition and with a full overprint of the present soil carbonate, post-depositional alteration processes of the $\delta^{13}\text{C}_{\text{som}}$ record might explain the behavior of this record in the Titel section. Enrichment of the values by micro-organisms in paleosols, but not in the loess parts implies that the $\delta^{13}\text{C}_{\text{som}}$ value has been higher in the paleosols in the past. This process has reduced the total variability in the section and even caused a negative correlation between $\delta^{13}\text{C}_{\text{som}}$ and $\delta^{13}\text{C}_{\text{sc}}$. However, the large difference between the $\delta^{13}\text{C}_{\text{som}}$ and $\delta^{13}\text{C}_{\text{sc}}$ values and the extremely low values of $\delta^{13}\text{C}_{\text{sc}}$ in glacial deposits in Titel remain unclear.

3.6 Conclusion

The $\delta^{13}\text{C}_{\text{som}}$ and the $\delta^{13}\text{C}_{\text{sc}}$ values in the studied loess section in Serbia do not show parallel behaviour, indicating at least one of the records is not representing paleo-precipitation conditions. Multiple proxy records that are sensitive for post-depositional climate conditions show high similarity to the $\delta^{13}\text{C}_{\text{sc}}$ record and (thus) not to the $\delta^{13}\text{C}_{\text{som}}$ record. This strongly suggests that $\delta^{13}\text{C}_{\text{sc}}$ in last glacial loess deposits is a more reliable proxy for paleo-precipitation than $\delta^{13}\text{C}_{\text{som}}$.

The $\delta^{13}\text{C}_{\text{som}}$ record in the studied section shows opposite behaviour in loess and paleosols compared to a section in Germany. This difference may be explained from differences in activity of micro-organisms between the two sections. Microbial and fungal decomposition of organic matter after deposition, mainly active in interglacial and interstadial conditions, may have enriched the $\delta^{13}\text{C}_{\text{som}}$ value more in paleosols than in loess parts in the Titel section. More research is needed to explain the degradation of the $\delta^{13}\text{C}_{\text{som}}$ signal in glacial deposits.

The difference in $\delta^{13}\text{C}_{\text{som}}$ signal behaviour between the sections underlines that care should be taken when this signal is interpreted as a proxy for paleo-precipitation. However, when $\delta^{13}\text{C}_{\text{sc}}$ is used for the same purpose, it has to be taken into account that all present soil carbonate was overprinted by the paleoclimate signal.



ATMOSPHERIC CIRCULATION PATTERNS IN EASTERN AND CENTRAL EUROPE DURING THE WEICHSELIAN PLENIGLACIAL INFERRED FROM LOESS GRAIN-SIZE RECORDS

With Jef Vandenberghe, Pal Sümeği, Maria Łanczont, Natalia Petrovna Gerasimenko, Zhanna Nikolajevna Matviishina, Slobodan Marković and Manfred Frechen. Submitted to Quaternary International.

ABSTRACT

This is a contribution to the reconstruction of the eolian transport processes and wind directions in south-eastern Europe during the Weichselian Pleniglacial. The study is based on eight loess sections: three west and five east of the Carpathian Mountains. The loess dispersal patterns in the area is interpreted by the loess grain-size distribution and mass accumulation rates (MARs) in relation to the topography. The grain-size dataset is subdivided in four endmembers (EMs) by means of the endmember modelling algorithm EMMA. The temporal evolution of the individual EMs is based on a number of absolute datings (25 IRSL and one ^{14}C). The MARs and proportions are calculated per unit of the Weichselian Pleniglacial (Early, Middle and Late). Both the MAR-results and the EM proportions suggest a prevailing western wind during the Early and Middle Pleniglacial and a dominant northwestern wind during the Late Pleniglacial.

4 Atmospheric circulation patterns in eastern and central Europe during the Weichselian Pleniglacial inferred from loess grain-size records

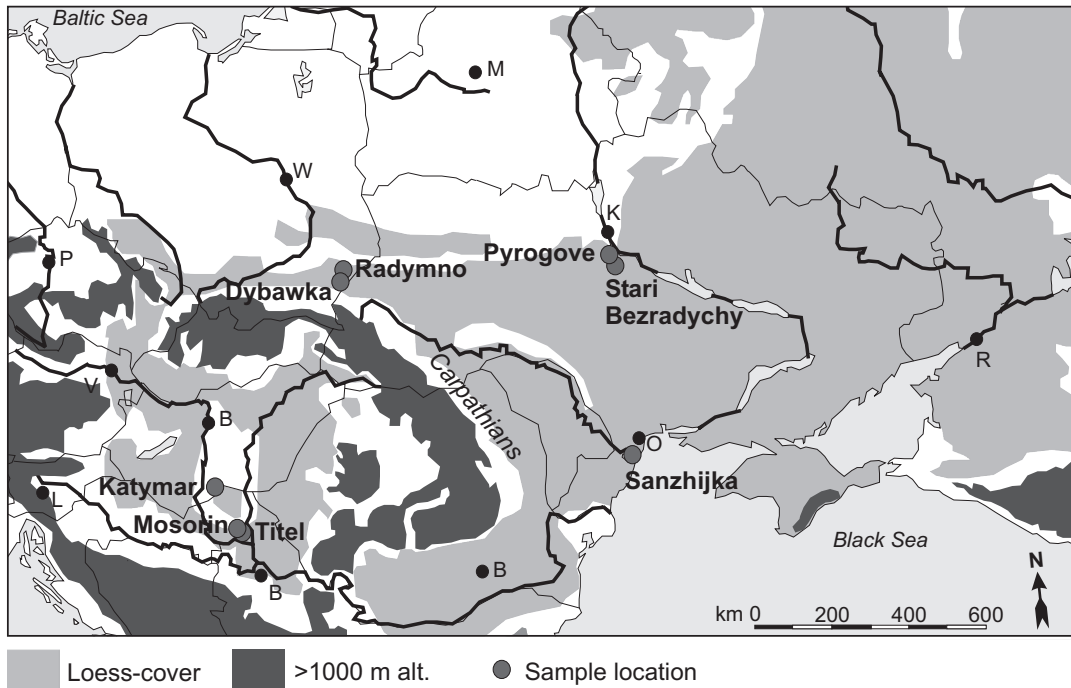
4.1 Introduction

The recognition of paleo-wind directions is of considerable importance in the reconstruction of atmospheric circulation patterns. Various suggestions of paleo-wind direction during the Last Glacial have been made, based on field data. Eolian dune morphology and orientation, grain-size trends of cover sands and loess, vertical relationships in cross sections, heavy metal provenance reconstructions, grain orientations and wind-polished rock surfaces have been investigated (for a detailed review, see Renssen et al., 2007). Most studies are done in western Europe (mainly The Netherlands and Belgium) focusing on the Weichselian Late Glacial and Late Pleniglacial. Most of these results indicate northern to western main wind directions. Some north-central European studies indicate also eastern directions.

Studies on wind directions in eastern and central Europe are scarcer. Geochemical and mineralogical bulk loess sediment analyses along the Danube in Romania have pointed out that the main loess sediment was transported by winds from a WNW to NNW/NNE direction, indicating forcing by northerly catabatic winds from the Fennoscandian ice sheet (Bugge et al., 2008). However, other authors state that the Black Sea shelf and the Aral and Caspian Sea arid lands also contributed to central and eastern European loess deposits (Conea et al., 1972, cited in Smalley and Leach, 1978; Stephens et al., 2003; Avramov et al., 2006), indicating southern and eastern winds must also have played a role. Nawrocki et al. (2006) derived a mean wind direction from W-SW during the Late Pleniglacial by the anisotropy of magnetic susceptibility on nine sites around the Polish-Ukrainian border.

Various modelling studies have been done to reconstruct the atmospheric circulation during (parts of) the Pleniglacial. Based on various data, Van Huissteden and Pollard (2003) modelled mean wind direction and intensity patterns in Europe. More recent modelling studies containing wind directions, focussed on the Late Pleniglacial and the Last Glacial Maximum (Renssen et al., 2007).

Studies on wind directions by field data never focussed on the Early, Middle and Late Pleniglacial separately. The geographical distribution patterns of loess occurrence and grain-size differentiation enable to reconstruct the wind direction. Such a procedure has shown, for instance, northern to northwestern wind directions for the loess supply into the Chinese loess plateau during the last 250 ka (Nugteren and Vandenberghe, 2004). Grain-size distributions revealed from endmember modelling algorithm (EMMA) studies of loess sediments showed promising detailed information on provenance,



4.1

transport and climate variability (Vriend, 2007; Prins et al., 2007; Prins and Vriend, 2007). They separated different loess components: a fine-grained signal that is mainly dominant in interglacial periods, and a coarse-grained signal that clearly decreases in relative amount in the direction away from the source area of the loess.

The loess in eastern and central Europe (for a general description on the characteristics see Haesaerts et al., 2003) was not studied in a similar way before. In this chapter we present new grain-size data from eight loess sections in eastern and central Europe, unmixed using the EMMA. The data are used to find the sources of the individual loess components in the study area, in order to derive the main wind directions during the Late, Middle and Early Pleniglacial in the region.

4.2 Methods

Sections

In paragraph 4.3 we describe eight sections from five locations in eastern and central Europe. At three of these locations we sampled two sections close to each other to separate local from regional variations (see also Chapter 1). Three of the eight analysed sections are situated west of the Carpathian Mountains, in the Pannonian (or Carpathian) Basin (fig. 4.1). This basin is completely surrounded by mountain ranges with peaks over 2000 m and is about 500 km from wide west to east.

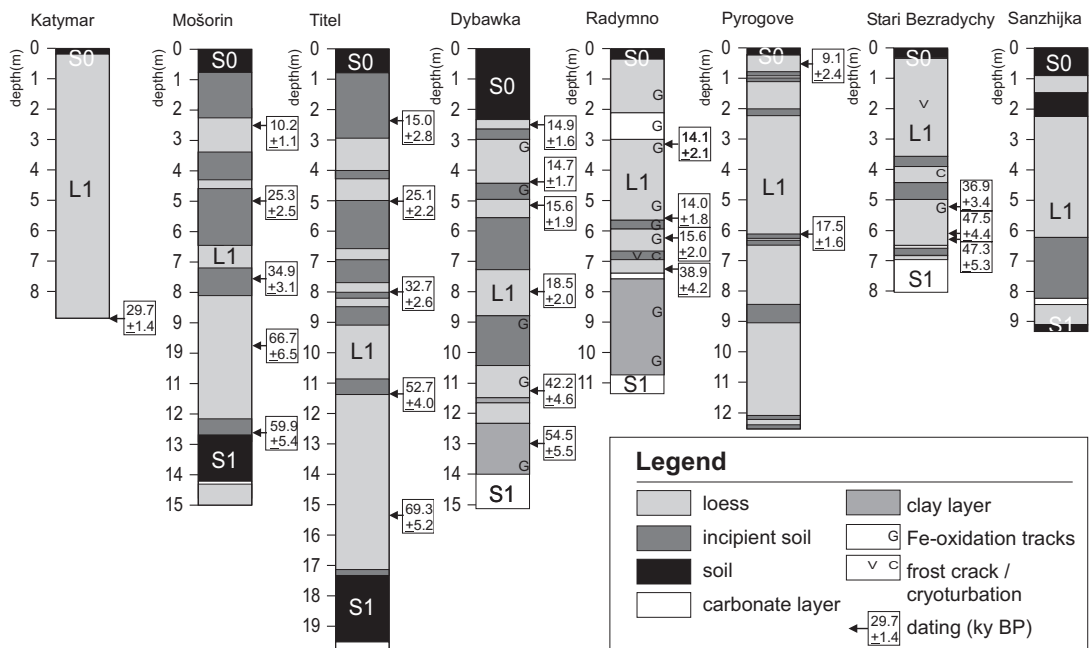
4.1 Locations of the eight sampled loess sections in eastern and central Europe. The dark shaded area indicates mountain ranges over 1000 m altitude, while the light shaded area indicates the loess distribution in the study area. P = Prague, W = Warszawa, M = Minsk, K = Kiev, R = Rostov, V = Vienna, L = Ljubljana, B = Budapest / Belgrade / Bucharest, O = Odessa.

The section Katymar is situated in southern Hungary, at the Serbian border, east of the valley of the Danube. The sections Mošorin and Titel are separated only 6 km from each other and are situated on the Titel Loess Plateau in the central part of Vojvodina, Serbia.

The other five sections are situated north and east of the Carpathian Mountains (fig. 4.1). The distance from the sections to the Carpathians varies between 50 km and 450 km. The sections Radymno and Dybawka are situated in Poland, near to the Ukrainian border. They are separated 20 km from each other. Section Radymno is situated on a large alluvial plain, 1 km south of the river San. Dybawka is situated in a more mountainous area in a large meander bench of the San. Pyrogove and Stari Bezradychy are both located at the west bank of the Dnepr, just south of Kiev, and are also separated 20 km from each other. Section Sanzhijka is located south of Odessa, at a Black Sea coastal cliff. Lithology and presence of (incipient) paleosols per section are plotted in fig. 4.2. The sections Stari Bezradychy, Pyrogove and Sanzhijka (Ukraine) are described in more detail Chapter 2, while the sections Titel and Mošorin (Serbia) are extensively described in Chapter 1.

Dating

25 samples, divided over six sections, were taken for IRSL dating. The analyses took place at the Institute for Applied Geosciences (GGA-Institut) in Hanover, Germany. The luminescence samples were pretreated under weak red light. The 4 to 11 μm fraction



4.2 Pedo-sedimentary logs of the eight sampled loess sections, showing macroscopic soil information. The dating results (IRSL and ^{14}C), are shown on the right side of each section.

Lab.nr.	Section	Depth (m)	Dose rate (Gy/ky)	Dose rate 1 σ (Gy/ky)	Paleodose (Gy)	Paleodose 1 σ (Gy)	Age (ky)	Age 1 σ (ky)	TL-age (ky) (Fedorowicz & Ł., 2004)	TL-age 1 σ (ky)
676	Dybawka	2.5			53.6	3.1	14.9	1.6	10.9	1.1
677	Dybawka	4.5			52.7	3.3	14.7	1.7	10.4	1.4
678	Dybawka	5.1			56.6	4.3	15.6	1.9	14.6	1.6
679	Dybawka	8.0			71.0	4.2	18.5	2.0	15.8	2.0
680	Dybawka	11.2			164.9	9.0	42.2	4.6	40.2	5.0
681	Dybawka	13.0			193.2	7.4	54.5	5.5	55.6	6.7
683	Radymno	3.1			50.2	4.1	14.1	2.1		
684	Radymno	5.6			48.4	2.9	14.0	1.8		
685	Radymno	6.2			57.6	3.7	15.6	2.0		
686	Radymno	7.2			145.4	5.4	38.9	4.2		
353	Pyrogove	0.55	3.06	0.22	27.8	7.1	9.1	2.4		
354	Pyrogove	6.1	3.14	0.22	55.0	3.3	17.5	1.6		
351	St. Bezradychy	5.17	3.21	0.25	118.5	5.8	36.9	3.4		
352	St. Bezradychy	6.07	3.64	0.27	173.0	9.2	47.5	4.4		
350	St. Bezradychy	6.10	3.00	0.24	142.0	11.5	47.3	5.3		
- (¹⁴ C)										
	Katymar	8.9	- (¹⁴ C)	- (¹⁴ C)	- (¹⁴ C)	- (¹⁴ C)	29.7	1.4		
345	Mošorin	2.5	3.82	0.28	38.6	3.0	10.2	1.1		
346	Mošorin	5.0	3.98	0.30	100.8	6.3	25.3	2.5		
347	Mošorin	7.55	3.83	0.29	133.4	6.4	34.9	3.1		
348	Mošorin	9.75	3.78	0.29	251.9	15.4	66.7	6.5		
349	Mošorin	12.55	3.92	0.30	234.5	10.9	59.9	5.4		
355	Titel	2.3	3.16	0.24	47.5	8.2	15.0	2.8		
356	Titel	5.0	3.89	0.29	97.7	3.6	25.1	2.2		
357	Titel	8.0	4.00	0.29	130.9	1.5	32.7	2.6		
358	Titel	11.35	3.54	0.26	186.6	4.0	52.7	4.0		
359	Titel	15.4	3.90	0.29	270.4	3.2	69.3	5.2		

T 4.1 Dating results of all samples from the study area. All samples are dated using the I¹⁴C-sample in Katymar (Hungary). The results of the Dybawka-section (Poland) are compared to TL-samples taken by Fedorowicz and Łanczont (2004).

was stimulated by infrared light (IRSL). The dose rate samples were calculated from the amounts of potassium (K), uranium (U) and thorium (Th). For measuring these elements the samples were grained, solved with concentrated HF-HNO₃-mixtures (10:1), dried, refluxed in 6 N HNO₃, dried and finally dissolved in a HNO₃ environment. The bulk concentrations of K, U and Th were measured by ICP-AES at the VU University Amsterdam (The Netherlands). A more detailed description of this measurement process is given by Eggins et al (1997). The average water content in the samples was estimated at 20%. For further information on the used dating method see Frechen et al. (1996).

At Katymar, Hungary, also a ¹⁴C-sample was taken from a charcoal layer. The sample was measured in the Laboratory of the Nuclear Research Centre of the Hungarian Academy of Sciences in Debrecen, Hungary (Willis et al., 2000). In the Dybawka section (Poland), Fedorowicz and Łanczont (2004) measured TL on samples from the same depths as we sampled in 2004.

Table 4.1 shows the dating results. In the Dybwaka section the upper two TL-samples are significantly younger than the IRSL-samples, while the others match better. The lowest IRSL sample in this section is estimated too young, while the TL sample from the same level is still in range with the other samples. All other IRSL samples are in chronological order.

Sedimentation and accumulation rate estimates

Loess appears often to be a mixture of eolian deposits from different sources. The transport of the components may take place by different mechanisms that are dependent – amongst others - on grain-size of the available sediment and the topography of the area. The geographical distribution pattern of loess and the dust sedimentation processes in the study region are controlled to some extent by the Carpathian Mountains with tops over 2000 m. These mountains behave as a filter for the dust supply to the sedimentation areas.

The mass accumulation rate (MAR in g/cm²/ky) indicates the amount of loess accumulated at a considered location. First, the absolute sedimentation rate per unit of the Pleniglacial (SR_{abs} in m/ky) was calculated based on the results of the grain size analysis. The calculation is done according to:

$$SR_{abs} = \frac{Unit_{th}}{Unit_d} \quad (4.1)$$

where Unit_{th} is the thickness of a sediment unit deposited during the Early, Middle or Late Pleniglacial (in m) and Unit_d is the duration of the relevant Unit (in ky). Second, the MAR was calculated using:

$$MAR = SR_{abs} \cdot BD \quad (4.2)$$

where BD is the bulk density of the sampled material in g/cm³. De value for BD is based

on field results by Nugteren (2002) and Kohfeld and Harrison (2003). The values used for calculation of the MAR are listed in table 4.2. We realise erosion or long periods of no sedimentation cannot be traced, but may influence our conclusions (see discussion section of this chapter). Soils and incipient soils are indicators for slower or no sedimentation, but an absolute quantification is hard to make.

Grain-size analyses and endmember modelling

All sections were sampled for grain-size analysis at 10-cm resolution. First the samples were pretreated with 1 M HCl and H₂O₂ to remove CaCO₃ and organic matter respectively. For a more detailed description of the pre-treatment process, see Konert and Vandenberghe (1997). The samples were measured for 56 intervals between 0.15 and 1682 µm using a Fritsch A22 Laser Particle Sizer.

The unmixing of the grain size dataset (n=957) was done using the inversion algorithm for endmember (EM) modelling of compositional data (EMMA) (Weltje and Prins, 2003; 2007). It constructs a mixing model that expresses the observations as mixtures of a limited number of EMs. First, the required amount of endmembers is defined by means of an 'error improvement significance' test. Second, the endmembers are composed and subsequently the calculation of the proportional contribution of the endmembers in each sample of the dataset. Model and procedure are described in detail by Weltje (1997). A more detailed description for application on loess can be found in Prins et al. (2007). The results by the EMMA model are used to calculate the proportion of each EM per unit of the Pleniglacial in all considered sections.

4.3 Descriptions of study regions and sites

West of the Carpathian Mountains

The Vojvodina region (northern Serbia) is mainly a lowland area covered by loess and loess-like sediments (Marković et al, 2008). Two sections on the Titel loess plateau, located in the central part of Vojvodina, were sampled for grain-size analyses. The plateau is situated between the rivers Danube and Tisa (Tisza/Theiss), about six kilometers north of their confluence, and is up to 55 meters high. The Danube and the

Depth	BD (coarse loess: U-ratio > 2.5) (g/cm ³)	BD (fine loess: U-ratio < 2.5) (g/cm ³)
0-4	1.5	1.6
4-7	1.5	1.7
7-12	1.6	1.7
12-14	1.6	1.8
14-25	1.7	1.8

T 4.2

T 4.2 Values for bulk density (BD) of loess deposits, used for the calculation of the mass accumulation rates for each Pleniglacial unit in the sampled sections. The value is dependent on the grain size and compaction. The values and transitions are based on Nugteren (2002) and Kohfeld and Harrison (2003).

Tisa eroded both sides of the loess plateau. The most detailed loess records are located north of Titel, at the southeastern part of the plateau. Katymar is located in southern Hungary, just 100 m from the Serbian border. Schematic logs of the sections west of the Carpathians are in fig. 4.2.

Katymar (Hungary)

A small brickyard exposes a 9 m section. The top contains a chernozem soil with a thickness of 1.2 m. At the base a charcoal layer was found. The loess is not disturbed by any other soils in between. The last interglacial soil (S1) is not reached. In the base of the section, at 8.9 m, a charcoal layer was found and ^{14}C -dated 29.7 ± 1.4 ka. Therefore we conclude almost the whole section was deposited during the Late Pleniglacial.

Mošorin (Serbia)

A valley cut is situated 6 km north of Titel, near the village of Mošorin. The sediments have a thickness of 15 m from the top of the Holocene soil (S0) down to the base of S1. The Holocene soil is clearly visible and consists of a 65-cm thick dark chernosem, followed by a thin transition horizon containing small CaCO_3 -nodules. The soil complex contains crotovinas. The Upper Pleniglacial loess contains an incipient soil of 1 m at the top and a smaller one between 3.40 m and 4.30 m. The top of the Middle Pleniglacial loess is marked by a more developed mollic horizon of 30 cm. The Middle Pleniglacial deposits are marked by two incipient soils with a thickness of 1.6 and 1 m respectively. The Lower Pleniglacial loess is slightly coarser and contains Mn-spots. The last interglacial deposit contains a soil complex, consisting of a 50 cm-thick weakly developed soil, followed by a 1.8 m-thick chernozem (S1). Both soils contain crotovinas. The lower part of S1 contains large nodules of CaCO_3 .

Titel (Serbia)

The brickyard under study is situated 1 km north of Titel. The sediments have a thickness of 19.8 m from the top of the Holocene soil (S0) down to the base of the last interglacial soil (S1). The Holocene soil consists of a chernozem of about 80 cm, followed by a thin transition horizon containing small CaCO_3 -nodules. The soil complex contains crotovinas. The Late Pleniglacial loess contains an incipient soil of 2 m at the top and a smaller one between 3.70 m and 4.10 m. The top of the Middle Pleniglacial loess is marked by a soil complex containing two incipient soils and a more developed mollic horizon, possibly representing a chernozem. The central part of the Middle Pleniglacial deposits contain three incipient soils, separated by loess containing Mn-spots, while the lower part becomes sandier. The base of the Middle Pleniglacial loess is marked with an incipient soil. The Early Pleniglacial loess becomes clearly coarser and contains many sandy layers. The lower part is finer and contains Mn-spots. The Last Interglacial deposit contains a soil complex, consisting of a 40 cm-thick weakly developed soil, followed by a 2 m-thick chernozem. Both soils contain crotovinas. The lower part of S1 contains large nodules of CaCO_3 .

East of the Carpathian Mountains

About 70% of the territory of Ukraine consists morphologically of flat land, almost completely covered with loess. The average thickness of the last glacial loess is smaller than it is in Serbia. Local paleo-depressions contain relatively thicker loess deposits. The Polish sections are situated a few kilometres from the border with Ukraine (fig. 4.1), near the city of Przemyśl. They are located in the forelands of the northern Carpathians. Schematic logs of the sections east of the Carpathians are in fig. 4.2. The IRSL-dating results are plotted next to each section.

Dybawka (Poland)

The Dybawka loess section is situated in the Przemyśl Foothills, about 7 km westwards of the city of Przemyśl (Łanczont, 1995). It represents loesses forming an eolian cover on the so-called middle (Vistulian) terrace of the San River. The section (a loess cliff) is located at the highest point of this terrace. The top of the exposure occurs at 223 m a.s.l., while the San River channel is at 196.7 m a.s.l. The top of the section contains a 2.3 m thick luvisol with a thick layered Bt-horizon. The loess contains some incipient soils and gley zones. From 11.45 m downward the loess becomes clayey. Sands and gravels of channel facies (Eemian and Wartanian) occur in the lower part of the section. The upper four dating results suggest relatively thick Late Pleniglacial deposits, as the top 8 meters of loess have been deposited in 18.5 ± 2.0 ka, while the 5 m below were deposited between 54.5 ± 5.5 ka and 18.5 ± 2.0 ka. Middle Pleniglacial sediments were deposited at a slower rate, or were eroded at times. They are more clayey than the Late Pleniglacial loess.

Radymno (Poland)

The Radymno section was recently described by Fedorowicz and Łanczont (2004) and Łacka et al. (2007). The loess profile is situated in a brickyard north-east of the town Radymno. The loess covers the Pleistocene terrace of the river San. The section shows a weakly developed, truncated chernozem at the top, overlying a loess that contains several carbonate concretion layers and gley zones. Below 5.70 m two soils appear. The lower soil and the clayey loess below are heavily cryoturbated and a frost crack occurs. From 9.55 m downward the deposits become extremely clayey, with dark grey, black and brown colours (see also fig. 4.2). They represent a humic floodplain sedimentation. The Eemian soil is represented by a gleyed illuvial horizon in the lowest part of this section. Also here the dating results suggest high sedimentation rates during the Late Pleniglacial: 6.2 m loess deposits in 15.6 ± 2.0 ka. The Middle Pleniglacial deposits are more clayey than the Late Pleniglacial loess.

Pyrogove (Ukraine)

The section at Pyrogove is located in a recent brickyard. The Late Pleistocene loess has a thickness of 12.80 m. The Holocene soil consists of 50-cm thick dark brown mollic

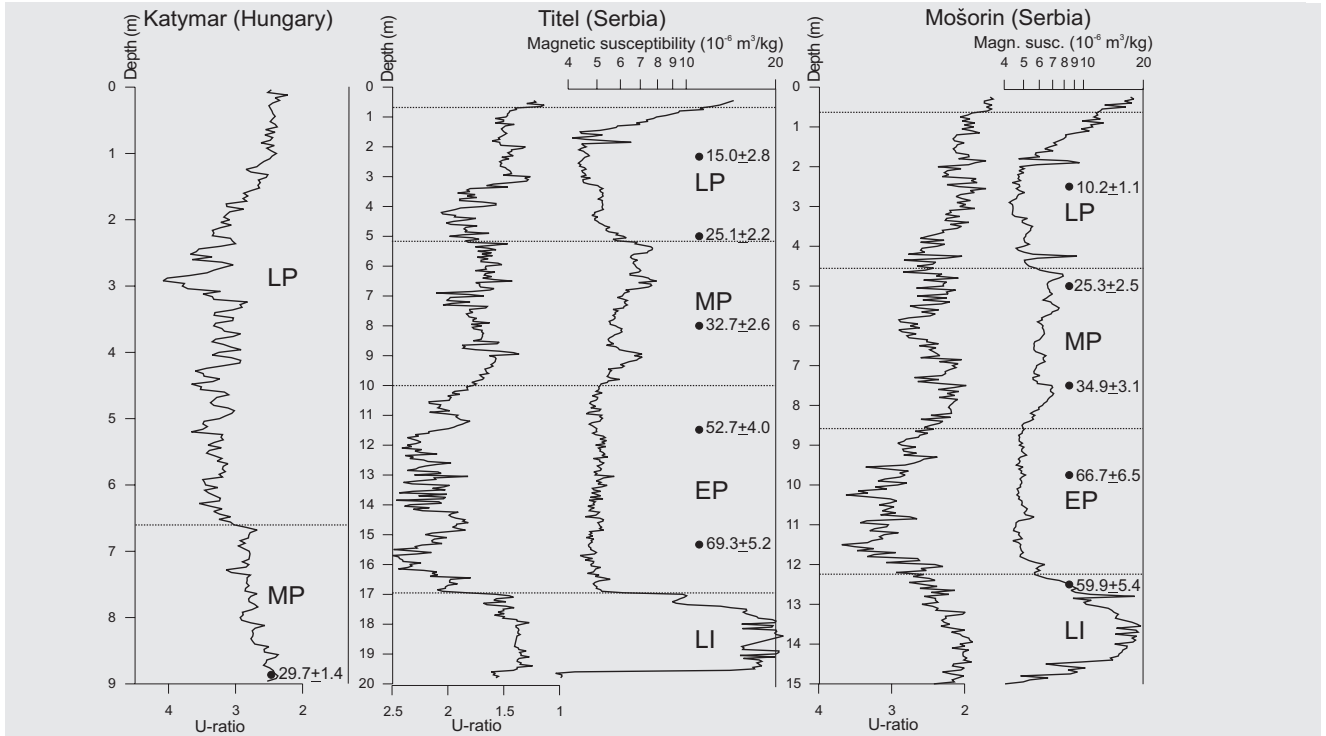
material. The upper 5.50 m of the loess is horizontally stratified in its lower part and contains seven incipient soils. Carbonate precipitation spots are found between these soils. Below 11.50 m the sediment is clearly more heterogeneous: coarser grained and gravelly on the average, but also more clayey than the overlying sediments. A humic soil occurs below 13.80 m. This lower part of the sequence is interpreted as Mid Pleistocene Dnieper till deposits. Again, the dating results suggest high sedimentation rates in the Late Pleniglacial. The uniformity of the section from 0.5 m down to 11.5 m and the dating at 6.1 m, suggest this whole part was deposited during the Late Pleniglacial.

Stari Bezradychy (Ukraine)

The total thickness of the Late Pleistocene loess is about 7 m and is exposed in a gully. The section was first described by Gerasimenko (2001) and Rousseau et al. (2001). The Holocene soil is exposed as an 80-cm thick remnant of a chernozem. The loess deposits below this soil contain an incipient soil and a brown rendzina containing frost cracks. The rendzina is situated between relatively coarse silt layers. About 4.10 m below surface, small cryoturbation structures were found. A frost crack occurs from 6.40 m downward. Two intersecting prismatic calcium-carbonate-rich layers are found at 6.50 m and at 6.80 m below surface. Below 6.80 a pedocomplex occurs, consisting of a truncated, thin, dark-brown soil, 10 cm loess and a chernozem soil. This soil superimposes the top of Mid-Pleistocene glaciofluvial deposits. Three IRSL-dating results between 5 m and 6.5 m suggest deposition during the Middle Pleniglacial. The upper 3.5 m contains no clear incipient soils and is therefore interpreted as deposited during the Late Pleniglacial. This interpretation corresponds with the conclusions of Gerasimenko (2001) and Rousseau et al. (2001).

Sanzhijka (Ukraine)

The Sanzhijka section (Matviishina, 1990) is located at a cliff along the Black Sea. The present soil is a chernozem, underlain by a carbonate rich layer. Beneath the Holocene soil a second soil complex is intercalated, consisting of three greyish to brown soils. The lowermost soil is a chernozem. A 20-cm thick loess layer marks the transition between the uppermost two soils. According to Matviishina (1990) a series of ice-wedge casts marks the transition between the second and the third soil. During the time of sampling these ice-wedge casts were not observed. The loess below 3.50 m is loamy at the base and contains interruptedly weak incipient soils. Three reddish-brown soils are intercalated in the loess between 6.50 and 8.70 m below surface. The uppermost soil contains abundant slats, mainly gypsum. The other two soils are loamy and somewhat browner than the first one. The loess below these soils is richer in clay than the loess deposited during the Late Pleniglacial and has a thickness of only 50 cm. It covers a loamy and brownish S1 with a prismatic structure. Down to 6.50 m the loess is not intersected by clear paleosols, indicating it is deposited during the Late Pleniglacial. The three reddish-brown soils of Middle Pleniglacial age overly a thin Early Pleniglacial deposit. The section was sampled until the top of the last interglacial paleosol.



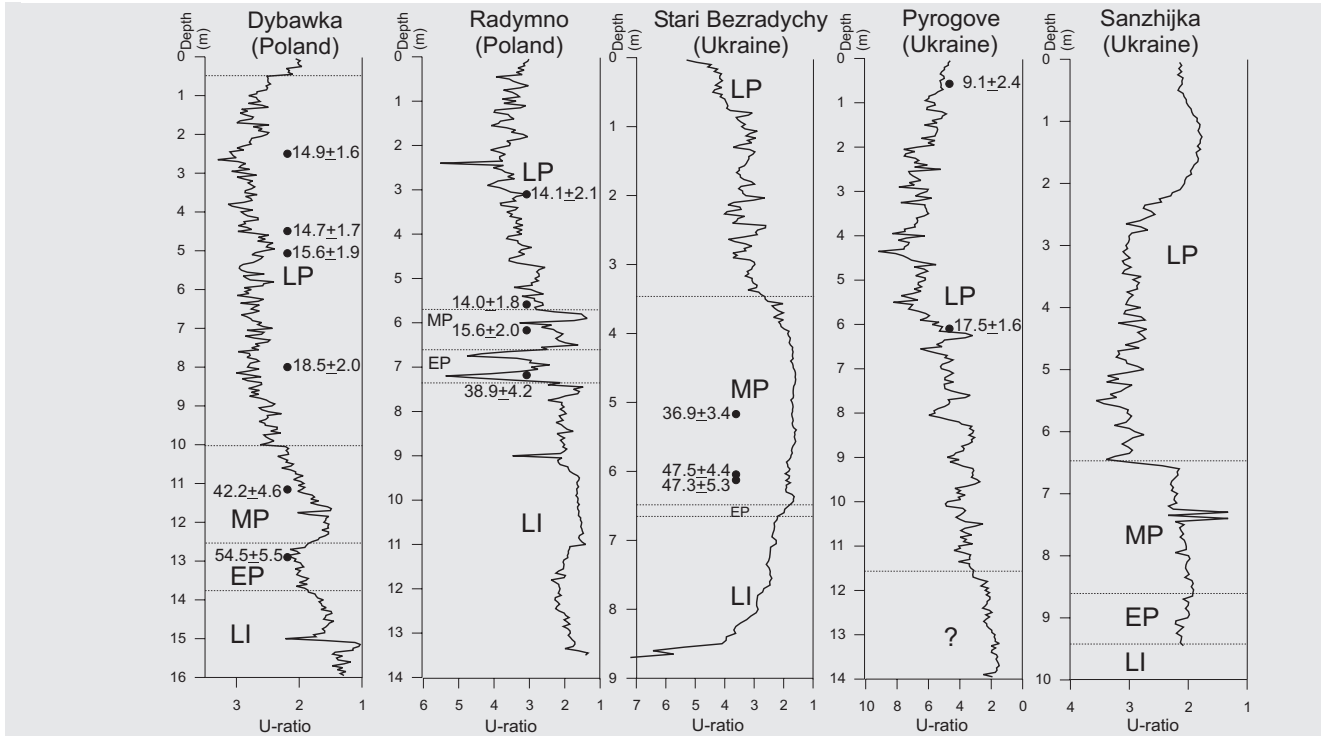
4.3a

4.4 Chronostratigraphic subdivision

Martinson et al. (1987) defined the transitions between marine isotope stages at 75 ka BP (transition MIS 5-4), 59 ka BP (transition MIS 4-3), 24 ka BP (transition MIS 3-2) and 12 ka BP (transition MIS 2-1). Following Woillard and Mook (1982) and Vandenberghe (1985), we assume that MIS 4, 3 and 2 roughly correspond with the Early, Middle and Late Pleniglacial respectively on the European continent. The transitions between the MIS-equivalent loess units in our sections are based on the field characteristics, the U-ratio and absolute datings (fig. 4.3a-b). The U-ratio is the ratio of two grain-size intervals: 16-44 μm / 5.5-16 μm (Vandenberghe et al., 1985). In addition, the transitions between the stages are also defined by magnetic susceptibility results from the Titel and Mošorin sections (fig. 4.3a) (see also Chapter 1).

The Last Interglacial is typified by a clear paleosol and in general a relatively low U-ratio. During the Early Pleniglacial the loess is characterised by a high U-ratio. It is generally very thin in the area east of the Carpathian Mountains. The transition of Early

4.3 U-ratios of the sections west (**4.3a**) and east (**4.3b**) of the Carpathian Mountains (U-ratio is defined as the ratio of the grain-size fraction (16-44 μm) / (5.5-16 μm) according to Vandenberghe et al. (1985)). The U-ratios, combined with datings and field descriptions, were used to subdivide the loess sections in Late, Middle and Early Pleniglacial loess. For the sections Titel and Mošorin also the magnetic susceptibility results were necessary to derive this subdivision. The numbers in the section plots represent dating results, including their standard deviations, expressed in ky BP. The dating in Katymar is an AMS-dating, while all others are IRSL datings.



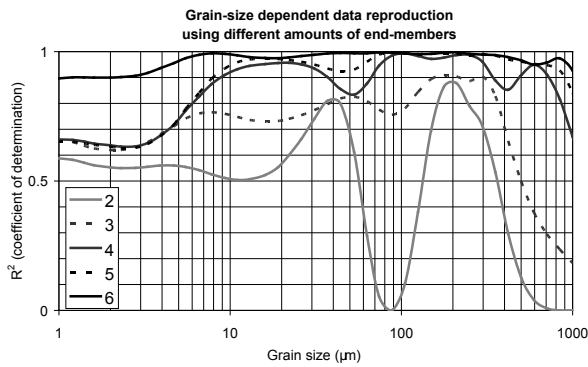
4.3b

to Middle Pleniglacial deposits is recognized by a fining trend in most cases (Dybawka (Poland), Mošorin and Titel (Serbia)). In addition, incipient soils may indicate Middle Pleniglacial deposits, sometimes underlain by a carbonate concretion layer. In this way we defined the Early to Middle Pleniglacial transition in Radymno (Poland), Stari Bezradychy and Sanzhijka (Ukraine).

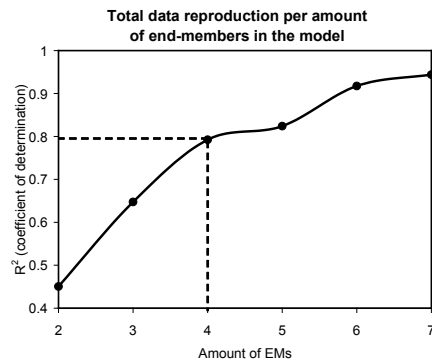
The Late Pleniglacial is characterized by relatively high U-ratio values and weak or no soils visible in the field. The transition from the Middle to the Late Pleniglacial is sometimes marked by a relatively clear incipient soil. We define this transition in this way in Dybawka (Poland), Stari Bezradychy and Sanzhijka (Ukraine). In Radymno (Poland) and Pyrogove the transition was based on low U-ratios in the Late Pleniglacial. At Mošorin and Titel (Serbia) a slight grain-size coarsening, the IRSL dates and the transition to low MS-values in the Late Pleniglacial mark the transition with the Middle Pleniglacial. The transition at Katymar (Hungary) is based on a small but distinct increase of the mean grain size and the position of a dated charcoal layer.

4.5 Endmember composition and interpretation

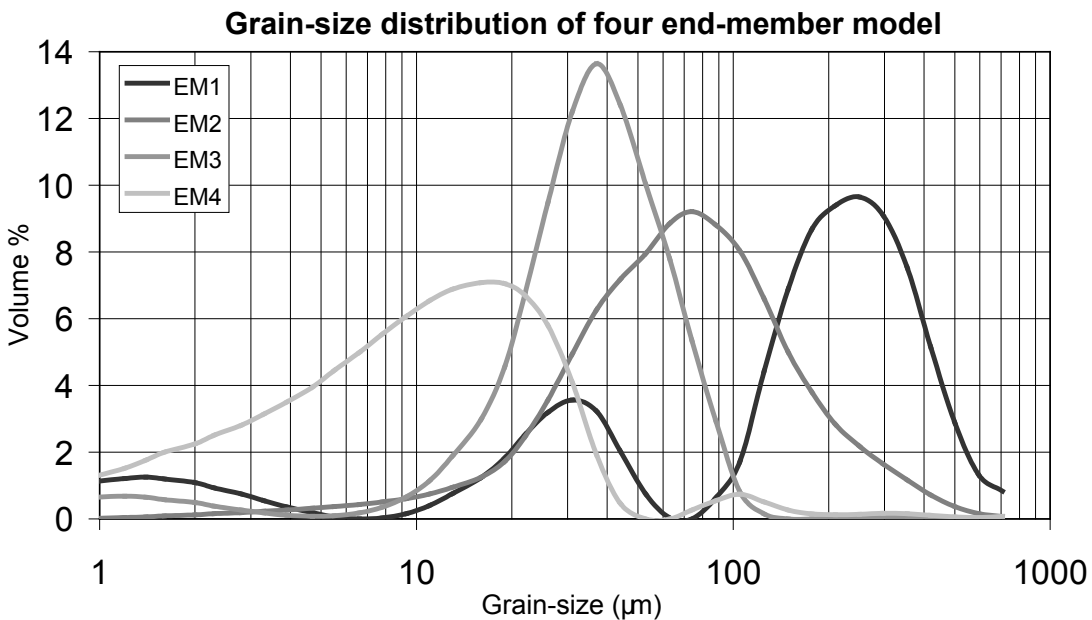
The EM-modeling results show that 80% of the data can be reproduced by using a four EM-model (fig. 4.4a). A smaller amount of EMs would result in insufficient data simulation, while more EMs will only significantly increase the data reproduction <10



4.4a1



4.4a2



4.4b

4.4a Data reproduction by the endmember model.

4.4a1 Each line represents a model run with a unique amount of endmembers. The more endmembers used in the model, the more data is reproduced, but the more difficult the interpretation of each endmember will be. In this case a four endmember model is chosen, as it explains 80% of the data in the grain-size range 5-850 μm . Model runs with less endmembers explain 75% or less of the silt-sized range, while models with more endmembers show only major improvements in data reproduction in the range $<10 \mu\text{m}$.

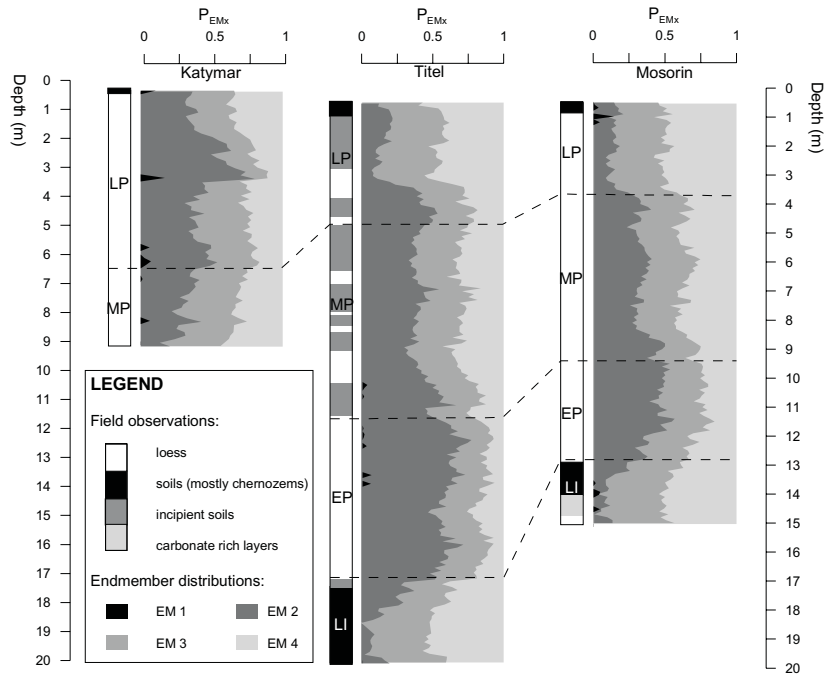
4.4a2 Total data reproduction per model run with different amounts of endmembers.

4.4b Distribution of the four-endmember model over the grain-size categories. Each endmember represents a distribution over a range of grain sizes with a specific optimum. The optima for the EMs 1 to 4 are respectively 250 μm , 74 μm , 37 μm and 16 μm .

μm and make the interpretation more complex. The resulting EMs have modal grain-sizes of 250 μm (EM1), 74 μm (EM2), 37 μm (EM3) and 16 μm (EM4) (fig. 4.4b). The optimum grain-sizes correspond roughly to the findings of EM-modelling results on the Chinese Loess Plateau by Prins et al. (2007, optima at 63, 40 and 19 μm) and Prins and Vriend (2007, optima at 63, 37 and 22 μm). They suggest that their two coarsest EMs are transported by low altitude dust outbreaks from the source areas. The ratio of both these EMs alternate strongly, parallel to loess-paleosol variations. The finest EM shows relatively constant behaviour in their study area, and is interpreted as partly being the result of fine dust transport by high altitude westerly airstreams, as suggested before by Sun et al (2004). We assume that the EMs in the European loess may be interpreted in a comparable way. As a consequence, the respective EMs may be considered as the sedimentary products that result from specific geomorphological or sedimentological processes. Mabutt (1977), Pye (1995) and Lehmkuhl and Haselein (2000) showed that grains with a diameter between ~ 90 and ~ 300 μm are mainly transported by eolian saltation and grains between ~ 15 and ~ 90 μm are mainly transported in low suspension clouds, while grains $< \sim 15$ μm can be transported highly in the atmosphere. EM1 is a sandy component, and thus mainly transported by saltation. As sands saltate mainly over relatively small distances, sandy areas in the direct neighbourhood of the section are probably the main source. Possibly the presence of such areas, like river beds, control the presence of this EM.

We interpret EM2 and EM3 deposits as the result of near-surface to low-altitude transport processes, as suggested by Prins et al (2007) and Prins and Vriend (2007) for EMs with a comparable grain-size. As the transport height of these processes is in actual situations maximum a few hundreds of meters above the surface, we assume that the transport ways of these silty deposits are strongly influenced by topography.

EM4 has a grain-size comparable to the finest EMs found on the Chinese Loess Plateau, so we assume that this EM is partly transported at high altitudes (Prins et al., 2007; Prins and Vriend., 2007). As a consequence, topography plays a smaller role in the spatial distribution of this EM. It is striking that EM4 has a fine-grained tail in fig. 4.4b. It might be possible that comparable tails in loess grain-size distributions from the Chinese Loess Plateau may be influenced by mineral-selective weathering processes and physical breakdown of grains into smaller ones by means of a secondary process (e.g. Xiao et al., 1995; Porter and An, 1995; Kemp, 2001). However, results of two loess-paleosol and red-clay sequences by Sun et al (2006) and Vandenberghe et al (2004), indicate that weathering processes are of negligible influence on grain-size distributions in loess deposits, except for extremely weathered interglacial soils in southerly locations on the Chinese Loess Plateau. The best explanation for the fine-grained tail is the transport of fine loess in aggregates, held together by electrostatic forces, salts or organic matter, as indicated by Pye (1995). The presence of these potential aggregates are found as a fine grained tail in our loess data, since they would be broken down in the grain-size preparation procedure.



4.5a

4.6 Analysis of the geographical variation and temporal evolution of EM proportions and mass accumulation rates

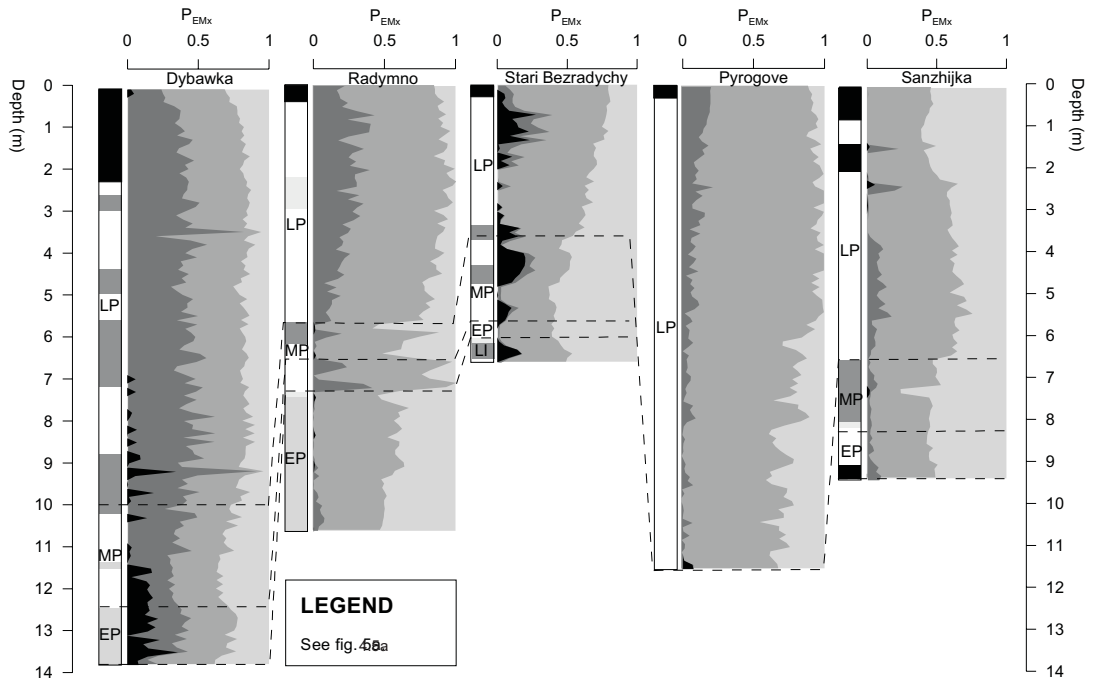
Endmember proportions

Figs. 4.5a and 4.5b show the results of the EM-proportions of each section. Both figures show a large variety between the sections. Generally, the Late and Early Pleniglacial show a large proportion of coarse EMs, while the Middle Pleniglacial shows a lower content of coarse EMs.

Figure 4.5b shows the data in the sections east of the Carpathians. Note that the sections Dybawka and Radymno (Poland) and the sections Stari Bezradychy and Pyrogove (Ukraine) are situated close to each other. The proportion of EM2 in the Late Pleniglacial deposits plays a more important role in the sections Dybawka and Radymno (proportion ~0.2 to 0.3) than in Stari Bezradychy and Pyrogove (proportion <0.1). In Sanzhijka the proportion of EM2 is about equal to or even less than in Stari Bezradychy and Pyrogove. The section Stari Bezradychy shows relatively large proportions of EM1. This EM behaves comparably to EM2, but almost independent of EM3 and EM4. In the other sections EM1 is not very abundant in our results (figs. 4.5a and 4.5b). For these reasons we assume that they have a comparable transport mechanism and/or source distance and take EM 1 and 2 together in our discussion from now on.

The results of the EM-proportions are plotted on a map for the Early, Middle and

4.5 Distributions of the endmember proportions over all samples of the sections west (**4.5a**) and east (**4.5b**) of the Carpathian Mountains. EM1+2+3+4 are always 100%.

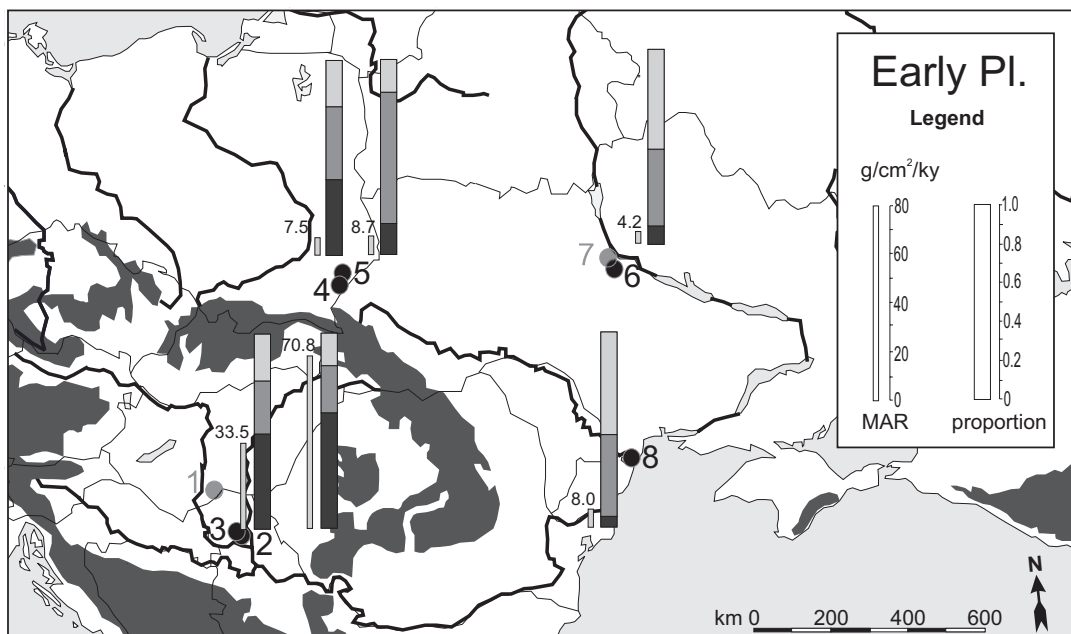


4.5b

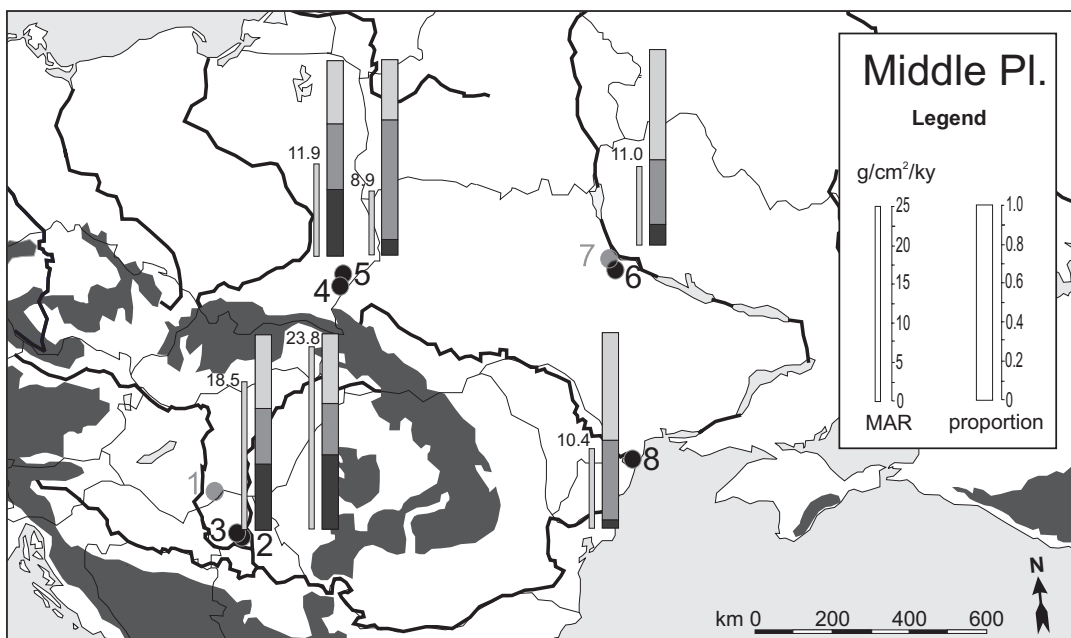
Late Pleniglacial in respectively figs. 4.6a, 4.6b and 4.6c. Fig. 4.6a, representing the Early Pleniglacial situation, shows a clear contrast of EM-proportions east and west of the Carpathian Mountains. Stari Bezradychy and Sanzhijka (Ukraine, east of the Carpathians) are very similar: both sections have very low proportions of EM1+2, while EM3 and EM4 are about equal. Dybawka and Radymno (Poland) show higher proportions of EM1+2, while EM3 is dominant in Dybawka. EM4 plays a minor role in these sections. However, west of the Carpathians, the sections Mošorin and Titel show a dominance of EM1+2 over EM3 and EM4.

Considering the sections east of the Carpathians during the Middle Pleniglacial (fig. 4.6b) and comparing them to the Early Pleniglacial situation (fig. 4.6a), there is a strong similarity of the EM-proportions. This contrasts with the sections west of the Carpathians where the proportions of EM1+2 have decreased in favour of EM3 and EM4. The proportions of EM3 and EM4 are about equal to each other (like during the Early Pleniglacial), while both EMs increase compared to the Early Pleniglacial deposits.

Strikingly, fig. 4.6c, representing the situation in the Late Pleniglacial, shows a different picture. In the area east of the Carpathians the proportions of EM3 increase relative to EM4, while the proportions of EM1+2 remain comparable to the Late and Early Pleniglacial situation. The Polish sections are an exception as the proportion of EM1+2 increases here in both sections. Loess sedimentation started at the section Pyrogove in the Late Pleniglacial. The EM proportions in this section show a striking dominance of EM3. The loess at Pyrogove probably accumulated in a paleo-depression,

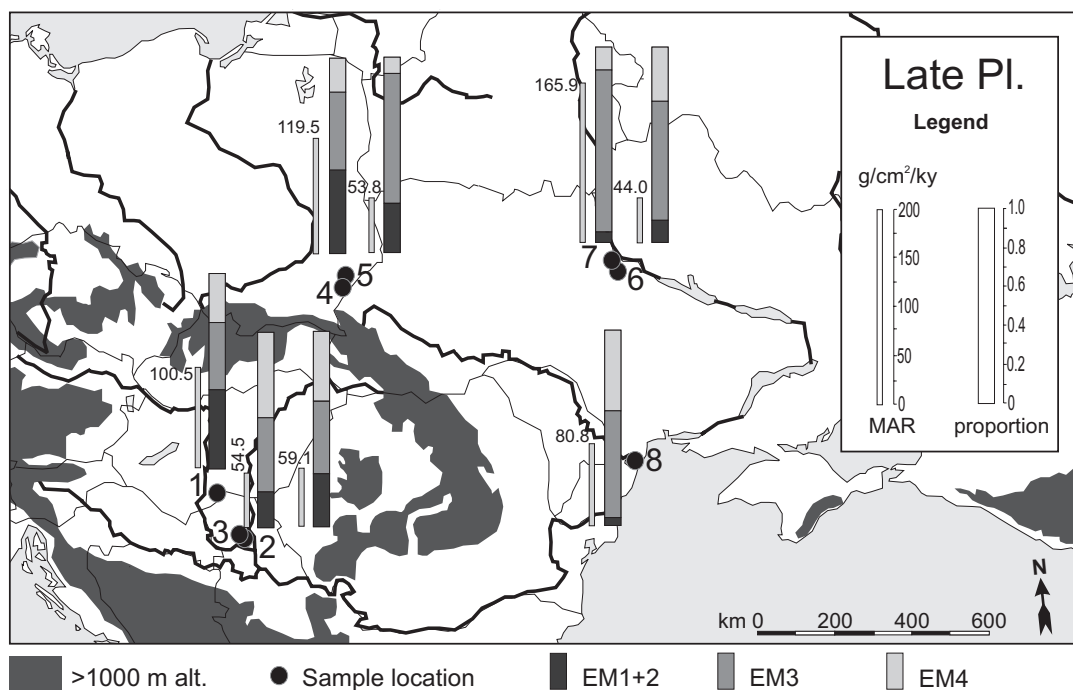


4.6a



4.6b

4.6 Mass accumulation rates (in $\text{g/cm}^2/\text{ky}$) of loess deposition and endmember proportions of the total sedimentation at each location at six studied sections during the Early Pleniglacial (**4.6a**), the Middle Pleniglacial (**4.6b**) and the Late Pleniglacial (**4.6c**). The proportions of EM1 and EM2 are taken together. At the sections Katymar and Pyrogove no or negligible deposits originating in the Early or Middle Pleniglacial were sampled. Note that the scale of the mass accumulation rates (MARs) differs on each map. The numbers refer to the studied loess sections: 1. Katymar (Hungary), 2. Titel (Serbia), 3. Mošorin (Serbia), 4. Dybawka (Poland), 5. Radymno (Poland), 6. Stari Bezradychy (Ukraine), 7. Pyrogove (Ukraine), 8. Sanzhijka (Ukraine).



4.6c

existing from the end of the Middle Pleniglacial onward, which was possibly sensitive for loess accumulation by one type of wind or transport mechanism, resulting in this EM3 dominance. Strikingly, in the area west of the Carpathians the proportion of EM1+2 has decreased in the Early Pleniglacial, while EM4 remains comparable to EM3. This drop of EM1+2 and rise of mainly EM4 was relatively abrupt, as clearly visible in fig. 4.5a, sections Titel and Mošorin. In contrast, loess deposition started only from the late Middle Pleniglacial onward at Katymar (Hungary) (like at Pyrogove in Ukraine), with high proportion of EM1+2 compared to the Serbian sections. The unexpected abrupt change in EM proportions in the Late Pleniglacial deposits in the Serbian sections is not found in Katymar (or any other section in the study area). Therefore we conclude it is probably of local origin.

Mass accumulation rates

The results of the mass accumulation rates and EM-proportions are plotted in figs. 4.6a, 4.6b and 4.6c, next to each proportion column. In the Early Pleniglacial situation (fig. 4.6a), there is a clear contrast of the MARs between both sides of the Carpathian Mountains. In the area west of the Carpathians, sedimentation rates range up to more than 70 g/cm²/ky on average. The large difference between Titel and Mošorin indicates that the sedimentation is controlled by local conditions. However, in the area east of the Carpathians sedimentation rates are extremely low at all sections, ranging from 4.2 to 8.7 g/cm²/ky on average. The structural character of these low sedimentation rates

during the Early Pleniglacial indicates control by low sediment availability and not by erosion processes.

Considering the sections east of the Carpathians during the Middle Pleniglacial (fig. 4.6b), it is striking that all sections in this area show a slight increase of MAR-values compared to the Early Pleniglacial Situation. Note that the scale of the MAR column has changed. The Middle Pleniglacial is generally considered warmer than the Early Pleniglacial. Therefore, the increase of the MARs east of the Carpathians is unexpected and contrasts with the sections west of the Carpathians where the MAR-values clearly decrease.

Fig. 4.6c, representing the situation in the Early Pleniglacial, shows a completely different picture. Note that the scale of the MAR column has changed again. During the Early Pleniglacial all sections east of the Carpathians have much higher MAR-values than before. The MAR-values west and east of the Carpathians are on average more equal to each other than during the Early and Middle Pleniglacial, but the variation between the sections is large, even between sections that are situated close to each other. Dybawka shows much higher MAR-values than Radymno. In northern Ukraine it is striking that the MAR is about four times higher in Pyrogove than in Stari Bezdychy, while the sedimentation rate of Pyrogove in general was insignificant during the Early and Middle Pleniglacial. West of the Carpathians the MAR-values have also increased compared to the Early and Middle Pleniglacial situation (figs. 4.6a and 4.6b). The MARs in this area are relatively low compared to the area east of the Carpathians, but about equal to each other. Sedimentation in Katymar started at the end of the Middle Pleniglacial (see also fig. 4.5a), showing higher MARs than in the Serbian sections.

Considering the whole picture, figures 4.6a-c indicate that the MARs in the study area are strongly varying in space and thus controlled by local factors, like (temporary) eolian morphology, vegetation and sediment availability. Erosion plays no controlling role, as most sections show a similar sedimentary evolution, for instance low MARs in all the sections east of the Carpathians during the Early and Middle Pleniglacial and high MARs in the Late Pleniglacial. The latter examples indicate that climate change or other general factors are also of major importance for the loess distribution in this area.

4.7 Discussion of grain-size variability

Various loess section studies spanning the whole Chinese Loess Plateau have shown a slight decrease from sandy loess in the north part, via silty loess in the central part to clayey loess in the south part of the plateau (e.g. Liu, 1985; Nugteren and Vandenberghe, 2004; Yang and Ding, 2004). The source areas of the loess are therefore most likely the Mongolian and Gansu desert areas on the north side of the Chinese Loess Plateau (e.g. Derbyshire et al., 1998; Sun et al., 2003; Ta et al., 2004). EM research has pointed out that the loess consists of a relatively constant fine-sized signal, becoming relatively more important towards the south, and a medium and a coarse silty loess component,

alternating parallel to loess-paleosol sequences, becoming less important southward (Prins et al., 2007; Prins and Vriend, 2007).

As stated before, the grain-size optima found over the whole Chinese Loess Plateau show a high similarity to our results. EM4 is a fine-grained loess component, while EM3 and EM1+2 are medium and coarse loess components respectively. A relative decreasing trend of medium and coarse grained components, would therefore point to a larger distance from the source area. However, the source area of the loess in the European situation is less clear than in the Chinese situation. Loess is suggested to have local sources like river plains (e.g. Buggle et al., 2007) as well as a large region, like the proglacial zone in north-central Europe (e.g. Nawrocki et al., 2006). Apart from that, the observed alternations of the two silt-sized EMs in China are less expressive in the European situation (in this paper these are EM2 and EM3). This indicates that the European loess distribution patterns are more complex than the Chinese ones.

The EM proportions and MARs indicate some general trends that may indicate generally valid conditions. A major change appears between the Middle and the Late Pleniglacial east of the Carpathians. During the Early and Middle Pleniglacial MARs were extremely low, while the MARs were very high during the Late Pleniglacial. The expected climate change to colder and drier conditions at this transition (e.g. Bos et al., 2001; Haesaerts et al., 2003) may partly explain the major increase in loess accumulation. Cold and dry conditions provoked a decrease of vegetation cover and thus a general increase in sediment availability. This explains the sudden increase at all locations east of the Carpathians. The different MARs throughout the region can be explained from varying local (e.g. geomorphological) conditions. However, the MARs in the area east of the Carpathians did not respond in an opposite way to the expected climate change to warmer and moister conditions between the Early and Middle Pleniglacial. In contrast, the sections in the area west of the Carpathians show clearly decreasing MARs and a decrease of EM1+2 relative to EM3 and EM4. Therefore a change to a drier and colder climate is not the only process responsible for the major change in sedimentation rates between the Middle and Late Pleniglacial.

Another factor that may change accumulation rates is an increase of wind speeds between the Middle and Late Pleniglacial. This would result in an increase of EM1+2 and EM3 compared to EM4. The Polish sections show this increase, while EM3 becomes more important in Stari Bezdychy. However, no increase can be seen in the proportions of EM1+2 or EM3 in Sanzhijka. Apart from that, the reduction of the EM1+2 proportions and the MARs in the Serbian sections can not be explained in this way. The different MARs and EM proportions at both sides of the Carpathians at the Middle and Late Pleniglacial transition indicate that both regions have different loess sources in both space and time.

A change of source areas may be explained by changing wind directions. These wind directions may be derived from the spatial distributions of EM proportions, similar to

the Chinese Loess Plateau situation, as described by Prins et al (2007) and Prins and Vriend (2007). During the Late Pleniglacial (fig. 4.6c) in the area east of the Carpathians the proportion of EM1+2 is higher in the northwestern (Polish) sections than in the eastern and southern (Ukrainian) sections, suggesting that the Polish sections were in an upwind position from the Ukrainian sections. In Sanzhijka the proportion of EM4 is more important than in the Polish or northern Ukrainian sections. From these data we can derive a wind direction in this period of north to northwest. If that is true, the proglacial zone in north central Europe is the obvious source of the large amounts of loess that have accumulated in our study area east of the Carpathians. On the other side of the Carpathians, Katymar shows a higher proportion of EM1+2 than the Serbian sections. Despite no conclusions can be made from this single situation, it fits our estimation of a general northern to northwestern wind. This area is surrounded by mountainous areas over 1000 m altitude, so that low altitude dust transport can probably not pass these mountains. Therefore, we assume that the loess sediments in this area originated from local river plains from the Danube, Sava and Tisa rivers in the Pannonian Basin, as well as from the ice margin of the eastern Alps. The abrupt decrease of EM1+2 relative to EM3 and EM4 in Titel and Mošorin may therefore also indicate a very local change in sediment availability.

The EM proportions during the Early and Middle Pleniglacial (fig. 4.6a and 4.6b) are slightly different at both sides of the Carpathians. Considering the east side of the Carpathians, EM4 is dominant in Stari Bezradychy and Sanzhijka, but not in the Polish sections. This may indicate that the sections Dybawka and Radymno (Poland) were in an upwind position from the sections Sanzhijka and Stari Bezradychy (Ukraine). The low MARs during the Early Pleniglacial in this area, indicate that the proglacial zone probably did not function as a source area. A different provenance and wind direction during the Early and Middle Pleniglacial in comparison with the Late Pleniglacial may therefore be assumed. Eastern winds would result in a proportional increase of EM4 in the Polish sections compared to the Ukrainian sections. A southern wind would result in higher EM1+2 and EM3 proportions in Sanzhijka, originating from the partly dry Black Sea shelf, and higher proportions of EM4 in Stari Bezradychy (Ukraine) and the Polish sections. Only a wind direction with a dominant western component can explain the dominance of EM3 and the relatively high proportions of EM1+2 in comparison to the relatively high proportions of EM4 in the sections Stari Bezradychy and Sanzhijka (Ukraine) that is seen in figs. 4.6a and 4.6b.

4.8 Implications for atmospheric circulation during the Weichselian Pleniglacial in central and eastern Europe

Comparison to model simulations

Van Huissteden and Pollard (2003) conclude from their simulation of winter conditions of MIS 3 both in the cold and the warm mode that central Europe was dominated by strong western winds, while the LGM was dominated by strong north-western winds.

Renssen et al. (2007) conclude that reconstructed winds from proxy-data indicate western to north-western winds during MIS 2 in central Europe. Both conclusions correspond to our findings. Van Huissteden and Pollard (2003) modelled weak northern winds in summer conditions during MIS 3 in a warm mode. Weak winds contribute relatively little on the total grain size population and could therefore probably not be recognized in our data. In MIS 3, cold mode (summer conditions) strong northern winds were modeled, but from our data no clear indications of northern wind dominance could be found. A probable explanation is the presence of some vegetation and as a consequence little sediment transport during summers.

Nawrocki et al. (2006) obtain quite similar results based on studies of the anisotropy of magnetic susceptibility which were carried out in order to define the directions and strength of paleowind during sedimentation of the youngest loesses (corresponding with LGM, MIS 2) in Poland and western Ukraine, in a small, more distant foreland of the Carpathians (about 100-200 km to the north of the mountain margin). The majority of the sections studied indicate a paleowind direction from W-SW to E-NE. A possible explanation for the differences with our findings, is that the part of the Carpathians south of their area locally deviates the north-western wind slightly to a western or even a south-western wind.

Wind directions derived from loess grain-sizes

The suggested change of wind direction from generally west during the Early and Middle Pleniglacial to north or northwest during the Late Pleniglacial may be explained by the position of the ice margin. During the Early Pleniglacial the ice margin was at about the present-day Polish coast, while during the Middle Pleniglacial it was located in southern Sweden and during the Late Pleniglacial the margin was at the line Hamburg, Berlin, Warszawa, Vilnius (Huijzer and Vandenberghe, 1998). Van Huissteden and Pollard (2003) and Renssen et al. (2007) modeled winds perpendicular to the ice margin in the proglacial zone. The area further south from the margin was dominated by western winds, being a part of counterclockwise circulating winds around the ice cap. Nawrocki et al. (2006) obtain quite similar wind directions, based on studies of the anisotropy of magnetic susceptibility in loess sections, indicating the inclination by the time of deposition, in Poland and western Ukraine. The majority of the studied sections indicate a paleo-wind direction from W-SW to E-NE.

The position change of the ice margin influenced also the wind directions. Obviously, during the Early and Middle Pleniglacial the ice margin, and thus the proglacial zone, being the obvious major source area of loess, was too far away for all sections to influence the main winds in the study region. In this period all sections were probably dominated by winds controlled by the Westerlies. These winds did not come across the proglacial zone on their way to the studied section locations, resulting in very low sedimentation rates. Obviously, during the Early and Middle Pleniglacial no material was available east of the Carpathians. In contrast, west of the Carpathians local river plains and tectonic

basins (e.g. the Pannonian Basin) functioned as source areas. During the Middle Pleniglacial these sources were more vegetated, resulting in a lower loess sedimentation (MAR) than during the Early and Late Pleniglacial.

During the Late Pleniglacial the ice margin and the proglacial source region were close enough to influence the study region. Isarin and Renssen (1999) modeled the European climate during the Younger Dryas, and concluded that the wind directions in Europe were strongly influenced by the position of the sea ice margin in the northern Atlantic. As a result the Icelandic Low was located south of Iceland. Winds from the ice caused high surface pressures in front of the sea ice. This caused a higher pressure gradient than nowadays, resulting in many northwestern storms over Europe. In this scenario the area at the east side of the Carpathians was also dominated by these northwestern winds, transporting loess from the proglacial zone to our study area. This explains the major increase in MARs at the Polish and northern Ukrainian sample locations and the decreased proportion of EM4 in northern Ukraine during the Late Pleniglacial (compared to the Middle Pleniglacial), resulting from increasing proportions of the silt-sized EMs. The initiation of loess sedimentation at Pyrogove may also be explained from increased loess transport towards the study location, while also the initiation at Katymar (Hungary) may be related to the changing main wind direction, in combination with local sediment availability or erosion processes.

Finally, Sanzhijka as the most southern location near the Black Sea shows also a major increase in MAR in the Late Pleniglacial. It occurs at a large distance from the ice margin. Apparently, the wind system was able to transport fine loess over the entire region.

4.9 Conclusions

The separation of the loess grain-size data into endmembers makes it possible to explain the differences in grain-size distribution in space and time in terms of wind-direction, source areas and sediment availability. The EM proportions and mass accumulation rates suggest a domination of western winds during the Early and Middle Pleniglacial in central and eastern Europe, while the Late Pleniglacial was dominated by north-western or northern winds. We base this conclusion on two major results:

First, during Late Pleniglacial a north-western wind transported silt-sized sediment (EM1+2 and EM3) from the proglacial plains of north-central Europe to the area east of the Carpathians. This resulted in the high MARs in this area. The MARs during the Early and Middle Pleniglacial, in contrast, are too low and do not show enough variability in space and time to be explained only by a large distance to the proglacial zone. A western wind during the Early and Middle Pleniglacial resulted in a much smaller transport from the northern proglacial source area to the region east of the Carpathians and thus very low sedimentation rates.

Second, the relative increase of the fine-grained sediment (EM4) in a south-eastern direction in the area east of the Carpathians during the Late Pleniglacial is best

explained by a north-western wind. The regional differentiation of the EM proportions distribution west of the Carpathians can be explained by a wind between northwest and north. During the Early and Middle Pleniglacial the spatial distribution of EM proportions in the research area suggests a western wind.

Besides large scale atmospheric circulation patterns, also local sedimentation conditions determined to a large extent the mass accumulation rates of loess. We base this conclusion on the difference in MARs between two sections situated close to each other being not smaller than differences in MARs at large distances in the study region.

Synthesis

New insights in the atmospheric circulation pattern during the Weichselian Pleniglacial in east and central Europe and proxies that register them in loess deposits are discussed in this thesis. Key questions were:

1. To what extent are millennial scale climate oscillations registered in the last-glacial loess deposits of central Europe? What is the reliability of these cycles? Can they contribute to bridge millennial scale climate information as derived from loess records on the Chinese Loess Plateau and from North Atlantic marine records?
2. To what extent can conclusions be drawn on the climatic conditions, mainly wind circulation patterns, over central Europe during the last glacial?

This chapter presents a review of the major results, and discusses them from the view of the general objectives. Objective 1 is discussed in the first three parts. The first section deals with the registration of millennial-scale climate oscillations in loess, while the second section discusses the reliability of these oscillations in proxy records as potential registrations of climate variability in the past. The third section deals with the perspective to bridge last glacial millennial scale climate information from the registrations on the Chinese Loess Plateau to those in the North-Atlantic region. Objective 2 is discussed in the fourth section. It deals with potential conclusions on changes of different climate parameters, especially wind strength and direction, during the Pleniglacial. The last section discusses suggestions for further research in the future.

Registration of millennial-scale climate oscillations in loess

The registration of a climate oscillation in loess is expressed by the change in one or more properties of the loess deposits. The alteration of loess properties depends on its sensitivity for climate change and registration starts once that a threshold value is passed. Different proxies react at different threshold values; this means that a certain climate parameter value may have crossed the threshold value of one proxy, but still shows noise for other proxies. For instance, figure 1.5 shows that some peaks are registered in the Ba/Sr-ratio, but not in the magnetic susceptibility (MS) record. As both proxies are mainly sensitive for precipitation, it may be stated that Ba/Sr is more sensitive for paleo-precipitation than MS. However, some oscillations (in the Late Pleniglacial deposits, fig. 1.5) show the opposite. Another example can be found in grain-size records. Section Stari Bezradychy (Ukraine) shows hardly any peaks in the Late Pleniglacial (fig. 2.3b), while the nearby section Pyrogove (Ukraine) shows about 22 peaks in the equivalent deposits (fig. 2.3c), indicating threshold values vary per section. Obviously, the registration of climate variability in loess is also dependent on local factors.

A peak in a proxy record may be interpreted as representative for external variation, when its value outranges the measurement error of the surrounding samples. However, a peak may consist of only one sample, and might result from a measurement error or a mistake during the sampling process. Therefore, the reliability of a peak increases with the number of samples in one peak rather than with the peak intensity of the proxy value. The difference between noise and a significant peak is not sharp as illustrated by some peaks in Early Pleniglacial deposits in the section Titel (Serbia) in fig. 1.5. The multi-proxy approach used in Chapter 1 anticipates this problem, by the comparison with other proxy records from the same samples. When different proxies are measured on the same data, some proxies may show a peak at a certain depth, while others do not. When there is doubt about a part of a proxy record being noise or a peak, the other proxy data confirm or disconfirm if a peak may be expected there.

From the previous considerations it may easily be understood that a multi-proxy approach leads to detecting more oscillations than a single-proxy approach (see for instance Chapter 1). The oscillations in the proxy records represent different climate situations. A change to a windier climate may be expressed in the grain-size record, while an increase of annual precipitation should be expressed in the Ba/Sr-ratio or MS. Figures 1.4a and 1.4b and table 1.2 show that measuring more than one proxy results in more peaks representing oscillations of different climate parameters.

Are the found proxy variations related to Dansgaard-Oeschger cycles?

The recorded variability in the studied proxy records indicates variations in environmental conditions by the time of sedimentation, or shortly after. In the past it was assumed that all variations were related to widespread climate changes, and wiggles were matched at thousands of kilometres distance, often using a 'counting from the top' method. Nowadays it is realized that interpretation of this variability in proxies is far more complex. Also in this thesis many features in the loess records indicate that the proxy variations cannot be directly related to climate changes at a large spatial scale.

First, loess sedimentation in the study area was not continuous, so that some climate oscillations are not registered in the deposits. Paleosols, containing high amounts of organic matter, indicate the presence of vegetation, which prevented the removal of loess by the wind and its redeposition at some distance. This may result in a temporary break in sedimentation. Strong soil formation as like the Late Pleniglacial soils in the Sanzhijka section (fig. 2.3d) may indicate a long period of a very slow deposition or non-deposition. This may also be the case at Stari Bezdrych, containing much stronger Middle Pleniglacial soils than other sections at comparable latitudes (fig. 2.3b). In the same way some peaks in magnetic susceptibility (MS) or Ba/Sr may indicate stagnation of sedimentation, while these peaks can not be separated from peaks originating from intensification of MS or Sr-transportation favouring climate conditions.

Second, erosion processes have removed loess that may have contained registrations of climate oscillations. Abrupt changes in grain-size properties indicate this, like e.g. in the Late Pleniglacial deposits in the Katymar section (Hungary) at 3.2 m depth or in the Titel section (Serbia) at 10.8 m depth (fig. 4.5a). In some cases sharp changes in the grain-size properties go hand in hand with sharp soil cut-offs like in the Radymno section (Poland) at 5.8 m depth or in the Sanzhijka section (Ukraine) at 6.5 m depth (fig. 4.5b). Erosion may be caused by water drainage, like sheet wash or gully erosion, when the section location is situated at a local slope. However, also eolian erosion may have occurred as indicated by thin layers of sandy loess, like in the Early Pleniglacial deposits in the Titel section (Serbia, fig. 2.3a), due to selective blow-out of the fine fraction, leaving the coarse fraction behind as a desert pavement. Fig. 1.5 shows that this loess trajectory forms only two peaks. When these peaks represent Dansgaard-Oeschger (D-O) cycles only a small part of the Early Pleniglacial (roughly corresponding to marine isotope stage (MIS) 4 (Vandenberghe 1985) and taking about 16 ka (Martinson et al., 1987)) only a small part of this period is represented here, also confirming strong erosion influenced these deposits.

Third, other factors than climate oscillations have caused loess property variations. Changes of vegetation cover at the sample location or changing topography, like dunes or depressions, may also cause property changes of the loess. Direct indications can not always be determined, while the results of Chapter 1 show that a separation can be made between peaks in loess property variability that are related to regional or larger spatial scale climate oscillations, and peaks that may be not. In this study we studied two sections (Titel and Mošorin, Serbia) at some distance from each other. We assumed that peaks in one section that are reproduced in the other section may be related to regional or larger scale climate changes. In both sections 11 peaks were found between S1 and S0. A matching based on three measured properties of the loess, points to 7 interrelated peaks that were linked to regional climate changes. The remaining peaks, 4 in both sections, were eroded or not registered in the other section.

Fourth, most peaks are related to regional scale instead of global scale climate variability as indicated by the strongly varying amount of grain-size peaks between the sections. For example the section at Stari Bezradychy (Ukraine) shows hardly any oscillations in the Late Pleniglacial (fig. 2.3b), while the nearby section Pyrogove (Ukraine) shows about 22 peaks in Late Pleniglacial deposits (fig. 2.3c). However, the Greenland ice sheet, for example the $\delta^{18}\text{O}$ record in the GISP2 core, shows 3 Dansgaard-Oeschger cycles in MIS 2, roughly corresponding to the Late Pleniglacial (Vandenberghe, 1985). This contrasts with the 22 peaks in Pyrogove and the c. 20 peaks in Dybawka (Poland, fig. 4.5b). This indicates that most oscillations we find in the central and eastern European loess deposits represent climate oscillations that did not influence the Greenland ice sheet. Assuming that the Late Pleniglacial had duration of about 12 ka (Martinson et al., 1987), each grain-size oscillation from that period in the Pyrogove section should represent $(12 / 22 =) 0.55$ ka, and probably less. This underlines that the peaks in this section (and other sections) are related to centennial scale oscillations

rather than to D-O cycles of c. 1450 years (Grootes and Stuiver, 1997).

To summarize, part of the loess proxy variability is related to past climate variability. Peaks related to regional or larger scale climate oscillations can be selected using a multi-proxy approach. However, it becomes not clear if these climate oscillations are related to D-O cycles. Some sections contain peaks that are related to centennial scale climate variations. In other sections indications of non-deposition and erosion point out that not all D-O cycles can be present. As a result, the loess in eastern and central Europe represents often random parts of a specific climate period and different sections may represent different parts and lengths of that climate period.

Can registered millennial scale climate oscillations in central and eastern Europe bridge Chinese and Atlantic climatic evolution?

The answer to this question may be found in the identification of registered climate oscillations. The most obvious way of correlation is accurate dating at high resolution. Specific oscillations and hiatuses have to be dated with standard deviations that are small enough to prevent misidentification. For Dansgaard-Oeschger cycles with duration of 1.5 ka a few centuries is the maximum standard deviation. The present-day dating methods are, however, insufficient.

Different and more or less independent proxies that register the same climate parameter may still show differences, depending on their sensitivity for that measured climate parameter. Precipitation influences the clay content, MS, Ba/Sr and $\delta^{13}\text{C}_{\text{sc}}$ (fig. 3.3). The resemblance between these proxies in Titel (Serbia) is promising (R^2 is never lower than 0.62), but also makes clear that the proxies are influenced by external factors other than precipitation. For example, changes in soil moisture content, long after the registration of a climate oscillation, may cause increased chemical weathering influencing the clay content and the Ba or Sr contents, breakdown of magnetic minerals and thus breakdown of the MS signal or partly overprinting of the registered $\delta^{13}\text{C}$ signal in the carbonates. Therefore, many proxies must be measured to identify an oscillation or a unique set of oscillations. Such a uniquely identified oscillation or specified set of oscillations may be 'followed' through a region, when the same procedure is applied on many sections. In this way a certain oscillation may be matched reliably throughout a whole loess area. However, loess is not present everywhere and climate changes spatially.

To conclude, at this moment it is impossible to match reliably long-distance registrations of climate variability. The main reasons are lack of accurate dating to date hiatuses and peaks and insufficient proxy data both at single locations and at a wide geographical scale.

What can be contributed to the reconstruction of the climate development in eastern and central Europe during the Weichselian Pleniglacial?

The translation of grain-size, MS, pedochemical and carbon isotope results into wind speed, wind direction, (annual) precipitation or temperature is not simple. Mass accumulation rates and endmember proportions of grain-size distributions show a promising new step in deriving wind directions in a large region. Chapter 4 shows how these expressions of grain-size data over a whole region point to a domination of western winds during the Early and Middle Pleniglacial. A major change in mass accumulation rates in the whole eastern and central European region points to a shift in dominant wind directions to north or northwest during the Late Pleniglacial.

Quantification of wind speeds is even more difficult as grain-sizes are not simply related to wind strength. Chapter 4 makes clear that MARs have no direct relation to grain-size. Sediment availability, distance to the source area, vegetation and local topography seem to have major influence. Proxies that result from post-depositional processes, like Ba/Sr or $\delta^{13}\text{C}_{\text{sc}}$ do not suffer from this problem. Tests of new more or less independent proxies that should theoretically be influenced by paleo-precipitation show promising results (Chapters 3 and 4). As stated before, Ba/Sr and $\delta^{13}\text{C}_{\text{sc}}$ show high similarity to each other and to MS and the clay fraction in the Titel section (Serbia) (fig. 3.3). However, the proxies do not match for 100% due to difference in sensitivity for the climate signal that they register. Most similarity is found in the central and top parts of the Middle Pleniglacial deposits. All proxies registered strong variation here, indicating that the climate signal, we assume mainly precipitation, was strongest in this period and thus, this was the wettest period of the Pleniglacial. The dating results indicate this part represents approximately the latest 10-15 ka of the Middle Pleniglacial (c. 40-25 ka BP).

The lowest part of the Middle Pleniglacial deposits in Titel is characterised by a certain oscillation in the Ba/Sr-ratio, the clay fraction and the $\delta^{13}\text{C}_{\text{sc}}$, while no oscillation can be found in the MS record (fig. 3.3). This indicates that this climate oscillation in the older part of the Middle Pleniglacial was characterized by less precipitation than the climate oscillations in the latest part, described above. In the same way, oscillations found in the clay record during the Early and Late Pleniglacial that were not registered in the Ba/Sr, MS or $\delta^{13}\text{C}_{\text{sc}}$ record indicate that the climate in these periods was dryer than the Middle Pleniglacial climate or characterized by other changes than precipitation increase.

To conclude, some statements about climate changes can be made, while the interpretation of most variations in the proxy records is difficult. Results in this thesis point out that a quantitative climate reconstruction can not be made, as too many unknown factors influence the measured proxy values.

Future research

The major issue that prevents us from bridging the registration of climate variability from the North-Atlantic region to China is accurate identification of climate oscillations. Improvement of the accuracy of dating is the first major step. Stevens et al. (2008), Buylaert et al. (2008) and Vriend (2007) have shown that high resolutions of OSL dating samples in Chinese loess can be used to create relatively precise age frames that were used to date (centennial- to) millennial-scale features. However, the uncertainty range is still too large to define the exact age of peaks with specific millennial-scale duration and to correlate them to D-O cycles. The position and size of hiatuses in loess deposits also have to be dated more accurately, to reduce the amount of wiggle matching possibilities.

More proxies need to be measured in each loess section. More proxy information will strongly improve the knowledge on properties of specific climate oscillations from the past. In this way peaks or sets of peaks may be recognized at new locations, which contribute to the knowledge of the spatial influence of these climate oscillations.

The same set of proxies, measured using the same techniques, must be applied in a dense network. In a test area an upscaling approach may be used to 'follow' specific peaks or sets of peaks throughout the region. When it is known in what density and set of proxies these peaks can be followed, a larger region may be sampled. In this way a connection may be made via Ukraine to the Russian Plain, the northern Caspian Sea and Central Asia to the Chinese Loess Plateau. In western direction a connection may be made via Poland, Czechia, southern Germany and northern France to the Atlantic region.

References

- Aitken MJ. 1985. Thermo-luminescence dating. London, Academic Press. 359 pp.
- Alley RB, Anandakrishnan S, Jung P. 2001. Stochastic resonance in the North Atlantic. *Paleoceanography* 16, 190-198.
- Avramov VI, Jordanova D, Hoffmann V, Roesler W. 2006. The role of dust source area and pedogenesis in three loess–paleosol sections from North Bulgaria: a mineral magnetic study. *Studia Geophysica et Geodaetica* 50(2), 259–282.
- Behre K-E, Van der Plicht J. 1992. Towards an absolute chronology for the last glacial period in Europe: radiocarbon dates from Oerel, Northern Germany. *Veget., Hist., Archaeobot.* 1, 111–117.
- Benner R, Fogel ML, Kent Sprague E, Hodsons RE. 1987. Depletion of ^{13}C in lignin and its implications for stable carbon isotope studies. *Nature* 329, 708–710.
- Blunier T, Chappellaz J, Schwander J, Dällenbach A, Stauffer B, Stocker TF, Raynaud D, Jouzel J, Clausen HB, Hammer CU, Johnsen SJ. 1998. Asynchrony of Antarctic and Greenland climate change during the last glacial period. *Nature* 394, 739–743.
- Bokhorst MP, Beets CJ, Markovic SB, Gerasimenko NP, Matviishina ZN, Frechen M. 2008. Pedochemical climate proxies in Late Pleistocene Serbian–Ukrainian loess sequences. *Quaternary International*, doi:10.1016/j.quaint.2008.09.003.
- Bond GC, Broecker W, Johnsen S, McManus J, Labeyrie LD, Jouzel J, Bonani G. 1993. Correlations between climate records from North-Atlantic sediments and Greenland Ice. *Nature* 365, 143–147.
- Bond GC, Showers W, Cheseby M, Lotti R, Almasi P, deMenocal P, Priore P, Cullen, H, Hajdas I, Bonani G. 1997. A pervasive millennial-scale cycle in North Atlantic Holocene and glacial climates. *Science* 278, 1257–1266.
- Bos JAA, Bohncke SJP, Kasse C, Vandenberghe J. 2001. Vegetation and Climate during the Weichselian Early Glacial and Pleniglacial in the Niederausitz, eastern Germany – macrofossil and pollen evidence. *Journal of Quaternary Science* 16, 269–289.
- Bowen DQ, Phillips FM, McCabe AM, Knutz PC, Sykes GA. 2002. New data for the Last Glacial Maximum in Great Britain and Ireland. *Quaternary Science Reviews* 21, 89–101.
- Brantley SL, Chesley JT, Stillings LL. 1998. Isotopic ratios and release rates of strontium measured from weathering feldspars. *Geochimica et Cosmochimica Acta* 62(9), 1493–1500.
- Buggle B, Glaser B, Zöller L, Hambach U, Marković S, Glaser I, Gerasimenko N. 2008. Geochemical characterization and origin of Southeastern and Eastern European loesses (Serbia, Romania, Ukraine). *Quaternary Science Reviews* 27(9–10), 1058–1075.
- Buylaert JP, Murray AS, Vandenberghe D, Vriend MGA, De Corte F, Van den Haute P. 2008. Optical dating of Chinese loess using sand-sized quartz: Establishing a time frame for Late Pleistocene climate changes in the western part of the Chinese Loess Plateau. *Quaternary Geochronology* 3(1–2), 99–113.
- Cerling TH. 1984. The stable isotopic composition of modern soil carbonate and its relationship to climate. *Earth and Planetary Science Letters* 71, 229–240.
- Cerling TH, Quade J, Wang Y, Bowman JR. 1989. Carbon isotopes in soils and paleosols as ecology and palaeoecology indicators. *Nature* 341, 138–139.
- Cerling TH, Quade J. 1993. Stable Carbon and Oxygen Isotopes in Soil Carbonates. In: Swart PK, Lohmann KC, McKenzie J, Savin S (eds.). *Climate Change in Continental Isotopic Records*. Geophysical Monograph 78, American Geophysical Union, pp 217–239.
- Chen FH, Bloemendal J, Wang JM, Li JJ, Oldfield F. 1997. High-resolution multi-proxy climate records from Chinese loess: evidence for rapid climatic changes over the last 75 kyr. *Palaeogeography, Palaeoclimatology, Palaeoecology* 130, 323–335.
- Clement AC, Cane MA. 1999. A role for the tropical Pacific coupled ocean-atmosphere system on Milankovitch and millennial timescales. Part I: A modelling study of tropical Pacific variability. In: Clark PU, Webb RS, Keigwin LD (eds.). *Mechanisms of Global Climate Change at Millennial Time Scales*. American Geophysical Union, Washington DC, pp 363–371.
- Cortijo E, Labeyrie L, Vidal L, Vautravers M, Chapman M, Duplessy J-C, Elliot M, Arnold M, Turon J-L, Auffret G. 1997. Changes in sea surface hydrology associated with Heinrich event 4 in the North Atlantic Ocean between 40° and 60°N. *Earth and Planetary Science Letters* 146(1–2), 29–45.

- Cosford J, Qing H, Yuan D, Zhang M, Holmden C, Patterson W, Hai C. 2008. Millennial-scale variability in the Asian monsoon: Evidence from oxygen isotope records from stalagmites in southeastern China. *Palaeogeography, Palaeoclimatology, Palaeoecology* 266(1-2), 3-12.
- Dansgaard W, Johnsen SJ, Clausen HB, Dahl-Jensen D, Gundestrup NS, Hammer CU, Hvidberg CS, Steffensen JP, Sveinbjörnsdóttir AE, Jøuzel J, Bond G. 1990. Evidence for general instability of past climate from a 250-kyr ice-core record. *Nature* 364, 218-220.
- Dekkers MJ. 1997. Environmental magnetism: an introduction. *Geologie en mijnbouw* 76, 163-182.
- Derbyshire E, Meng X, Kemp RA. 1998. Provenance, transport and characteristics of modern aeolian dust in western Gansu Province, China, and interpretation of the Quaternary loess record. *Journal of Arid Environments* 39(3), 497-516.
- Ding ZL, Rutter N, Liu TS. 1993. Pedostratigraphy of Chinese Loess deposits and climatic cycles in the last 2.5 Myr. *Catena* 20, 73-91.
- Ding ZL, Sun JM, Liu TS, Zhu RX, Yang SL, Guo B. 1998. Wind-blown origin of the Pliocene red clay formation in the central Loess Plateau, China. *Earth and Planetary Science Letters* 161(1-4), 135-143.
- Ding ZL, Derbyshire E, Yang S, Yu Z, Xiong S, Liu T. 2002. Stacked 2.6-Ma grain size record from the Chinese loess based on five sections and correlation with the deep-sea $\delta^{18}\text{O}$ record. *Paleoceanography* 17(1033), 1-21.
- Eggins SM, Woodhead JD, Kinsley LPJ, Mortimer GE, Sylvestre P, McCulloch MT, Hergt JM, Handler MR. 1997. A simple method for the precise determination of >40 trace elements in geological samples by ICPMS using enriched isotope internal standardisation. *Chemical Geology* 134, 311-326.
- Ehlinger JR, Cerling TE, Helliker BR. 1997. C4 photosynthesis, atmospheric CO_2 and climate. *Oecologia* 112, 285-299.
- Ehlinger JR, Buchmann N, Flanagan LB. 2000. Carbon isotope ratios in belowground carbon cycle processes. *Ecological applications* 10(2), 412-422.
- Engels S. 2008. Exploring early- and mid- Weichselian climate variability in Europe by applying chironomids as a proxy. PhD-thesis Vrije Universiteit Amsterdam, The Netherlands. 160 pp.
- Fedorowicz S, Łanczont M. 2004. The age of loess deposits at Dybawka, Tarnawce and Zarzecze (SE Poland) based on luminescence dating. *Geologija* 47, 8-14.
- Frechen M, Schweitzer U, Zander A. 1996. Improvements in sample preparation for the fine grain technique. *Ancient TL* 14(2), 15-17.
- Frechen M, Van Vliet-Lanoë B, Van den Haute P. 2001a. The Upper Pleistocene loess record at Harmignies/Belgium; high resolution terrestrial archive of climate forcing. *Palaeogeography, Palaeoclimatology, Palaeoecology* 173(3-4), 175-195.
- Frechen M, Vanneste K, Verbeeck K, Paulissen E, Camelbeek T. 2001b. The Deposition of the Coversands along the Bree Fault Escarpment, NE Belgium. *Netherlands Journal of Geosciences* 80(3-4), 171-185.
- Frechen M, Oches EA, Kohfeld KE. 2003. Loess in Europe; mass accumulation rates during the Last Glacial Period. *Quaternary Science Reviews* 22(18-19), 1835-1857.
- Gallet S, Jahn B-m, Torii M. 1996. Geochemical characterization of the Luochuan loess-paleosol sequence, China, and paleoclimatic implications. *Chemical Geology* 133 (1-4), 67-88.
- Gallet S, Jahn B-m, Van Vliet Lanoë B, Dia A, Rossello E. 1998. Loess geochemistry and its implications for particle origin and composition of the upper continental crust. *Earth and Planetary Science Letters* 156 (3-4), 157-172.
- Ganopolski A, Rahmstorf S. 2001. Rapid changes of glacial climate simulated in a coupled climate model. *Nature* 409, 153-158.
- Genty D. 2003. Dansgaard-Oeschger events recorded in a stalagmite from SW-France between 83 and 32 ka. *Lettre pigb-pmrc France* 15, 16-20.
- Gerasimenko NP. 2001. Late Pleistocene vegetation and soil evolution at the Kyiv loess plain as recorded in the Stari Bezradychy section, Ukraine. *Studia Quaternaria* 17, 19-28.
- Gerasimenko NP. 2006. Upper Pleistocene loess-paleosol and vegetational successions in the Middle Dnieper Area, Ukraine. *Quaternary International*, 149(1), 55-66.
- Goodfriend G, Lain Ellis G, Toolin LJ. 1999. Radiocarbon age anomalies in land snail shells from Texas: ontogenetic, individual, and geographical patterns of variation. *Radiocarbon* 41(2), 149-156.
- Goossens D, Gross J. 2002. Similarities and dissimilarities between the dynamics of sand and dust during wind erosion of loamy sandy soil. *Catena* 47(4), 269-289.

- GRIP Members. 1993. Climate instability during the last interglacial period recorded in the GRIP ice core. *Nature* 364, 203-207.
- Grootes PM, Stuiver M, White JWC, Johnsen S, Jouzel J. 1993. Comparison of oxygen isotope records from the GISP2 and GRIP Greenland ice cores. *Nature* 366, 552 – 554.
- Grootes PM, Stuiver M. 1997. Oxygen 18/16 variability in Greenland snow and ice with 103 to 105-year time resolution. *Journal of Geophysical Research* 102, 26,455–26,470.
- Gu Z, Liu R, Liu Y. 1991. Response of stable isotopic composition of loess-paleosol carbonate to paleoenvironmental changes. In: Tungsheng L (ed.). *Loess, Environment and Global Change*. Science Press, Beijing, China, pp 82-92.
- Guo ZT, Peng SZ, Hao QZ, Biscaye PE, Liu TS. 2001. Origin of the Miocene–Pliocene Red-Earth Formation at Xifeng in Northern China and implications for paleoenvironments. *Palaeogeography, Palaeoclimatology, Palaeoecology* 170(1-2), 11-26.
- Haesaerts P, Borziak I, Chirica V, Damblon F, Koulakovska L, Van der Plicht J. 2003. The east carpathian loess record: a reference for the middle and late pleniglacial stratigraphy in central Europe. *Quaternaire* 14(3), 163-188.
- Hatté C, Antoine P, Fontugne M, Rousseau D-D, Tisnérat-Laborde N, Zöller L. 1999. New chronology and organic matter $\delta^{13}\text{C}$ paleoclimatic significance of Nussloch loess sequence (Rhine Valley, Germany). *Quaternary International* 62, 85-91.
- Hatté C, Antoine P, Fontugne M, Lang A, Rousseau D-D, Zöller L. 2001. $\delta^{13}\text{C}$ of loess organic matter as a potential proxy for paleoprecipitation. *Quaternary Research* 55, 33-38.
- Hays JD, Imbrie J, Shackleton NJ. 1976. Variations in the earth's orbit: pacemaker of the ice ages. *Science* 194, 1121-1132.
- Heinrich H. 1988. Origin and consequences of cyclic ice rafting in the Northeast Atlantic Ocean during the past 130,000 years. *Quaternary Research* 29(2), 142-152.
- Heller F, Liu TS. 1982. Magnetostratigraphical dating of loess deposits in China. *Nature (London)* 300, 431-433.
- Heller F, Liu TS. 1984. Magnetism of Chinese loess deposits, *Geophys. J.R. Astron. Soc.* 77, 125-141.
- Heller F, Liu TS. 1986. Paleoclimatic and sedimentary history from magnetic susceptibility of loess in China. *Geophys. Res. Lett.* 13, 1169-1172.
- Heller F, Evans ME. 1995. Loess magnetism. *Rev. Geophys.* 33, 211-240.
- Hemming SR. 2004. Heinrich events. Massive late Pleistocene detritus layers of the North Atlantic and their global climate imprint. *Reviews of Geophysics* 42(1), RG1005, doi:10.1029/2003RG000128.
- Hiller A, Junge FW, Geyh MA, Krbetschek M, Kremenetski C. 2004. Characterising and dating Weichselian organogenic sediments: a case study from the Lusatian ice marginal valley (Scheibepencast mine, eastern Germany). *Palaeogeography, Palaeoclimatology, Palaeoecology* 205(3-4), 273-294.
- Huijzer B, Vandenbergh J. 1998. Climatic reconstruction of the Weichselian Pleniglacial in northwestern and Central Europe. *Journal of Quaternary Science* 13(5), 391-417.
- IPCC. 2007. *Climate change 2007: The Physical Science Basis*. Contribution of working group I to the Fourth Assessment Report of the Intergovernmental Panel on Climate Change. Solomon S, Qin D, Manning M, Chen Z, Marquis M, Averyt KB, Tignor M, Miller HL (eds.). Cambridge University Press, Cambridge United Kingdom and New York, NY, USA. 996 pp.
- Isarin RFB, Renssen H. 1999. Reconstructing and modelling Late Weichselian climates: the Younger Dryas in Europe as a case study. *Earth-Science Reviews* 48(1-2), 1-38.
- Jahn B, Galler S, Han J. 2001. Geochemistry of the Xining, Xifeng and Jixian sections, Loess Plateau of China: eolian dust provenance and paleosol evolution during the last 140 ka. *Chemical Geology* 178, 71-94.
- Kaakinen A, Sonninen E, Pekka Lunkka J. 2006. Stable isotope record in paleosol carbonates from the Chinese Loess Plateau: Implications for late Neogene paleoclimate and paleovegetation. *Palaeogeography, Palaeoclimatology, Palaeoecology* 237(2-4), 359-369.
- Kasse C, Vandenbergh J, Van Huissteden J, Bohncke SJP, Bos JAA. 2003. Sensitivity of Weichselian fluvial systems to climate change (Nochten mine, eastern Germany). *Quaternary Science Reviews* 22(20), 2141-2156.
- Kemp RA. 2001. Pedogenic modification of loess: significance for paleoclimatic reconstructions. *Earth-Science Reviews* 54(1-3), 145-156.
- Kitagawa H, Van der Plicht J. 2000. Atmospheric radiocarbon calibration beyond 11,900 calBP from Lake Suigetsu laminated sediments. *Radiocarbon* 42, 369-380.

- Koarashi J, Iida T, Asano T. 2005. Radiocarbon and stable carbon isotope compositions of chemically fractionated soil organic matter in a temperate-zone forest. *Journal of environmental Radioactivity* 79, 137-156.
- Kohfeld KE, Harrison SP. 2003. Glacial-interglacial changes in dust deposition on the Chinese Loess Plateau. *Quaternary Science Reviews* 22, 1859-1878.
- Konert M, Vandenberghe J. 1997. Comparison of layer grain-size analysis with pipette and sieve analysis: a solution for the underestimation of the clay fraction. *Sedimentology* 44, 523-535.
- Kukla GJ, An ZS. 1989. Loess stratigraphy in central China. *Palaeogeography, Palaeoclimatology, Palaeoecology* 72, 203-225.
- Kukla GJ, Heller F, Liu XM, Xu TC, Liu TS, An ZS. 1988. Pleistocene climates in China dated by magnetic susceptibility. *Geology* 16, 811-814.
- Łacka B, Łanczont M, Madeyska T. 2007. Morphological forms of authigenic carbonates and their isotopic composition (stable isotopes of carbon and oxygen) in loess profiles at the Carpathian Margin and Podolia. *Annales UMCS(B)*, 93-112.
- Łanczont M. 1995. Stratigraphy and paleogeography of loess on the Przemyśl Foothills (SE Poland). *Annales UMCS(B50)*, 91-126.
- Land M, Ingri J, Andersson P, Öhlander B. 2000. Ba/Sr, Ca/Sr and $^{87}\text{Sr}/^{86}\text{Sr}$ ratios in soil water and groundwater: implications for relative contributions to stream water discharge. *Applied Geochemistry* 15(3), 311-325.
- Landais A, Masson-Delmotte V, Jouzel J, Raynaud D, Johnsen J, Huber C, Leuenberger M, Schwander J, Minster B. 2006. The glacial inception as recorded in the NorthGRIP Greenland ice core: timing, structure and associated abrupt temperature changes. *Climate Dynamics* 26(2-3), 273-284.
- Lang A, Hatté C, Rousseau D-D, Antoine P, Fontugne M, Zöller L, Hambach U. 2003. High-resolution chronologies for loess: comparing AMS ^{14}C and optical dating results. *Quaternary Science Reviews* 22(10-13), 953-959.
- Lehman S. 1993. Ice sheets, wayward winds and sea change. *Nature* 365, 108-110.
- Lehmkuhl F, Haselein F. 2000. Quaternary paleoenvironmental change on the Tibetan Plateau and adjacent areas (Western China and Western Mongolia). *Quaternary International* 65-66, 121-145.
- Leuschner DC, Sirocko F. 2000. The low-latitude monsoon climate during Dansgaard-Oeschger cycles and Heinrich Events. *Quaternary Science Reviews* 19, 243-254.
- Lin B, Liu R, An ZS. 1991. Preliminary research on stable isotopic compositions of Chinese loess. In: Tungsheng L (ed.). *Loess, Environment and Global Change*. Science Press, Beijing, pp 124-131.
- Little MG, Schneider RR, Kroon D, Price B, Summerhayes CP, Segl M. 1997. Trade wind forcing of upwelling, seasonality, and Heinrich events as a response to sub-Milankovitch climate variability. *Paleoceanography* 12(4), 568-576.
- Liu T. 1985. *Loess and the environment*. China Ocean Press, Beijing. 174 pp.
- Liu W, Huang Y, An Z, Clemens SC, Li L, Prell WL, Ning Y. 2005. Summer monsoon intensity controls C_4/C_3 plant abundance during the last 35 ka in the Chinese Loess Plateau: Carbon isotope evidence from bulk organic matter and individual leaf waxes. *Palaeogeography, Palaeoclimatology, Palaeoecology* 220, 243-254.
- Lowe JJ, Blockley S, Trincardi F, Asioli A, Cattaneo A, Matthews IP, Pollard M, Wulf S. 2007. Age modelling of late Quaternary marine sequences in the Adriatic: Towards improved precision and accuracy using volcanic event stratigraphy. *Continental Shelf Research* 27(3-4), 560-582.
- Mabutt JA. 1977. *Desert Landforms*. Australian National University Press, Canberra.
- MacAyeal DR. 1993. Binge/Purge oscillations of the Laurentide Ice-Sheet as a cause of the North Atlantic Heinrich Events. *Paleoceanography* 8(6), 775-784.
- Maher BA, Thompson R, Zhou LP. 1994. Spatial and temporal reconstructions of changes in the Asian palaeomonsoon: A new mineral magnetic approach. *Earth and Planetary Science Letters* 125(1-4), 461-471.
- Maher BA, Thompson R. 1995. Paleorainfall reconstructions from pedogenic magnetic susceptibility variations in the Chinese loess and paleosols. *Quaternary Research* 44, 383-391.
- Maher BA. 1998. Magnetic properties of modern soils and loessic paleosols: implications for paleoclimate. *Palaeogeography, Palaeoclimatology, Palaeoecology* 137, 25-54.
- Maher BA, Alekseev A, Alekseeva T. 2002. Variation of soil magnetism across the Russian steppe: its significance for use of soil magnetism as a palaeorainfall proxy. *Quaternary Science Reviews* 21, 1571-1576.

- Marković SB, Oches EA, Gaudenyi T, Jovanović M, Hambach U, Zöller L, Sümegi P. 2004. Paleoclimatic record in the Late Pleistocene loess-paleosol sequence at Miseluk (Vojvodina, Serbia). *Quaternaire* 15(4), 305-315.
- Marković SB, McCoy WD, Oches EA, Savić S, Gaudenyi T, Jovanović M, Stevens T, Walther R, Ivanišević P, Galić, Z. 2005. Paleoclimate record in the Late Pleistocene loess-paleosol sequence at Petrovaradin Brickyard (Vojvodina, Serbia). *Geologica Carpathica* 56, 483-491.
- Marković SB, Oches E, Sümegi P, Jovanović M, Gaudenyi T. 2006. An introduction to the Upper and Middle Pleistocene loess-paleosol sequences of Ruma section (Vojvodina, Serbia). *Quaternary International* 149, 80-86.
- Marković SB, Oches EA, McCoy WD, Gaudenyi T, Frechen M, Jovanović M. 2007. Malacological and sedimentological evidence for "warm" climate from the Irig loess sequence (Vojvodina, Serbia). *Geophys., Geochem., Geosystems* 8, Q09008.
- Marković SB, Bokhorst MP, Vandenberghe J, Oches EA, Zöller L, McCoy WD, Gaudenyi T, Jovanović M, Hambach U, Machalett B. 2008. Late Pleistocene loess-paleosol sequences in the Vojvodina region, North Serbia. *Journal of Quaternary Science* 23(1), 73-84.
- Martinson D, Pisias MG, Hays JD, Imbrie J, Moore TC, Shackleton NJ. 1987. Age dating and the orbital theory of ice ages: development of a high-resolution 0 to 300,000-year chronostratigraphy. *Quaternary Research* 27, 1-30.
- Matviishina ZN, Perederij VI, Ivchenko AS. 1990. Late Cenozoic paleostages in the Lower Dniester area. *VINITI, Moscow* (in Russian).
- Mayewski PA, Bender M. 1995. The GISP2 ice core record - Paleoclimate highlights. *Reviews of Geophysics* 33(S1), 1287-1296.
- McBride MB. 1994. *Environmental chemistry of soils*. Oxford University Press, New York, Oxford. 406 pp.
- Merian E. 1991. *Metals and their compounds in the environment; occurrence, analysis, and biological relevance*. VCH, Weinheim, New York, Basel, Cambridge. 1438 pp.
- Milankovitch M. 1941. *Kanon der Erdbestrahlung und seine Anwendung auf das Eiszeitenproblem*. R. Acad. Spec. Publ. 133.
- Mol J. 1997. Fluvial response to Weichselian climate changes in Niederausitz (Germany). *Journal of Quaternary Science* 12, 43-60.
- Mudelsee M. 2001. The phase relations among atmosphere CO₂ content, temperature and global ice volume over the past 420 ka. *Quaternary Science Reviews* 20, 583-589.
- Nawrocki J, Bakhmutov V, Bogucki A, Dolecki L. 1999. The Paleo- and Petromagnetic record in the Polish and Ukrainian Loess-Paleosol Sequences. *Phys. Chem. Earth (A)* 24(9), 773-777.
- Nawrocki J, Polechońska O, Boguckij A, Łanczont M. 2006. Palaeowind directions recorded in the youngest loess in Poland and western Ukraine as derived from anisotropy of magnetic susceptibility measurements. *Boreas* 35(2), 266-271.
- Négrel P. 2006. Water-granite interaction: Clues from strontium, neodymium and rare earth elements in soil and waters. *Applied Geochemistry* 21(8), 1432-1454.
- Nesbitt HW, Mrkovic G, Price RC. 1980. Chemical processes affecting alkalis and alkaline earths during continental weathering. *Geochimica et Cosmochimica Acta* 44, 1659-1666.
- NorthGRIP (North Greenland Ice Core Project). 2004. High-resolution record of Northern Hemisphere climate extending into the last interglacial period. *Nature* 431, 147-151.
- Novothny Á, Frechen M, Horváth E, Bradák B, Oches EA, McCoy WD, Stevens, T. In press. Luminescence and amino acid racemization chronology of the loess-paleosol sequence at Süttő, Hungary. *Quaternary International*, doi:10.1016/j.quaint.2008.01.009.
- Nugteren G. 2002. *Reconstruction of aeolian distribution patterns on the Central Loess Plateau (China) and their palaeoclimatic implications*. PhD-thesis Vrije Universiteit Amsterdam, The Netherlands.
- Nugteren G, Vandenberghe J. 2004. Spatial climatic variability on the Central Loess Plateau (China) as recorded by grain-size for the last 250 kyr. *Global and Planetary Change* 41(3-4), 185-206.
- O'neil JR, Clayton RN, Mayeda T. 1969. Oxygen isotope fractionation in divalent metal carbonates. *Journal of Chemical Physics* 51, 5547-5558.
- Perelman AI. 1977. *Geochemistry of elements in the supergene zone*. Keterpress enterprises, Jerusalem. 266 pp.
- Pigati JS, Quade J, Shahanan TM, Vance Haynes Jr. C. 2004. Radiocarbon dating of minute gastropods and new constraints on the timing of late Quaternary spring-discharge deposits in southern Arizona, USA. *Palaeogeography, Palaeoclimatology, Palaeoecology* 204(1-2), 33-45.
- Porter SC, An Z. 1995. Correlation between climate events in the North Atlantic and China during the last glaciation. *Nature* 375, 305-308.

- Porter SC, An ZS, Zheng HB. 1992. Cyclic Quaternary alleviation and terracing in a nonglaciated drainage basin on the north flank of the Qinling Shan, Central China. *Quaternary Research* 38, 157-169.
- Porter SC, Hallet B, Wu X, An Z. 2001. Dependence of near-surface MS on dust accumulation rate and precipitation on the Chinese Loess Plateau. *Quaternary Research* 55, 271-283.
- Powers JS, Schlesinger WH. 2002. Geographic and vertical patterns of stable carbon isotopes in tropical rain forest soils of Costa Rica. *Geoderma* 109, 141-160.
- Prescott JR, Hutton JT. 1995. Environmental dose rates and radioactive disequilibrium from some Australian luminescence dating sites. *Quaternary Science Reviews* 14(4), 439-448.
- Prins MA, Vriend MGA. 2007. Glacial and interglacial eolian dust dispersal patterns across the Chinese Loess Plateau inferred from decomposed loess grain-size records. *Geochemistry, Geophysics, Geosystems* 8, doi:10.1029/2006GC001563.
- Prins MA, Vriend MGA, Nugteren G, Vandenberghe J, Lu H, Zheng H, Weltje GJ. 2007. Late Quaternary Aeolian dust flux variability on the Chinese Loess Plateau: Inferences from unmixing of loess grain-size records. *Quaternary Science Reviews* 26, 242-254.
- Puchelt H. 1972. Barium. In: Wedepohl KH (ed.). *Handbook of Geochemistry*. Springer, Berlin, pp 56D1-56D18.
- Pye K. 1995. The nature, origin and accumulation of loess. *Quaternary Science Reviews* 14, 653-667.
- Rahmstorf S. 2002. Ocean circulation and climate during the past 120,000 years. *Nature* 419, 207-214.
- Reille M, De Beaulieu JL. 1990. Pollen analysis of a long upper Pleistocene continental sequence in a Velay maar (Massif Central, France). *Palaeogeography, Palaeoclimatology, Palaeoecology* 80(1), 35-48.
- Reille M, De Beaulieu JL, Svobodova H, Andrieu-Ponel V, Goeury C. 2000. Pollen analytical biostratigraphy of the last five climatic cycles from a long continental sequence from the Velay region (Massif Central, France). *Journal of Quaternary Science* 15(7), 665-685.
- Renssen H, Kasse C, Vandenberghe J, Lorenz SJ. 2007. Weichselian Late Pleniglacial surface winds over northwest and central Europe: a model-data comparison. *Journal of Quaternary Science* 22(3), 281-293.
- Retallack GJ. 1994. A pedotype approach to latest Cretaceous and earliest Tertiary paleosols in eastern Montana. *Bull. Geol. Soc. Am.* 106, 1377-1397.
- Rousseau D-D, Gerasimenko NP, Matviishina ZN, Kukla G. 2001. Late Pleistocene environment of the Central Ukraine. *Quaternary Research* 56, 349-356.
- Rousseau D-D, Antoine P, Hatté C, Lang A, Zöller L, Fontugne M, Ben Othman D, Luck JM, Moine O, Labonne M, Bentaleb I, Jolly D. 2002. Abrupt millennial climatic changes from Nussloch (Germany) Upper Weichselian eolian records during the Last Glaciation. *Quaternary Science Reviews* 21, 1577-1582.
- Rousseau D-D, Derbyshire E, Antoine P, Hatté C. 2007. Loess records; Europe. *Encyclopedia of Quaternary Science*, pp 1440-1456.
- Sage RF, Monson RK. 1999. *C4 plant biology*. Academic Press, San Diego, USA.
- Salomons W, Mook WG. 1986. Isotope geochemistry of carbonates in the weathering zone. In: Fritz P, Fontes JCh (Eds.). *Handbook of Environmental Isotope Geochemistry* 2. The Terrestrial Environment B., Elsevier, pp 239-270.
- Schwertmann U, Taylor RM. 1977. Iron oxides. In: Dixon JB, Weed SB (eds.). *Minerals in Soil Environments*. Soil Science Society America, Madison, pp 45-180.
- Smalley I, Leach JA. 1978. The origin and distribution of the loess in the Danube Basin and associated regions of East-Central Europe - a review. *Sedimentary Geology* 21, 1-26.
- Spötl C, Mangini A. 2002. Stalagmite from the Austrian Alps reveals Dansgaard-Oeschger events during isotope stage 3: Implications for the absolute chronology of Greenland ice cores. *Earth and Planetary Science Letters* 203(1), 507-518.
- Spötl C, Mangini A, Richards DA. 2006. Chronology and paleoenvironment of Marine Isotope Stage 3 from two high-elevation speleothems, Austrian Alps. *Quaternary Science Reviews* 25(9-10), 1127-1136.
- Stephens M, Krzyszkowski D, Ivchenko A, Majewski M. 2003. Palaeoclimate and pedosedimentary reconstruction of a Middle to Late Pleistocene loess-palaeosol sequence, Prymorske, SW Ukraine. *Studia Quaternaria* 19, 3-17.
- Stevens T, Lu H, Thomas DSG, Armitage SJ. 2008. Optical dating of abrupt shifts in the late Pleistocene East Asian Monsoon. *Geology* 36(5), 415-418.

- Stueber AM. 1978. Strontium. In: Wedepohl KH (ed.). *Handbook of Geochemistry*, vol. II-4. Springer, Berlin, pp 38D1-38D17.
- Sun D, Bloemendal J, Rea DK, Vandenberghe J, Jiang F, An Z, Su R. 2002. Grain-size distribution function of polymodal sediments in hydraulic and aeolian environments, and numerical partitioning of the sedimentary components. *Sedimentary Geology* 152, 263-277.
- Sun D, Chen F, Bloemendal J, Su R. 2003. Seasonal variability of modern dust over the Loess Plateau of China. *Journal of Geophysical Research* 108(D21), 4665.
- Sun D, Bloemendal J, Rea DK, An Z, Vandenberghe J, Lu H, Su R, Liu T. 2004. Bimodal grain-size distribution of Chinese loess, and its palaeoclimatic implications. *Catena* 55, 325-340.
- Sun J. 2002. Provenance of loess material and formation of loess deposits on the Chinese Loess Plateau. *Earth and Planetary Science Letters* 6403, 1-15.
- Sun Y, Lu H, An Z. 2006. Grain size of loess, palaeosol and Red Clay deposits on the Chinese Loess Plateau: Significance for understanding pedogenic alteration and palaeomonsoon evolution. *Palaeogeography, Palaeoclimatology, Palaeoecology* 241(1), 129-138.
- Ta W, Xiao H, Qu J, Xiao Z, Yang G, Wang T, Zhang X. 2004. Measurements of dust deposition in Gansu Province, China, 1986-2000. *Geomorphology* 57, 41-51.
- Tang Y, Jia J, Xie X. 2003. Records of magnetic properties in Quaternary loess and its paleoclimatic significance: a brief review. *Quaternary International* 108(1), 33-50.
- Újvári G, Varga A, Balogh-Brunstad Z. 2008. Origin, weathering, and geochemical composition of loess in southwestern Hungary. *Quaternary Research* 69(3), 421-437.
- Van der Hoven SJ, Quade J. 2002. Tracing spatial and temporal variations in the sources of calcium in pedogenic carbonates in a semiarid environment. *Geoderma* 10(3-4), 259-276.
- Van Geel B, Raspopov OM, Renssen H, Van der Plicht J, Dergachev VA, Meijer HAJ. 1999. The role of solar forcing upon climate change. *Quaternary Science Reviews* 18(3), 331-338.
- Van Huissteden J. 1990. Tundra Rivers of the Last Glacial: sedimentation and geomorphological processes during the Middle Pleniglacial in the Dinkel valley (eastern Netherlands). *Mededelingen Rijks Geologische Dienst* 44, 3-138.
- Van Huissteden J, Pollard D. 2003. Oxygen isotope stage 3 fluvial and eolian successions in Europe compared with climate models. *Quaternary Research* 59(2), 223-233.
- Vandenberghe J. 1985. Palaeoenvironment and stratigraphy during the last glacial in the Belgian-Dutch border region. *Quaternary Research* 24(1), 23-38.
- Vandenberghe J, Múcher HJ, Roebroeks W, Gemke D. 1985. Lithostratigraphy and palaeoenvironment of the Pleistocene deposits at Maastricht-Belvédère, southern Limburg, The Netherlands. *Mededelingen Rijksgeologische Dienst* 39(1), 7-29.
- Vandenberghe J, An Z, Nugteren G, Lu H, Van Huissteden K. 1997. New absolute time scale for the Quaternary climate in the Chinese loess region by grain-size analysis. *Geology* 25(1), 35-38.
- Vandenberghe J, Huijzer BS, Múcher H, Laan W. 1998. Short climatic oscillations in a western European loess sequence (Kesselt, Belgium). *Journal of Quaternary Science* 13(5), 471-485.
- Vandenberghe J, Nugteren G. 2001. Rapid climatic changes recorded in loess successions. *Global and Planetary Change* 28(1-4), 1-9.
- Vandenberghe J, Lu H, Sun D, Van Huissteden J, Konert M. 2004. The late Miocene and Pliocene climate in East Asia as recorded by grain-size and magnetic susceptibility of the Red Clay deposits (Chinese Loess Plateau). *Palaeogeography, Palaeoclimatology, Palaeoecology* 204(3-4), 239-255.
- Veres DS. 2007. Terrestrial response to Dansgaard-Oeschger cycles and Heinrich events: the lacustrine record of Les Echets, south-eastern France. *Dissertations from the department of Physical Geography and Quaternary Geology* 6, Stockholm University. 110 pp.
- Voelker AHL. 2002. Global distribution of centennial scale records for Marine Isotope Stage (MIS) 3: a database. *Quaternary Science Reviews* 21(10), 1185-1212.
- Von Richthofen F. 1882. On the mode of origin of the loess. *The Geological Magazine (II)* 9(7), 293-305.
- Vriend MGA. 2007. Lost in loess. Late Quaternary eolian dust dispersal patterns across central China inferred from decomposed loess grain-size records. PhD-thesis Vrije Universiteit Amsterdam, The Netherlands.
- Wang H, Ambrose SH, Liu C-LJ, Follmer LR. 1997. Paleosol stable isotope evidence for early hominid occupation of east asian temperate environments. *Quaternary Research* 48, 228-238.
- Wang H, Follmer LR. 1998. Proxy of monsoon seasonality in carbon isotopes from paleosols of the southern Chinese Loess Plateau. *Geology* 26(11), 987-990.

- Ward PJ, Aerts JCJH, De Moel H, Renssen H. 2007. Verification of a coupled climate-hydrological model against Holocene palaeohydrological records. *Global and Planetary Change* 57(3-4), 238-300.
- Watts WA, Allen JRM, Huntley B. 1996. Vegetation history and palaeoclimate of the last glacial period at Lago Grande di Monticchio, Southern Italy. *Quaternary Science Reviews* 15, 133-153.
- Wedin DA, Tieszen LL, Dewey B, Pastor J. 1995. Carbon isotope dynamics during grass decompositions and soil organic matter formation. *Ecology* 76(5), 1383-1392.
- Weltje GJ. 1997. Endmember modeling of compositional data: Numerical-statistical algorithms for solving the explicit mixing problem. *Journal of Mathematical Geology* 29, 503-549.
- Weltje GJ, Prins MA. 2003. Muddled or mixed? Inferring paleoclimate from size distributions of deep-sea clastics. *Sedimentary Geology* 162, 39-62.
- Weltje GJ, Prins MA. 2007. Genetically meaningful decomposition of grain-size distributions. *Sedimentary Geology* 202(3), 409-424.
- Willis KJ, Rudner E, Sümegi P. 2000. The Full-Glacial Forests of Central and Southeastern Europe. *Quaternary Research* 53(2), 203-213.
- Woillard G, Mook, W. 1982. Carbon-14 dates at Grande Pile: correlation of land and sea-chronologies. *Science* 215, 159-161.
- Wright JS. 2007. An overview of the role of weathering in the production of quartz silt. *Sedimentary Geology* 202(3), 337-351.
- Wu N, Pei Y, Lu H, Guo Z, Li F, Liu T. 2006. Marked ecological shifts during 6.2–2.4 Ma revealed by a terrestrial molluscan record from the Chinese Red Clay Formation and implication for palaeoclimatic evolution. *Palaeogeography, Palaeoclimatology, Palaeoecology* 233(3-4), 287-299.
- Xiao J, Porter SC, An Z, Kumai H, Yoshikawa S. 1995. Grain size of quartz as an indicator of winter monsoon strength on the Loess Plateau of Central China during the last 130,000 yr. *Quaternary Research* 43, 22–29.
- Xie S, Guo J, Huang J, Chen F, Wang H, Farrimond P. 2004. Restricted utility of $\delta^{13}\text{C}$ of bulk organic matter as a record of paleovegetation in some loess–paleosol sequences in the Chinese Loess Plateau. *Quaternary Research* 62, 86-93.
- Yang SL, Ding ZL. 2004. Comparison of particle size characteristics of the Tertiary ‘red clay’ and Pleistocene loess in the Chinese Loess Plateau: implications for origin and sources of the ‘red clay’. *Sedimentology* 51, 77–93.

Summary

Climate change is a hot topic these days. It may harm our economies and even our safeties. However, climate has always changed. New insight in the functioning of our climate and the resulting changes on scales of centuries to millennia is therefore possible from information about past climate changes. Such research is only possible when information from past climate changes is registered somewhere. Ocean floor sediments and land ice record climate changes relatively well and may provide a database of the climate of the past. The climate of the last glacial, or last ice age, is therefore very well registered in land ice and ocean floor deposits, mainly in the North Atlantic region. The records are very complete in time as signal forming processes continuously take place and erosion processes play hardly any role on these deposits.

New insights on relatively short-scale climate changes require information from the land. However, finding suitable information carriers on land is not that easy. Many deposits are the product of discontinuous processes, while destructive erosion processes are common. Very thick deposits of eolian dust in China seem to provide a resolution that potentially registered these oscillations. However, the information on short scale climate changes during the last glacial in China cannot reliably be linked to information from the North Atlantic. This thesis investigates the eastern and central European loess as a possible carrier of information on millennial scale climate oscillations during the last glacial. It is tested to what extent information from these loess deposits may function as a bridge between China and the North Atlantic. Besides, conclusions are drawn on the climate conditions, mainly wind directions, in central Europe during the last glacial.

Thick loess deposits are best suitable for this purpose, as they indicate a high time resolution. Paleosols, soils developed during the accumulation history of a loess deposit, may indicate slower deposition rates and thus lower resolution. They are therefore unwanted. Loess deposits are mainly found as blanket deposits on relatively low altitudes in the landscape, sometimes as relics of fluvial erosion. Exposures are often fluvial erosion cliffs or (former) brickyards.

For this research eight loess sections of last glacial age were sampled in 5-cm resolution. Three sections are situated on the west side of the Carpathian Mountains, in the Pannonian or Carpathian Basin: two in northern Serbia and one in southern Hungary. Five sections were sampled on the east and north side of the Carpathians: three in Ukraine and two in southeastern Poland. In northern Serbia, northern Ukraine and southeastern Poland two sections that are situated close to each other were sampled, in order to make comparisons possible. The section with the highest average resolution, with a total thickness of 20 m last glacial deposits, was found in Serbia.

Several signals (or proxies), sensitive for climate changes, were measured in the loess. They show a certain vertical variability through a loess section. During the research it became clear that correlating the wiggles of the different proxies between two sections is impossible without very precise dating techniques. However, dating techniques for the loess provide at present only about 8-10% uncertainty within one standard deviation (optical stimulated luminescence or OSL). This is not accurate enough to match millennial scale oscillations of the last glacial age (between 75 and 12 ka BP).

Chapter 1 describes a pilot study of a first step towards reliable matching of two records using a multi-proxy approach. Three, more or less independent proxies (grain-size fraction $<5.5\ \mu\text{m}$, magnetic susceptibility and the Ba/Sr ratio (see also Chapter 2)) were used in two Serbian sections that are separated only 6 km. First, different single-proxy record combinations were matched, using the available datings and field information. Using only this information, generally up to five wiggles can be matched. However, in most cases there are different matching possibilities; never more than two matches are unique and thus relatively reliable.

Finally all three proxy records were combined before the matching. In this way, more information is assembled for each wiggle. This gives a significantly better result: 8 matches could be established now, while all are unique. To conclude, two records with comparable sedimentation conditions can be matched reliably only when sufficient information on sediment properties is available. In this way, larger distances may be bridged in correlating the paleoclimatic variation from different regions.

Chapter 2 deals with new ways of extracting climate information from loess records. Grain-size is accepted as a reliable proxy for wind intensities, generally associated with cold periods. Proxies for temperature and precipitation, generally associated with warm periods, are more difficult to interpret. For example, magnetic susceptibility is accepted as a proxy for paleo-precipitation. However, the signal is unreliable in some environments and it is also sensitive for post-depositional processes that breakdown the signal. Therefore, new proxies that are relatively easily measured are more than welcome in terrestrial paleo-climatology. Peto-chemical elements may be used as such a proxy. They weather from primary minerals and have different solubility in acid, percolating rainwater. Ratios from hardly soluble elements and well soluble elements may provide a new proxy for the amount of percolating water through the loess column in the past, and thus for paleo-precipitation. Ratios were made in the elemental sequence Ca-Sr-Ba, and applied on four locations in Serbia and Ukraine with different present-day climate conditions. The Ba/Sr and Sr/Ca ratios show high similarities with magnetic susceptibility and the clay fraction. Sr/Ca is mainly sensitive in the Ukrainian test sites. Ba/Sr shows the similarity at all locations and is therefore a promising proxy for paleo-weathering intensity, especially paleo-precipitation. Further research may point out the further applicability of this ratio in different paleo-climatic environments.

Chapter 3 also focuses on new proxies that may indicate warm climate conditions. The climate dependent $\delta^{13}\text{C}$ -value of CO_2 in the air is transferred via plants to soil organic matter and then to soil carbonates where it is recorded. Water plays a controlling role in the type of plants (C3 or C4) that register the $\delta^{13}\text{C}$ -signal from the air, so this signal may well be interpreted as a registration of paleo-precipitation. In the continuous and relatively well dated section Titel in Serbia $\delta^{13}\text{C}$ of both soil organic matter ($\delta^{13}\text{C}_{\text{som}}$) and soil carbonate ($\delta^{13}\text{C}_{\text{sc}}$) are measured, next to total organic carbon, the CaCO_3 content and the C/N ratio. The $\delta^{13}\text{C}$ signals are compared to the clay fraction (grain-size $<5.5\ \mu\text{m}$), magnetic susceptibility and Ba/Sr records. The results are remarkable, as the $\delta^{13}\text{C}_{\text{sc}}$ correlates very well to these proxies, while the $\delta^{13}\text{C}_{\text{som}}$ does not at all. As the signal in soil carbonate is registered via the soil organic matter, it must be concluded that post-depositional processes have affected the signal in the soil organic matter. The reliability of the $\delta^{13}\text{C}_{\text{sc}}$ -signal was checked by comparing it to the $\delta^{18}\text{O}$ signal, and confirmed. This study suggests that $\delta^{13}\text{C}_{\text{sc}}$ may very well be a good proxy for paleo-precipitation, while care should be taken when using $\delta^{13}\text{C}_{\text{som}}$ as a proxy.

Chapter 4 describes an overview of the paleoclimatic results as derived from all sampled loess sections. Especially the grain-size information from these sections is used to reconstruct atmospheric circulation patterns during the last glacial. The reconstruction is based on the assumption that loess is a mixture of aeolian deposits from different origins and transport mechanisms. Sand and coarse silt are transported by saltation and in very low suspension, while medium-fine silt is transported in suspension clouds up to a few hundreds of meters above the ground surface. The bulk of these sediments can therefore not pass large water surfaces and mountain ranges. Very fine-grained loess, on the contrary, can be transported in dust plumes high in the atmosphere and can even cross oceans.

An end-member model separates the loess samples in coherent groups, or end-members. The mass accumulation rate was calculated for the Weichselian Early, Middle and Late Pleniglacial for each section. The end-member proportions and mass accumulation rates through time were related to the topography of the region. A large difference in mass accumulation rates is derived between the Early-Middle and the Late Pleniglacial east of the Carpathian Mountains. This difference, low accumulation rates in the Early and Middle, and high rates in the Late Pleniglacial, was not found on the west side of the Carpathians. There the sedimentation rates show more equal rate over time. This distribution of loess in space and time can not be explained by distance to the proglacial zone in front of the Scandinavian ice cap alone. A dominantly western wind during the Early and Middle Pleniglacial and a northwestern wind during the Late Pleniglacial in combination with the position of the Carpathians explains the observed loess distribution in the study area over time and space.

The distribution of the end-member results can also be interpreted – assuming that the proportions of fine endmembers increase and the proportion of coarse endmembers

decreases downwind – from this change in wind directions in the Early-Middle and Late Pleniglacial, confirming the hypothesis.

In the Synthesis it is concluded that it is probable that millennial scale oscillations of the last glacial climate are registered in the eastern and central European loess. It is also probable that these oscillations are related to the same climate oscillations that were responsible for variations in proxies from the Greenland ice sheet and from North Atlantic ocean floor deposits. However, problems still rise with attempts to match the wiggles in the proxy records on a long distance. Slight upscaling of wiggle-match distance, using many datings and proxies, may give new insight in the stability of a climate signal through a region.

New proxy information on the eight locations in eastern and central Europe, that is presented in this thesis, has contributed to the knowledge on the climate of the last glacial in this region. Mainly large differences in mass accumulation rates through time have pointed out that the total amount of dust transport varied more than was expected, while it could confirm modelled wind directions during this period. Also pilot studies on new proxies indicating post-depositional processes show promising results. They may also contribute to more reliable wiggle matching in the future. In this way, newly established proxy information may open new ways for the development of a better insight in the spatial influence of millennial scale climate oscillations.

Samenvatting

Klimaatverandering is hot. Vooral omdat onze economie er aanzienlijk door beïnvloed kan worden. Meer inzicht in hoe het klimaat functioneert en in de snelheid van bijbehorende processen is van wezenlijk belang om in te kunnen spelen op de gevolgen van klimaatverandering. Om een beeld te krijgen van die processen kunnen we naar klimaatfluctuaties in het verleden kijken. Informatie over klimaatveranderingen op eeuw- tot millenniumschaal in het verleden zijn echter alleen te vinden als deze in het verleden ook ergens opgeslagen zijn. Skeletjes van algen, of foraminiferen, op de oceaانبodem en luchtbelletjes in het ijs van bijvoorbeeld Groenland of Antarctica hebben zich al bewezen. Omdat het zinken van skeletjes naar de bodem en het vastvriezen van sneeuw op de ijskappen een vrijwel continu proces is, is er in het begin van de jaren negentig al zeer gedetailleerde informatie over het Holocene en de laatste ijstijd verzameld. Zo ontdekte men dat het klimaat van de laatste ijstijd sterk wisselend is geweest op millenniumschaal.

Deze nieuwe inzichten hebben veel vragen opgeroepen naar de aard en verspreiding van deze abrupte klimaatveranderingen. Om die aard en verspreiding in beeld te krijgen moet uitgezocht worden hoe deze veranderingen zich op verschillende plaatsen op aarde hebben gemanifesteerd. Hoge-resolutie informatie van de landmassa's is echter erg moeilijk, omdat de afzettingsprocessen waarmee signalen afkomstig van klimaatveranderingen opgeslagen worden, discontinu zijn. Bovendien zijn ze onderhevig aan erosie. Echter, dikke pakketten door de wind afgezet stof, of löss, in China lijken gedetailleerde informatie te bevatten over deze abrupte klimaatveranderingen. Om een brug te kunnen slaan tussen de informatie die in het Noordatlantisch gebied is gevonden en die in China is gevonden, richt het in dit proefschrift beschreven onderzoek zich op de löss van Europa.

Löss is in het landschap aanwezig als alles bedekkende afzettingen op lage hoogte ten opzichte van het zeeniveau. Afzettingen uit de laatste ijstijd bereiken in China diktes tot dertig meter. De löss is vaak ontsloten door eroderende rivieren of in (voormalige) baksteengroeves. Voor dit onderzoek zijn acht ontsluitingen van löss uit de laatste ijstijd in oost en centraal Europa gemonsterd in 5-cm resolutie. Drie secties liggen ten westen van de Karpaten, in het Pannonisch of Karpatisch Bekken, waarvan één in het zuiden van Hongarije en twee in het noorden van Servië. De overige vijf secties liggen ten oosten en noorden van de Karpaten, waarvan drie in Oekraïne en twee in zuidoost Polen. In Servië, Polen en noordelijk Oekraïne zijn steeds twee secties bij elkaar in de buurt gemonsterd, om onderling vergelijk mogelijk te maken. De dikste sectie, welke daarmee de hoogste gemiddelde tijdsresolutie heeft, werd gevonden in Servië, waar de löss uit de laatste ijstijd ongeveer 20 m dik is.

Verschillende signalen die gevoelig zijn voor klimaatverandering, meestal aangeduid als proxy's, zijn aan de lössmonsters gemeten. Deze signalen vormen verticaal een bepaalde variabiliteit, waaruit informatie over het klimaat uit de periode van afzetting af te leiden is. Echter, om deze informatie te koppelen aan klimaatinformatie uit een ander gebied zijn ook precieze gegevens nodig over de ouderdom van de löss. Gedurende het onderzoek is duidelijk geworden dat de precisie van bestaande (luminescentie) dateringstechnieken onvoldoende is om oscillaties op millenniumschaal met een ouderdom van 75 tot 12 duizend jaar met elkaar op afstand te kunnen correleren.

Hoofdstuk 1 beschrijft een eerste proefstudie naar mogelijkheden om toch betrouwbaar te correleren, zonder nauwkeuriger dateringsmethoden. Hiertoe is uitgegaan van drie min of meer onafhankelijke proxy's (korrelgrootte $<5.5\ \mu\text{m}$, magnetische susceptibiliteit (MS) en de Ba/Sr-ratio, zie ook hoofdstuk 2), welke zijn gemeten aan twee löss secties in Servië die slechts 6 km uit elkaar liggen. Eerst zijn matches gemaakt met één proxy per sectie, zowel twee verschillende als twee dezelfde. In de meeste gevallen kunnen maximaal vijf matches worden gemaakt op deze manier. Echter, meestal zijn er meerdere correlatiemogelijkheden. Slechts maximaal twee matches zijn uniek en dus relatief betrouwbaar.

Tot slot wordt per sectie alle informatie eerst gecombineerd, waardoor van iedere klimaatoscillatie meer informatie bekend is. Daarmee kan makkelijker onderscheid gemaakt worden tussen de oscillaties onderling, waardoor ze makkelijker uniek te correleren zijn op afstand. Deze benadering gaf een structureel beter resultaat: er kunnen nu acht matches gemaakt worden, die alle uniek zijn. Wanneer dus voldoende informatie per klimaatoscillatie bekend is, kan er op kleine afstand vrij betrouwbaar gecorreleerd worden. Met nog meer informatie per oscillatie kunnen in de toekomst mogelijk grotere afstanden worden overbrugd.

Hoofdstuk 2 beschrijft een onderzoek naar een nieuwe manier om extra klimaatinformatie af te leiden uit löss, met een relatief eenvoudige meetmethode. Korrelgrootte van löss is geaccepteerd als proxy voor wind intensiteit, meestal geassocieerd met koude periodes. Proxy's die gevoelig zijn voor temperatuur en neerslag, en dus voor warmere periodes, zijn moeilijker interpreteerbaar. Bijvoorbeeld MS wordt vaak gebruikt als neerslagproxy, maar is in sommige milieus onbetrouwbaar omdat bepaalde processen het opgeslagen klimaatsignaal juist weer afbreken. Daarom zijn nieuwe proxy's die neerslag en/of temperatuur indiceren nodig. Het hoofdstuk beschrijft hoe ratios van chemische elementen in de löss, die in meer of mindere mate vrij kunnen bewegen door het profiel, getest worden op hun betrouwbaarheid als neerslagproxy. De keuze van de geteste ratios is gebaseerd op het verschil in mobiliteit van de elementen en de processen waarmee ze vrij verweren uit de minerale structuur van de lösskorrels. Iedere ratio bestaat uit een relatief immobiel element, gedeeld door een relatief mobiel element, welke onder invloed van neerslag en zuur in de bodem uit het profiel kan spoelen. Bij veel neerslag zorgt water dat door het löss profiel sijpelt, voor een uitslag van de ratio-waarde. De ratios zijn gekozen in de reeks Ca-Sr-Ba en toegepast op vier secties

met uiteenlopende actuele klimaatsituaties: van een sectie in een relatief nat milieu in Servië, via twee secties dicht bij elkaar in noord Oekraïne naar een sectie in een relatief droog milieu in het zuiden van Oekraïne. De dubbele sectie is gekozen om onderling vergelijk mogelijk te maken. Uit de tests komt naar voren dat ratios van Ba/Sr en Sr/Ca grote overeenkomsten laten zien met het MS-sigitaal. De Ba/Sr-ratio doet dat zelfs in alle secties en lijkt daarom een veelbelovend proxy te kunnen zijn als indicator voor verweringsintensiteit in het verleden, in het bijzonder neerlag. Toekomstig onderzoek kan uitwijzen of dit proxy ook in andere milieus toepasbaar is.

Hoofdstuk 3 beschrijft een onderzoek naar twee andere neerslaggevoelige proxy's. De klimaatafhankelijke $\delta^{13}\text{C}$ -waarde van CO_2 in de lucht is via planten vastgelegd in organische stof en vervolgens via de CO_2 in de bodem in calciumcarbonaat. Water speelt een bepalende rol bij het type planten (C3 of C4) dat samen de vegetatie vormt en het $\delta^{13}\text{C}$ -sigitaal vastlegt in de bodem. Om die reden kan dit sigitaal als neerslagproxy worden beschouwd. In de relatief continue löss-afzettingen in de Titel-sectie in Servië werd het $\delta^{13}\text{C}$ -sigitaal zowel in organische stof als in de calciumcarbonaten gemeten. Vervolgens werden deze signalen vergeleken met elkaar en met het MS- en korrelgrootte(<5.5 μm)-sigitaal. Daarnaast werd gekeken naar de totale hoeveelheid organische stof, calciumcarbonaat en de C/N-ratio. De resultaten zijn opmerkelijk. Het $\delta^{13}\text{C}$ -sigitaal in het calciumcarbonaat laat een zeer goede correlatie zien met het korrelgrootte- en MS-sigitaal, terwijl het geen enkele correlatie laat zien met het $\delta^{13}\text{C}$ -sigitaal in de organische stof. Dit is vreemd, gezien het sigitaal in het calciumcarbonaat via de organische stof is vastgelegd. De betrouwbaarheid van het $\delta^{13}\text{C}$ -sigitaal in het carbonaat is gecheckt met het $\delta^{18}\text{O}$ -sigitaal, en bevestigd. Deze studie laat zien dat er waarschijnlijk processen spelen die het $\delta^{13}\text{C}$ -sigitaal in organische stof na verloop van tijd afbreken en dat daarom voorzichtigheid is geboden met het gebruik van $\delta^{13}\text{C}$ in organische stof als neerslagproxy. $\delta^{13}\text{C}$ in calciumcarbonaat lijkt echter goed toepasbaar als zodanig.

Hoofdstuk 4 beschrijft een totaalbeeld van klimatologische informatie uit het laatste glaciaal uit korrelgrootteonderzoek aan alle voor dit promotieonderzoek gemonsterde secties. Atmosferische circulatiepatronen in oost en centraal Europa zijn per deel van het laatste glaciaal bediscussieerd op basis van deze gegevens. Hiertoe is uitgegaan van de aanname dat de löss afzettingen zoals ze nu aangetroffen worden het resultaat zijn van verschillende transportmechanismen van löss die afkomstig kan zijn uit verschillende brongebieden. De fijnste löss kan door de hoge atmosfeer continenten en oceanen oversteken (zie de omslag van dit boek). De middelste löss verplaatst zich in grote suspensiewolken tot enige honderden meters hoogte en kan geen hoge bergruggen of grote wateroppervlakken oversteken. De grofste löss, gedeeltelijk bestaande uit zand, verplaatst zich middels saltatie, een soort springende beweging waarbij de korrels iedere paar meter de grond raken.

Een endmember-model scheidt de gemeten korrelgrootteverdelingen van de lössmonsters in coherente groepen, of endmembers. Op basis van deze endmembers

is de massa accumulatiesnelheid (MAR) berekend. De verschillende endmember proporties en MARs zijn per deel van het laatste glaciaal in relatie gebracht met de aanwezige topografie. Een groot verschil in MAR is aangetroffen tussen de west- en oostzijde van de Karpaten en tussen het Vroeg-Midden en het Laat Pleniglaciaal van de laatste ijstijd. Dit verschil, lage MAR's in het Vroeg en Midden en hoge MAR's in het Laat Pleniglaciaal werd echter niet gevonden aan de westzijde van de Karpaten, waar de MAR constanter is geweest over de gehele periode. Deze opmerkelijke verdeling van de löss over het onderzoeksgebied kan niet alleen verklaard worden vanuit de afstand tot het voor de hand liggende brongebied voor de Skandinavische ijskap. Een verandering van de dominante windrichting van westelijk in het Vroeg en Midden Pleniglaciaal naar noordwestelijk in het Laat Pleniglaciaal is de voor de hand liggende manier om de verdeling de löss over het gebied en door de tijd heen te verklaren.

Wanneer aangenomen wordt dat grove endmembers kleiner worden in verhouding tot fijne endmembers, naarmate de afzetting verder van de bron verwijderd is, bevestigt de verdeling van de endmembers de hypothese van een veranderende dominante windrichting tussen het Midden en Laat Pleniglaciaal.

In de synthese wordt geconcludeerd dat het waarschijnlijk is dat er klimaatoscillaties op millenniumschaal geregistreerd zijn in de oost en centraal Europese löss. Het is ook waarschijnlijk dat deze oscillaties verband houden met de klimaatveranderingen welke de variaties in de eigenschappen van het Groenlandse ijs en de oceaanbodemaafzettingen in de noord Atlantische regio hebben veroorzaakt. Echter, er blijven fundamentele problemen met betrekking tot het onderling correleren van deze informatie. Nieuwe studies die langeafstandscorrelaties steeds verder opschalen, gebruik makend van veel verschillende proxy's en dateringen, zullen nieuw inzicht kunnen verschaffen in de ruimtelijke stabiliteit van een klimaatsignaal.

Nieuwe proxy-informatie op de acht locaties in oost en centraal Europa die bestudeerd zijn voor dit onderzoek, hebben bijgedragen aan de kennis over het klimaat van de laatste ijstijd in deze regio. In het bijzonder grote verschillen in de MAR's door de tijd heen hebben uitgewezen dat de totale hoeveelheid verplaatst stof veel variabelere was dan verwacht, naast het feit dat modelreconstructies van de windrichting gedurende het laatste glaciaal bevestigd zijn. De teststudies naar nieuwe proxy's die gevoelig zijn voor warmere en nattere klimaatcondities hebben nieuwe inzichten verschaft. In de toekomst kunnen zij tevens bijdragen aan betrouwbare teleconnecties van klimaatgerelateerde data op millenniumschaal. Op die manier kan nieuwe proxy-informatie nieuwe mogelijkheden creëren voor de ontwikkeling van een beter inzicht in de ruimtelijke verbreiding van de invloed van klimaatfluctuaties op korte tijdschaal.



Colofon

This research was carried out at, and funded by:

VU University Amsterdam
Faculty of Earth and Life Sciences
Department of Climate Change and Landscape Dynamics
De Boelelaan 1085
1081 HV Amsterdam
The Netherlands

ISBN 978 90 8659 305 7

Last Glacial climate variability in eastern and central Europe as recorded in loess deposits
[PhD dissertation, VU University Amsterdam]

In Dutch: Klimaatvariabiliteit in het laatste glaciaal in oost en centraal Europa, afgeleid uit loess afzettingen
[Academisch proefschrift, Vrije Universiteit Amsterdam]

Author: M.P. Bokhorst

Cover design

Kaftwerk / Janine Hendriks

Cover photo

Dust storm off the coast of western Africa. Earth Observatory, NASA

Photos inside

p. 20: Sampling the lower part of the Titel section (Serbia) from a rope *Photographer: Jef Vandenberghe*
p. 40: Reaching the top part of the Pyrogo section (Ukraine) with Erhard Pots *Photographer: Jef Vandenberghe*
p. 62: Investigating the Stari Bezradychy section (Ukraine) with Natasha Gerasimenko *Photographer: Erhard Pots*
p. 76: Sampling the Dybawka section (Poland) with Jasper Wassenburg *Photographer: Sander Zwart*
p. 127: Discussing periglacial features in the Radymno section (Poland) with Maria Łanczont *Photogr.: Sander Zwart*

Printed by:

Ipskamp Drukkers BV, Enschede, The Netherlands